Population pharmacokinetic modelling to address the gaps in knowledge of commonly used HIV and TB drugs in children

BY
Tjokosela Tikiso

Thesis Presented for the Degree of

DOCTOR OF PHILOSOPHY

in the Division of Clinical Pharmacology
Department of Medicine
University of Cape Town

Supervisor: Associate Professor Paolo Denti
Co-supervisor: Professor Helen McIlleron

Contributions to the field

This thesis includes some of the following contributions to the field of pharmacometrics and clinical pharmacology:

Full length original articles

1. Rabie H, Tikiso T, Lee J, et al. Abacavir exposure in children cotreated for tuberculosis with rifampin and superboosted lopinavir-ritonavir. *Antimicrob Agents Chemother* 2020; 64.

2. Tikiso T, McIlleron H, Rabie H, Lee J, Archary M, Hennig S, Cotton M, Lallemant M, Gibb D, Burger D, Denti P. Abacavir pharmacokinetics in African children living with HIV: a pooled analysis describing the effects of age, malnutrition and common concomitant medications. *Submitted*

Scientific conference presentations

1. Tikiso T, McIlleron H, Rabie H, Lee J, Archary M, Hennig S, Cotton M, Lallemant M, Gibb D, Burger D, Denti P. A pooled analysis of abacavir pharmacokinetics in HIV-infected African children: the effect of age, malnutrition, and common concomitant co-medications. In: *Population Approach Group Europe (PAGE) 28th meeting,* Stockholm, Sweden. Abstr 9165

2. Tikiso T, Rabie H, McIlleron H, Lee J, Isabelle Andrieux-Meyer I, Cotton M, Lallemant M, Denti P. TB/HIV co-treatment with superboosted lopinavir lowers abacavir concentrations in children. 22nd International AIDS Conference (AIDS 2018), Amsterdam, Netherlands [presentation in a poster discussion session] Abstr wePDB0201

3. Tjokosela Tikiso, Helena Rabie, Helen McIlleron, Janice Lee, Isabelle Andrieux-Meyer I, Mark Cotton, Marc Lallemant, Paolo Denti. TB/HIV co-treatment with superboosted lopinavir lowers abacavir concentrations in children. Population Approach Group Europe (PAGE) 27th meeting, Montreux, Switzerland. Abstr 8702

4. Tjokosela Tikiso, Andrzej Bienczak, Diana Gibb, David Burger, Helen McIlleron, Paolo Denti. Population Pharmacokinetics of Abacavir in HIV-infected African children. Population Approach Group Europe (PAGE) 26th meeting, Budapest, Hungary. Abstr 7308

The author also made the following contributions not included in the thesis to the field of clinical pharmacology and pharmacometrics at the time when registered for doctoral studies:

Full length original articles

1. Van Der Laan LE, Garcia-Prats AJ, Simon Schaaf H, *et al.* Pharmacokinetics and drug-drug interactions of lopinavir-ritonavir administered with first- and second-line antituberculosis drugs in HIV-infected children treated for multidrug-resistant tuberculosis. *Antimicrob Agents Chemother* 2018; **62**.

Declaration of work

I Tjokosela Tikiso, hereby declare that the work on which this thesis is based is my original work (except where acknowledgements indicate otherwise) and that neither the whole work has been, is being, or is to be submitted for another degree in this or any other university. Chapter 3 and 4 of the thesis have been respectively published and submitted in an international journal and contents remain unchanged from the printed versions excepted where formatting was required to maintain consistency in the thesis. All co-authors gave their written consent to include the publications as part of the PhD. I confirm that co-authors of manuscript presented in chapter 5 (not published) are aware that the manuscript is part of the PhD.

I empower the university to reproduce for the purpose of research either the whole or any portion of the contents in any manner whatsoever.

I confirm that I have been granted permission by the University of Cape Town's Doctoral Degrees Board to include the following publication(s) in my PhD thesis, and where co-authorships are involved, my co-authors have agreed that I may include the publication(s):

1. Rabie H, Tikiso T, Lee J, et al. Abacavir exposure in children cotreated for tuberculosis with rifampin and superboosted lopinavir-ritonavir. *Antimicrob Agents Chemother* 2020; 64.
2. Tikiso T, McIlleron H, Rabie H, Lee J, Archary M, Hennig S, Cotton M, Lallemant M, Gibb D, Burger D, Denti P. Abacavir pharmacokinetics in African children living with HIV: a pooled analysis describing the effects of age, malnutrition and common concomitant medications. *Submitted*

Signature: Signed by candidate Date: 17/10/2021

Student Name: Tjokosela Tikiso Student Number: TKSTJO002

Acknowledgements

The time spent during my PHD has been an emotionally and mentally challenging experience. The completion of this research would have not been possible without the support of a number of people that I owe huge amount of gratitude to.

First and foremost, I would like to thank my supervisor associate professor Paolo Denti who provided mentorship and guidance in the field of pharmacometrics which was very new to me. He also provided funding to attend conferences and supported my applications for funding. Professor Helen McIlleron for critically reviewing the modelling work from a medical perspective and assistance with interpreting modelling results

I would like to thank everyone who contributed to the data used in this research and all co-authors for their feedback on my research outputs. I would also like to thank all my colleagues in the pharmacometrics modelling group for the interesting discussions, useful advice, and general support.

I am grateful for the opportunity and experience I got as an intern in the Next Generation Scientist program at Novartis. The mentorship, support and training of Dr Ivan Demin the Novartis Pharma modelling and simulation group will forever be remembered.

I would like to thank the ICTS High-Performance Computing team, provided by the University of Cape town, for providing computing power for some of the modelling carried out in this research.

I would like to thank the National Research Foundation for financial assistance. All the opinions and conclusions expressed are those of the author and were not influenced in any way by the funders of this research.

To my friends, thank you multitudes for all the encouragement, support and all the laughter we shared together

To my family, Rets'elisitso, Madeze, Deneze and Motsobunyane Tikiso. It is through your love and support that I was able to have the strength to carry on in this journey.

Abstract

Population pharmacokinetic modelling to address the gaps in knowledge of commonly used HIV and TB drugs in children

Tjokosela Tikiso -2020

The epidemiology of HIV and TB are overlapping, particularly in sub-Saharan Africa, and TB infection remains common in HIV-positive children. The combined administration of anti-tubercular and antiretroviral therapies (ART) may lead to drug-drug interactions potentially needing to be addressed with the adjustment of doses. This thesis assessed the pharmacokinetics of abacavir and ethambutol and evaluated the influence of covariates such as age and concomitant medication on the PK parameters across different studies using nonlinear mixed-effects modelling. The models developed were used to estimate area under the concentration-time curve (AUC) and maximum concentrations (C_{max}) achieved with the currently-recommended weight-adjusted doses. A web-based paediatric dosing tool, which is meant to be used as a first step in the design of clinical trials for paediatric dosing was also developed.

The model describing the pharmacokinetics of abacavir found: a) abacavir exposure to be 18.4% larger (CI:7.50-32.2) after the first dose of ART compared to abacavir co-treated with standard lopinavir/ritonavir for over 7 days, possibly indicating that clearance is induced with time on ART, b) malnourished HIV-infected children had much higher exposures but this effect waned with a half-life of 12.2 (CI: 9.87-16.8) days as children stayed on nutritional rehabilitation and recovered, c). during co-administration of rifampicin-containing antituberculosis treatment and super-boosted lopinavir/ritonavir, abacavir exposure was decreased by 29.4% (CI: 24.3-35.8), d) children receiving efavirenz had 12.1% (CI: 2.57-20.1) increased abacavir clearance compared to standard lopinavir/ritonavir. The effects did not result in abacavir exposures lower or higher than those reported in adults and are not likely to be clinically important.

The ethambutol model found lower concentrations than those reported in adults. The predicted ethambutol median (IQR) C_{max} was 1.66 (1.21-2.15) mg/L for children on ethambutol with or without ART (excluding super-boosted lopinavir/ritonavir) and 0.882 (0.669-1.28) mg/L for children on ethambutol with super-boosted lopinavir/ritonavir, these are below the lower limit of the recommended C_{max} range of 2 mg/L. During co-administration with super-boosted lopinavir, ethambutol exposure was decreased by 32% (CI: 23.8-38.9), likely due to drug-drug interaction involving absorption, metabolism or elimination. Bioavailability was decreased in children who were administered ethambutol in a crushed form, with an estimate decrease of 30.8% at birth, and an increase of 9.6% for each year of age up to 3.2 years where bioavailability was now similar to children taking EMB full tablet.

The developed paediatric dosing tool contains two major sections. a) the 'generic module' which uses allometric scaling -based predictions to explore the expected AUC for a generic drug, b) the 'drug-specific module' which can simulate entire pharmacokinetic profiles (concentration over time after dose) by using a drug-specific population pharmacokinetic model.

In summary, under the current weight-adjusted doses, abacavir exposure remained within the adult recommended levels. Ethambutol dose adjustment would be required in order to achieve adult exposures. A web-based paediatric dosing tool that uses allometric scaling -based predictions as well as drug specific predictions based on published pharmacokinetic models was successfully developed.

Table of Contents

List of figures

List of Tables

LIST OF ABBREVIATIONS

95% CI	95 Percent Confidence Interval
3TC	Lamivudine
ABC	Abacavir
ALAG	Absorption Lag Time
AIC	Akaike Information Criterion
ART	Antiretroviral Therapy
ARV	Antiretrovirals
AUC	Area under the Concentration Time Curve
AZT	Zidovudine
BID	Bis in Die (Twice Daily)
BLQ	Below the Limit of quantification
BOV	between-occasion variability
BSV	Between-subject variability
CL/F	Clearance
CYPs	Cytochrome P450 Enzymes
CV	Co-efficient of Variation
Cmax	Maximum Concentration
Cmin	Minimum Concentration
EBEs	Empirical Bayes Estimates
EFV	Efavirenz
EMB	Ethambutol
FOCE	First Order Conditional Estimation
FOCEI	First Conditional Estimation with Interaction
HAZ	Height for Age Z-Scores
HIV	Human Immune-Deficiency Virus
hr	Hour(s)
IIV	Inter-individual Variability

IOV	Inter-occasion Variability
IPREDs	Individual Predications
IQR	Interquartile Range
IWRES	Individual Weighted Residuals
KA	Absorption Rate Constant
kg	Kilogram
KTR	Transit Time Rate Constant
L/kg	Litres per Kilogram
LPV	Lopinavir
LPV/r	Ritonavir-Boosted Lopinavir
Pg-p	P-glycoprotein
PI	Protease Inhibitor
PK	Pharmacokinetics
PREDs	Predictions
PsN	Perl Speaks NONMEM
mg	Milligrams
mg/kg	Milligram Per Kilogram
mg/L	Milligram Per Litre
MTT	Mean Transit Time
NNRTI	Non-nucleoside Reverse Transcriptase Inhibitor
NRTI	Nucleoside Reverse Transcriptase Inhibitor
NVP	Nevirapine
PMA	Post Menstrual Age
PMA50	Post Menstrual Age Half Life
OFV	Objective Function Value
RTV	Ritonavir
RUV	Random Unexplained Variability
UGTs	Uridine 5' Diphospho-Glucuronosyltransferases
V/F	Volume of Distribution

VPC	Visual Predictive Check
WHO	World Health Organization
WAZ	Weight for Age Z-scores

Chapter 1: Introduction and literature review

1.1 Introduction

In 2018, human immunodeficiency virus (HIV) and tuberculosis (TB) were among the major sources of death worldwide, with TB the number one cause of death in infectious diseases and HIV following closely behind at second. [1] In the same year, it was predicted that 37.9 million people were living with HIV in the world, [2] whilst 10 million were estimated to have TB. [1] Of these 10 million, 8.6% were people living with HIV. The number of people living with HIV and TB-coinfection was observed more in the African Region particularly in Southern Africa where it exceeds 50% of TB cases.[1] HIV and TB co-infection has been shown to influence the progression and outcome of both diseases. [3] For instance, a person living with HIV has one of the highest possibilities to develop active TB (about 15 to 22 more times), and TB is the number one cause of mortality in HIV-positive people, with the proportion of deaths around 33%. [1,4] The influence of HIV and TB in children has been immense. It is believed that about 1.7 million children are currently living with HIV and over 1 million have TB worldwide. In 2018, 13% of HIV-positive people who died from TB were children. Additionally, children with HIV are estimated to be 8 times more likely to be infected with TB.[5]

The introduction of antiretroviral therapy, substantially decreased the rapid mortality rate due to HIV infection, changing it from a deadly condition into a chronic condition. Antiretroviral treatment suppresses HIV replication, decreases viral levels, and aids in maintaining optimal immunologic function allowing for normal growth and development in paediatric patients. [6–8] Without antiretroviral treatment, children living with HIV in surroundings with scarce resources

have a mortality rate of 45-59% by 2 years of age. But ever since the availability of antiretroviral therapy, people living with HIV now have lower TB-associated mortality. [9–13] Despite declines in HIV and TB mortality in paediatrics, the numbers are still high. Thus, plenty of work is still required to decrease new infections, improve treatment efficacy and safety, and identify and manage drug interactions to further improve treatment outcome.

The optimal dose of a drug is one which provides the maximum benefit with reduced risk to the patient. For children, dose optimization is challenging because of the little research performed in this population group, limited availability of paediatric drug formulations, and complexity of prescribing drugs in children. [14–16] Most medicines used in children are originally developed for adults, and historically many drugs were developed when paediatric assessments were not required by regulatory authorities, so the development and implementation of paediatric therapy has significantly been impacted by the lack of evidence from safety and dose-finding trials of drugs already approved in adults. [6] Such poor turnover may partly be due to unaccounted differences in pharmacokinetics and pharmacodynamics of drugs in paediatrics and adults. For example, until recently, children's doses have been widely derived by simply assuming linear scaling of the adult dose based on weight, but this over-simplification generally leads to under-dosing in children. [17] Out of all the licensed antiretroviral drugs by regulatory agencies (i.e. European Medicines Agency and the US Food and Drug Administration), only 25% are approved for treating children younger than 2 years. [18] In infectious diseases, it is widely accepted during optimization of paediatric dosing to target similar exposure proven to be effective in adults while monitoring safety. To achieve this, it is crucial to understand the pharmacokinetics of the drug of interest and the paediatric and environmental factors responsible for the pharmacokinetic

variability of the drug. It is also very important to utilize analytical techniques that make optimal use of the limited available clinical paediatric data.

1.2 Paediatric factors affecting pharmacokinetics

The pharmacokinetics (absorption, distribution, metabolism, elimination) of a drug are influenced by a number of factors, including the drug's physicochemical properties (e.g., lipophilic or water soluble, degree of ionization), physiological parameters of the person receiving the drugs (e.g., gastric pH, protein binding, drug-metabolizing enzymes) and environmental factors (e.g., food administration with the dose, method of drug administration). The main differences in pharmacokinetics between adults and children relate to the anatomical, biochemical, and physiological changes that occur from birth throughout childhood. The impact of these factors may differ significantly with growth and development and can play a major role in the age-related pharmacokinetic differences seen between adults and paediatrics. The complexity of paediatric pharmacokinetic variability arises from the multiple age groups. The international regulation on paediatric clinical trials defines paediatric population to be all age groups from birth to 18 years, including premature neonate (born before 37 weeks' gestation), neonates (within first month of life), infants (1 to 23 months), children (2 to 11 years), and adolescents (12 to 18 years). [19] The most important factors that can impact pharmacokinetics processes of antiretroviral therapy and anti-TB drugs in paediatrics are discussed below.

1.2.1 Absorption

Several differences in physiology between adults and children may affect drug absorption. The rate at which a lot of drugs are absorbed is mostly slower in younger children compared to adults,

with gastrointestinal function achieving adult levels and functionality by the age of 2 years. Intraluminal pH is higher in neonates and infants (less acidic) and gets to adult levels by 3 years, this difference in pH can directly affect dissolution of the drug with a consequent influence on drug absorption. [20–23] Age-dependent changes in the functionalities of efflux transporters and metabolizing enzymes found in the intestines can also change absorption of a drug, i.e., uridine 5'-diphospho-glucuronosyltransferase (UGT) 2B7 enzyme that is responsible for zidovudine metabolism is highly expressed in adults but not in neonates. [24] However, data on the intestinal expressions of drug metabolizing enzymes and efflux transporters in children is scarce. [20]

Another important source of differences in absorption between adults and children is associated with drug administration, drug formulation and the method of drug administration, these factors play a crucial role in the pharmacokinetics of drugs. Children cannot swallow adult tablets, so alternative methods are necessary to give drugs orally. A widely-spread approach is crushed adult tablets or sprinkled capsule content, sometimes taken with food to improve palatability. These dosing procedures or use of other formulations can erratically alter a drugs pharmacokinetics and subsequently contribute towards treatment failure. [25] In particular, food intake around the time of drug dosing can impact bioavailability of drugs. Not only can it interfere with the dissolution and transit time of the drug, but it can also influence metabolic transformation of drugs. [26] The effect of tablet crushing/dissolving and food can greatly vary from drug to drug and hard to predict *a priori*.

1.2.2 Distribution

Developmental changes that occur in the body can profoundly alter drug distribution. Infants have higher total body water (80-90% of the body weight) and decreased fat content (10-15% of

body weight) compared to adults, with the levels of both reaching adult values around 1-2 years. [22,24,27] These changes can result in either higher or lower volume of distribution of water-soluble and lipophilic drugs, respectively. Also, infants and children have low levels of important plasma binding proteins in comparison to adults. [22,24,28] Overall , acidic drugs generally bind to albumin, whereas basic drugs bind to globulins, α1-acid glycoprotein, and lipoproteins. [22] The effect of reduced protein binding is more detrimental for highly protein-bound drugs such as lopinavir/ritonavir. These changes in protein binding can affect volume of distribution and subsequently drug activity.

Drug distribution may further be affected by disease-related changes in body composition. Malnutrition is particularly of importance due to its common occurrence and association with severe forms of HIV and TB [29–31] in paediatrics. During malnutrition, the total body water is increased and adipose mass is reduced, these alterations in physiology can impact pharmacokinetic processes, drug responses and toxicity. [31] Whether these processes are increased or decreased will depend on the physiochemical characteristics of the drug. Malnutrition does not only affect distribution, but also other pharmacokinetic processes to some extent.

1.2.3 Metabolism

Drug metabolism predominantly takes place in the liver. The effect age-related changes have on hepatic metabolism mainly depends on the family of enzymes. Most of the commonly used ART and anti-TB drugs are catalysed by the cytochrome P450 (CYP) and uridine diphosphate glucuronosyltransferase (UGT) enzymes. Total cytochrome P450 levels are low at birth (about 50–70% of adult values), exceed adult values by 2–3 years and stabilize to adult levels by puberty.

[28,32,33] These fluctuations have been reported in various CYP isozymes, including CYP1A2, CYP2C, and CYP3A.[28] UGT enzymes, particularly UGT1A1, UGT1A4, UGT1A6, UGT2B7, UGT1A9, UGT2B15, and UGT2B17 are also significantly impacted by age. UGT-dependent metabolism is low in neonates and reaches adult levels by the age of 3–4 years. [28,34,35] These changes may be partly driven by hormonal signaling during development. [34,36]

1.2.4 Excretion

Excretion of drugs by the kidneys is influenced by age related changes. The main processes behind excretion (glomerular filtration rate, tubular secretion and reabsorption) depend on renal blood flow, which is highly affected by growth and development. At birth it is 5 to 6% of adult cardiac output, by 1 year it increases to 15 to 25% and reaches adult levels ~ 2 years of age. Overall, renal function at birth is~25–30% of adult values, by 6 months it is 50–75%, and reaches full maturation by age 2–3 years. [22,24,28]

1.3 HIV and tuberculosis

This section will discuss the Pathogenesis and treatment of HIV and TB in paediatrics.

1.3.1 HIV Pathogenesis

HIV is a retrovirus belonging to a subgroup called lentiviruses (viruses that cause disease slowly). A HIV viral particle contains 2 enzymes (the reverse transcriptase and integrase molecule) that are important for HIV replication and 2 strands of RNA that contain the genetic material and are located in the virus capsid. [37] The replication cycle of HIV starts with the virus attaching to the hosts CD4 receptors on the surface of immune system cells like T-lymphocytes, monocytes,

macrophages and dendritic cells as well as either CCR5 or CXCR4 chemokine coreceptors. [37–39] After attachment, HIV fuses with the host membrane therefore making it possible for the HIV capsid to enter the host cell where HIV converts RNA into HIV DNA through its transcriptase enzyme. Once the HIV DNA enters the host cell nucleus, it integrates to the host cell DNA with the help of Integrase, HIV then instructs the host cell to start making new HIV proteins, these long chain proteins are broken down by HIV protease enzyme into smaller protein parts that join together with copies of HIV's RNA making up a new virus. The viral particles are then released out of the cell to infect other target cells.[37–40] As the virus is actively replicating in the lymph nodes and blood stream, the infected individuals may look healthy without symptoms. This stage lasts up to three months after infection, until seroconversion, i.e. when HIV-specific antibodies can be detected. The outcome of infection and duration for disease progression with clinical symptoms may vary greatly between individuals, but often it progresses fairly slowly. It takes several years from primary infection to the development of symptoms of advanced HIV disease and immunosuppression.[41]

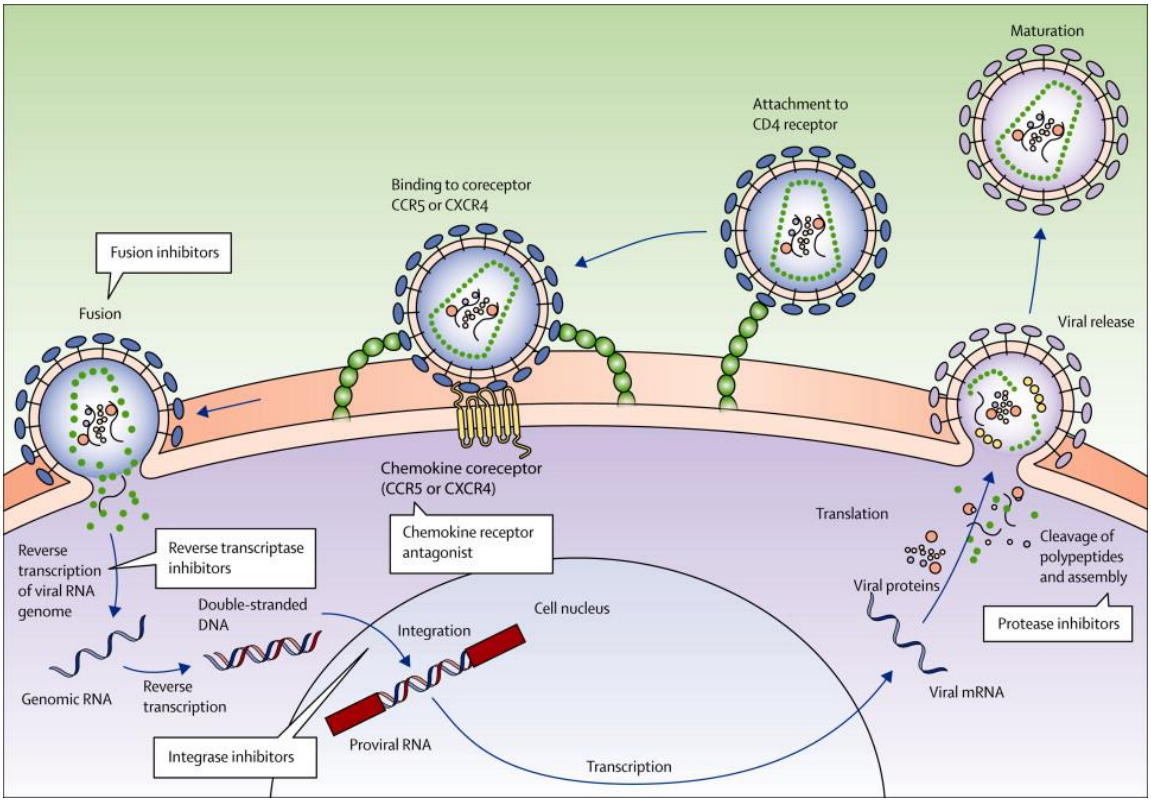

Figure 1.1 HIV life cycle with antiviral targets. Taken from Maartens *et al* 2014

1.3.2 Tuberculosis Pathogenesis

Tuberculosis is caused by Mycobacterium tuberculosis (*M. tuberculosis*), a rod-shaped, slow growing aerobic bacterium. Infection starts when inhaled droplet containing *M. tuberculosis* migrates to the alveoli of the lungs where *M. tuberculosis* is phagocytosed by alveolar macrophages. The infected macrophages transport the bacteria to regional lymph nodes and other organs.[42,43] This process of distribution activates the immune system for response. Macrophages release pro inflammatory cytokines and mycobacterial antigens responsible for inducing activation of CD4+ cells are presented, and this leads to the formation of granulomas. [42,44–46] Granulomas are barriers that keep the bacilli under control, they are made up of monocytes, macrophages, and neutrophils. People in this stage cannot spread the infection even

though they have *M. tuberculosis* in their bodies, this is identified as the latent infection stage. Once the immune system struggles to keep *M. tuberculosis* under control, the bacteria multiply rapidly until the granuloma erupts causing the distribution of *M. tuberculosis* into the alveoli and bronchi, ready to infect other individuals, this is when TB disease begins. [42,47]

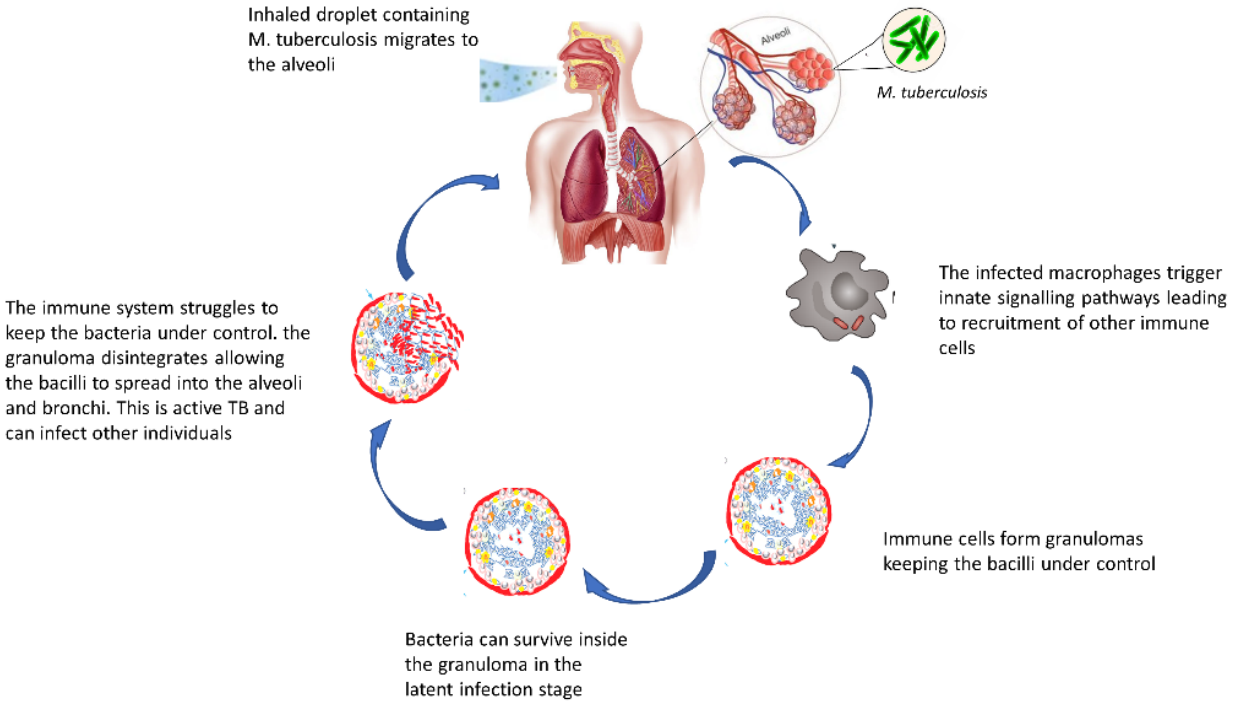

Figure 1.2 TB life cycle.

1.3.3 Pathogenesis of HIV and TB co-infection

Both TB and HIV "attack" the immune system of the body, HIV causes a decline in immune system cells, this in turn affects the immune systems response to TB infection. Macrophages and CD4+ cells are important immune system cells in the fight against TB, they form most of the granulomas which are responsible for keeping TB in the latent stage. HIV uses these immune cells to multiply, this eventually leads to reduced integrity of granulomas and thus decrease the ability to contain

M. tuberculosis, this increases the likelihood of activation of a latent TB infection as well as reactivation of tuberculosis. [48,49] On the other hand, TB increases the expression of CXCR4 in alveolar macrophages and suppresses CCR5, thus creating an environment that promotes rapid HIV replication. HIV predominantly utilizes CCR5 early in the development of infection and CXCR4 mostly as the disease progresses.[49–51]

1.3.4 HIV treatment

Antiretroviral therapy uses a combination (three being the standard) of 5 classes of ARV: entry and fusion inhibitors prevent HIV from attaching to target CD4 cells by binding to the viral envelope proteins, nucleoside reverse transcriptase inhibitors (NRTIs) inhibit HIV reverse transcription and thus viral replication after they are incorporated inside the viral DNA, non-nucleoside reverse transcriptase inhibitors (NNRTIs) inhibit HIV reverse transcription similar to NRTIs just at a different site, integrase strand transfer inhibitors (INSTIs) block HIV integrase enzyme activity and thus prevents incorporation of HIV DNA into the host genome, Protease inhibitors (PIs) prevents HIV replication by blocking HIV protease enzyme activity, this enzyme is responsible for breaking down HIV proteins into smaller particles.[52–54]

The world health organization (WHO) recommends a first-line regimen of two NRTIs, abacavir (ABC) and lamivudine (3TC) combined with a PI lopinavir/ritonavir (LPV/r) in children weighing less than 15 kg, while children weighing more than 15 kg, lopinavir/ritonavir is replaced with dolutegravir (DTG).[55] In South Africa, the currently preferred first-line ART option for children over 4 weeks old and less than 20 kg includes abacavir and lamivudine plus lopinavir/ritonavir. For children 20-35 kg, abacavir plus lamivudine and dolutegravir are preferred. [56,57] Previously,

children older than 3 years of age were given the non-nucleoside reverse transcriptase inhibitor (NNRTI) efavirenz instead of dolutegravir.

1.3.5 TB treatment

The main aim of TB treatment is to eradicate *M. tuberculosis,* prevent transmission and relapse of disease, as well as prevent development of drug resistance. For treatment of drug-susceptible Tb in children living in settings where HIV prevalence is high or resistance to isoniazid is frequent, the World Health Organisation currently recommends a daily six-month regimen of isoniazid, rifampicin, pyrazinamide and ethambutol. With administration of all the drugs during the intensive phase (first two months) and only rifampicin and isoniazid during the continuation phase (four months). [1]

1.3.6 HIV and TB treatment during coinfection

During co-infection of HIV and TB, WHO recommends TB treatment to be initiated as soon as diagnosis is confirmed, whereas antiretroviral therapy should be started 2-8 weeks after TB treatment is initiated.[1,58] The combined administration of anti-TB treatment and antiretroviral therapy can be complicated by a range of possible drug-drug interactions and adverse effects. Sometimes, the interactions are not similar for both adults and children, meaning that the same dose adjustment strategy that works in adults may not necessarily work in children. An example of this is the interaction between rifampicin (main drug for TB) and boosted protease inhibitors lopinavir/ritonavir, doubling the dose works in adults but not in children.

1.4 Drugs of Interest in This Thesis

In the following section, the key drugs of the present thesis, abacavir and ethambutol will be introduced. And a brief summary of the co-administered drugs that might impact abacavir and ethambutol pharmacokinetics will be discussed.

1.4.1 Abacavir

Abacavir is a nucleoside reverse transcriptase inhibitor that that prevents HIV replication by inhibiting HIV reverse transcriptase. It is licensed for paediatric patients above 3 months and can be taken 1-2 times per day at a dosage of 16 mg/kg and 8 mg/kg respectively.[59] A single abacavir dose of 300 mg and 600 mg attain mean maximum plasma concentrations (C_{max}) of 2.39–3.11 µg/mL and 4.10–5.46 µg/mL respectively, with time to C_{max} (T_{max}) between 0.63-1 hour. [59,60] Its oral bioavailability is indicated to be around 83% while plasma protein binding is approximately 50% irrespective of plasma concentrations. Concomitant intake with food does not affect abacavir bioavailability but might decrease the rate of absorption. The hepatic enzymes responsible for abacavir metabolism are alcohol dehydrogenase (ADH) and uridine diphosphate glucuronyltransferase (UGT) which produce inactive carboxylate and glucuronide metabolites. Abacavir has a terminal elimination half-life of about 1.5 hours. [59–61]

The population pharmacokinetics of abacavir has been described by a one–[62,63] or two-compartment [64,65] disposition model with first-order absorption and elimination. The absorption was generally implemented with no delay in most of the models except for one model which implemented a delay characterised by lag. [63] Allometric scaling by body weight was applied on disposition parameters to account for the effect of body size on pharmacokinetics in most of the

models. However, the models did not account for the effect of age or the maturation process. Moreover, they did not explore the impact co-administered drugs have on abacavir pharmacokinetics. The 12-hour median AUC of 6.02 mg·h/L obtained in adults has been recommended as the therapeutic target. When lopinavir/ritonavir was co-administered with abacavir in adults, a 30% reduction in abacavir exposure was reported. [66] The most common adverse effect associated with abacavir intake is optic hypersensitivity, the risk for this adverse effect is very low in African children. [67]

1.4.2 Ethambutol

Ethambutol inhibits bacterial growth by inhibiting biosynthesis of the arabinan component of the mycobacterial cell wall core, but its primary inclusion in the first-line anti-TB therapy is for protection against resistance to co-administered first line anti-TB drugs. [68,69] Ethambutol is indicated for the paediatric population at 15-25 mg/kg once daily. Its oral bioavailability is indicated to be approximately 80% and Plasma protein binding around 70–80%. Ingesting food around the same time ethambutol is administered decreases the rate of ethambutol absorption but not its overall bioavailability. Peak plasma concentrations of ethambutol are between 2–4 hours after dose. The peak concentrations between 2 to 6 mg/L has been proposed as a therapeutic target in adults on 25 mg/kg. [68–70] Ethambutol is mostly excreted unchanged in urine, around 50 to 70% of oral doses are recovered unchanged in the urine of subjects with normal renal function. [70] Ethambutol is metabolised by alcohol dehydrogenase to an aldehyde intermediate, with its metabolite additionally oxidised to dicarboxylic acid by aldehyde dehydrogenase. [71,72] Co-administration of ethambutol with antacids decreases ethambutol exposure, with 29% and 10% reduction in C_{max} and AUC0–∞ respectively.[69]

Population pharmacokinetics of ethambutol has been reported in adults. [69,73–76] Ethambutol plasma concentrations have generally been reported as a two-compartment disposition model with first-order absorption with/without delay. [74,75,76] Ethambutol has also been described by a zero-order process by Peloquin et al. and Zhu et al. All the models included elimination as a first-order process and included allometric scaling on all clearance and volume of distribution parameters to account for the effect of body size. Denti et al. and Jönsson et al. described this effect of body size with total body weight [75,76] whereas Smythe used total body weight on volume of distribution and fat-free mass on clearance. [77] A decrease in ethambutol AUC and C_{max} has been reported in HIV co-infected patients compared to those without HIV coinfection: a 20% decrease in $C_{max,}$ and a 27% decrease in AUC was reported by Zhu et al. and McIlleron et al. respectively.[73,78] HIV co-infected patients have also been reported to have 15% reduction in bioavailability.[76] The major adverse effect related to ethambutol is dose-dependent ocular toxicity which resolves upon stopping ethambutol intake. [79,80] Patients with renal failure are most likely to experience toxicity with the currently recommended dose. Similarly, doses of at least 30 mg/kg are likely to incite toxicity. Higher plasma uric acid levels have also been noted, though less likely.[81]

1.4.3 Lopinavir/ritonavir

Lopinavir selectively inhibits HIV-1 protease-mediated cleavage of gag and gag-polypolyprotein leading to production of non-infectious HIV virions. [82] Lopinavir is highly metabolised by hepatic cytochrome P450 (CYP) 3A4 isoenzyme. However, co-administration with ritonavir, a protein inhibitor of hepatic CYP3A4 and drug-transporting cellular efflux proteins such as P-glycoprotein, increases lopinavir plasma concentrations to required therapeutic levels.[82–84] Therefore, lopinavir

is commercially available co-formulated with ritonavir. Administration of the capsule or liquid formulations with moderate to high fat food increases bioavailability of lopinavir/ritonavir. Binding to plasma proteins for both lopinavir and ritonavir is about 98-99%. The mean plasma C_{max} of lopinavir/ritonavir is 9.8+3.7 μg/mL, occurring approximately 4 hours post dose, with the mean elimination half-life of 2-3 hours after single dose administration.[82–84] Drug-drug interactions have also been reported between lopinavir/ritonavir with NNRTIs efavirenz and nevirapine. Both NNRTIs are metabolized by CYP3A4 and both act as CYP3A inducers. Likewise, co-administration of lopinavir/ritonavir with rifampicin, a potent CYP3A4 inducer results in decreased lopinavir concentrations.[82–84]

1.4.4 Rifampicin

Rifampicin is the main drug in the treatment of drug-susceptible tuberculosis. It works by preventing bacterial DNA-directed mRNA synthesis via binding to the β subunit of DNA dependent RNA polymerase leading to a suppression of RNA synthesis and cell death. Food decreases rifampicin C_{max} and increases T_{max}. [69,85] In the absence of food, rifampicin absolute bioavailability was found to be 87%. [86] Rifampicin is metabolised by liver esterase, [85] and binding to plasma protein is about 80%. [87,88] Rifampicin is a potent inducer of a number of drug metabolising enzymes via activation of nuclear pregnane X receptor which regulates the transcription of metabolizing enzymes of multiple drugs and drug transporters like the P-glycoprotein .[89] Time to full induction is estimated to be between one week to one month. [90] In the first two weeks of rifampicin treatment, a dose-dependent autoinduction which decreases the elimination half-life has been reported.

1.4.5 Efavirenz

Efavirenz is a non-nucleoside reverse transcriptase inhibitor that inhibits HIV by binding to a non-catalytic site of the HIV reverse transcription enzyme. [91] Its intake with food is associated with increased plasma concentrations and side effects. [92] The mean plasma C_{max} occurs approximately 5 hours post dose, with steady-state attained in 6 to 7 days. Efavirenz has a half-life of about 45 hours and binds highly to proteins, with a strong affinity for albumin. [93] Efavirenz is metabolized rapidly by CYP2B6 and slowly metabolized by CYP3A4. It enhances its own metabolism (autoinduction) by inducing the expression of CYP2B6 and CYP3A4 via activation of pregnane X receptor and constitutive androstane receptor. [92,94–97]

1.5 Techniques for analysis of clinical data

1.5.1 Pharmacometrics

Unlike adults, children cannot easily undergo drug testing. For example, there are many practical and ethical barriers, like limited amount of blood samples that can be collected from children. To address these challenges, International Council on Harmonisation of Technical Requirements for Registration of Pharmaceuticals for Human Use urged development and implementation of novel approaches to drug testing, and pharmacometrics is one of them.

Pharmacometrics is a science that develops and applies mathematical, statistical and computational methods with the overall aim to understand, characterise, and predict a drug's pharmacokinetic and pharmacodynamic behaviour.[98–100] Pharmacometrics was originally developed to help with analysis of clinical data from drug development. In the recent years pharmacometric modelling has gained increasing attention in clinical research due to the ability

to characterize sources and levels of variability, compile data from different sources and the ability to simulate clinical trials based on various circumstances (set of assumptions). The simulations can further be used in trial optimization and decision making.[101] The main benefit in paediatric medicines is the ability to use of all the available limited data to make decisions and optimize paediatric medicines. [102]

1.5.2 R Shiny

Interactive web applications are ideal for communicating complex models to a non-technical audience, the dynamic visualizations of data make decision-making quicker and easier. However, creating web applications is very difficult due to the deep knowledge of web technologies like HTML, CSS and JavaScript required. The introduction of Shiny has made it significantly easier for R users to build interactive web tools that enhance data visualization and facilitate data and information sharing. Shiny can empower a non-technical audience to explore and visualize their data or perform their own analyses with methods pre-developed. Shiny has been used for visualizing clinical trials and pharmaceutical data, as well as aiding in study design and analysis.

Shiny is an open-source R package of RStudio that uses R programming language to build interactive web applications. [103] RStudio is a free integrated development environment for R. Shiny provides a set of user interface (UI) functions that generate the HTML, CSS, and JavaScript. Therefore, prior knowledge of HTML/CSS/JavaScript is not required. And, through the use of reactive programming, Shiny can quickly and automatically update all related dependencies of a code chunk. The UI.R and server.R make up a shiny application.[103,104]

1.6 Thesis objectives

The currently recommended paediatric doses used for antiretroviral and first-line antituberculosis drugs were derived from adult dosage with the assumption that the same dose per kg is suitable across all age groups. Even though abacavir and ethambutol have been available for many years, pharmacokinetic knowledge of these drugs in paediatrics is limited and the majority of the studies used NCA for analysis. In paediatrics, age-dependent changes such as maturation of metabolizing enzymes and transporters, body composition and nutritional status, can influence pharmacokinetics and toxicity. Hence there is a need to describe the population pharmacokinetics of abacavir and ethambutol through a pharmacometric approach, and use final models to predict AUC and C_{max} and compare them with adult pharmacokinetic levels. Pharmacometric models are complex to interpret and use for non-modelers like clinicians, the value of the evidence generated by pharmacometric models cannot be appreciated if such information does not reach other scientists who can use it to inform decision making. There is therefore a need for easy-to-use tools like Shiny that can be used to help interpret pharmacometrics models and concepts in a user-friendly manner to other scientists who are not familiar with modelling.

The specific aims of the thesis were to:

1 To describe the population pharmacokinetics of abacavir using several available clinical datasets to take advantage of the increased sample size and perform a more robust analysis to investigate the consequence of differences in body size, age, concomitant TB co-medications, malnutrition, and drug formulation on abacavir pharmacokinetics in children.

2 To characterize the population pharmacokinetics of ethambutol in African children with TB, infected and uninfected with HIV, and identify factors that impact ethambutol pharmacokinetics in order to guide dosing.

3 To implement a web-based paediatric dosing tool used to visualize alternative dosing regimens by displaying exposure across weight bands, which is meant to be used as a first step in the design of clinical trials for paediatric dosing was also developed.

Chapter 2: Methodology

2.1 Study designs and data description

2.1.1 CHAPAS-3

CHAPAS-3 (Children with HIV in Africa – Pharmacokinetics and Adherence of Simple Antiretroviral Regimens) was a multicentre, open-label, randomised, phase II/III trial assessing acceptability, adherence, cost-effectiveness, pharmacokinetics, toxicity and virological efficacy of three first-line antiretroviral regimens in 478 African children aged 3 months to 13 years. The children were either previously untreated or treated for at least 2 years with stavudine-based regimens and showing viral suppression during testing. The regimens under study were abacavir + lamivudine, stavudine + lamivudine and zidovudine + lamivudine, in combination with nevirapine or efavirenz. The trial was conducted at four African sites: one in Zambia (University Teaching Hospital, Lusaka) and three in Uganda (Bristol Myers Squibb Children's Clinical Centre of Excellence, Baylor College of Medicine, Kampala; Joint Clinical Research Centre, Kampala; Joint Clinical Research Centre, Gulu) during November 2010 and December 2013. The children were all administered paediatric fixed dose combination (FDC) tables and dosed according to the WHO 2010 recommendations. Intensive pharmacokinetic sampling (draws at 0, 1, 2, 4, 6, 8, and 12 hours after dose, plus 24 hours if taking abacavir once daily) was done in children with TB and those enrolled at week 6. Measurements of viral loads were done at baseline, weeks 48, 96, and 132 (or 144). Children were followed for at least 2 years after inclusion in the study. [105] The trial diagram is presented in Figure 2.1. Abacavir clinical data taken from CHAPAS was used in chapter 4 for population pharmacokinetics meta-analysis of abacavir in children.

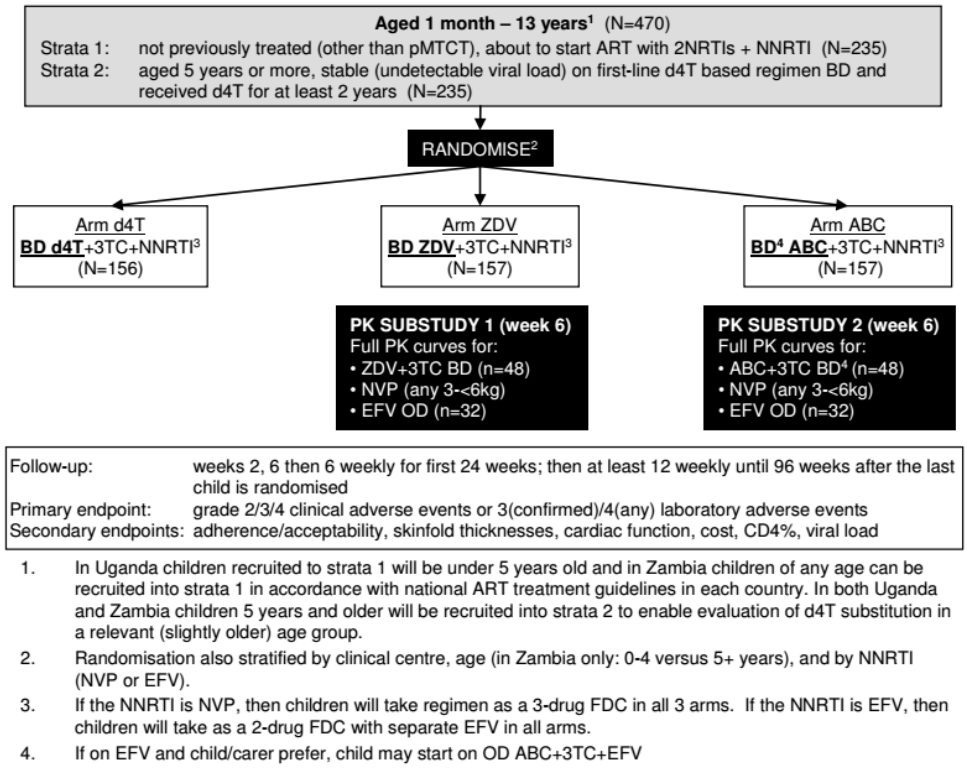

Figure 2.1 CHAPAS-3 study diagram from the study protocol.

3TC - lamivudine, ABC – abacavir, BD – twice a day, d4T - stavudine, NNRTI – non-nucleoside reverse transcriptase inhibitor, EFV - efavirenz, NVP - nevirapine, OD –once a day. ZDV - zidovudine

2.1.2 Arrow

ARROW (Antiretroviral Research for Watoto) was a parallel group, open-label, multicentre, randomised controlled, clinical trial conducted at four African sites: one in Zimbabwe (University of Zimbabwe-Clinical Research Centre, Harare) and 3 in Uganda (Joint Clinical Research Centre, Kampala; Medical Research Council/Uganda Virus Research Institute, Entebbe; Paediatric Infectious Disease Clinic/Mulago, Kampala). The main objective of the trial was to assess management of antiretroviral therapy by (i) using clinically driven monitoring as well as laboratory plus clinical monitoring and (ii) by using first line antiretroviral therapy that included three drugs (two nucleoside reverse transcriptase inhibitors and one non-nucleoside reverse

transcriptase inhibitor), with induction with four drugs of two classes then maintenance with three drugs. Two further randomisations were performed after at least 36 and 96 weeks on antiretroviral therapy, with the aim of assessing approaches that could aid in antiretroviral therapy adherence. These were, (i) once versus twice daily abacavir + lamivudine dosing and (ii) stopping versus continuing daily cotrimoxazole prophylaxis. A total of 1200 symptomatic HIV infected African infants and children from 3 months to 17 years were enrolled and followed from March 2007 to March 2012. Most of the children were given the paediatric FDC tablets and dosing was based on the WHO 2006 recommendations.[106,107] Pharmacokinetic samples were collected before drug intake and then at 1, 2, 4, 6, 8 and 12 hours after dose, plus 24 hours if taking abacavir once daily. Measurements of viral loads were done at baseline and then every 12 weeks. The trial diagrams showing the first and second phases of the trial are shown in Figures 2.2 and 2.3 (respectively). Abacavir clinical data taken from ARROW was used in chapter 4 for the population pharmacokinetics meta-analysis of abacavir in children.

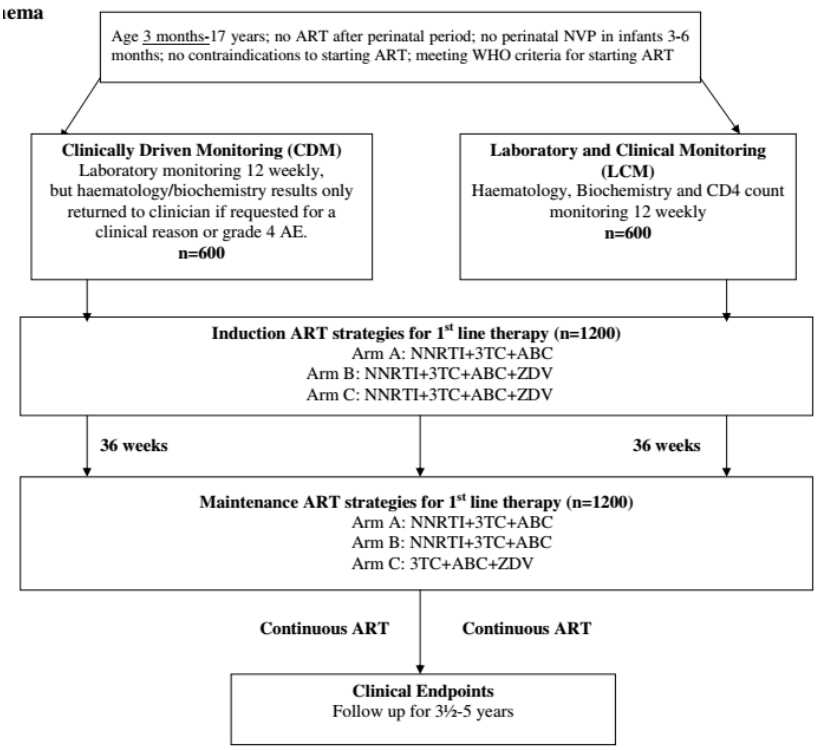

Figure 2.2 ARROW study diagram showing 1st phase of the study. 3TC - lamivudine, ABC – abacavir, AE – adverse event, NRRTI – non-nucleoside reverse transcriptase inhibitor, ZDV - zidovudine.

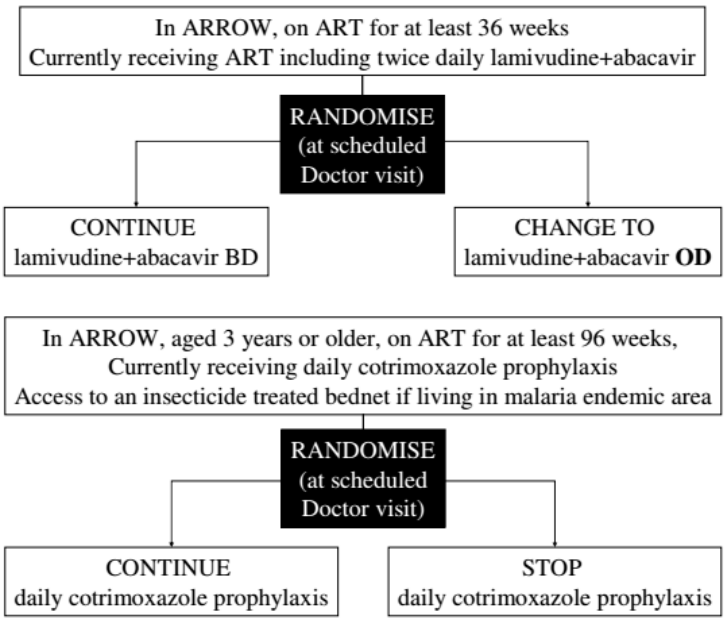

Figure 2.3 ARROW study diagram showing 2nd phase of the study. ART – antiretroviral treatment, BD – twice daily, OD – once daily,

2.1.3 DNDI

The study was a multicentre, non-randomized, prospective, Phase I/II, open label, noninferiority study in 87 South African infants and children weighing 3 to 15 kg. The key objective of the trial was to compare pharmacokinetics of rifampicin-based anti-TB treatment and super-boosted lopinavir (LPV/r 1:1) with standard lopinavir (LPV/r 4:1) without rifampicin-based anti-TB treatment. Another goal of the study was to evaluate lopinavir safety, tolerance, and virological effect in HIV-TB co-infected infants and children. The study was conducted in 5 South African sites: The Enhancing Care Foundation; the Family Centre for Research with Ubuntu (FAM-CRU); Wits RHI Shandukani Research Unit; the Empilweni Services and Research Unit (ESRU); the Perinatal HIV Research Units (PHRU). The children were enrolled between January 2013 and November 2015, with follow-up completed in July 2016. Drugs were provided by the South African Department of Health ART-program. Doses for both ART and anti-TB drugs were based on the South African 2012 dosing recommendations. [108,109] Pharmacokinetic samples were drawn before the observed dose and after 1, 2, 4, 6, and 10 hours postdose. Measurements of viral loads were assessed at the onset of therapy, and on the final PK day (4 to 6 weeks after discontinuing the TB treatment). Abacavir clinical data taken from DNDI was used in chapter 3 and 4 for the population pharmacokinetics of abacavir in children, while ethambutol clinical data was used in chapter 5 for the population pharmacokinetics of ethambutol in African children.

2.1.4 MATCH

MATCH (Malnutrition and Antiretroviral Timing in Children with HIV) was a multicentre, open label, Phase I/II, prospective, non-randomized, noninferiority study that enrolled 82 newly diagnosed HIV-infected infants and children between 1 month to 12 years. The main objective of

the study was to compare the nutritional, immunological, and virological responses to Highly active antiretroviral therapy (HAART) in severely malnourished (weight-for-length Z-scores < −3, mid-upper arm circumference < 115 mm or peripheral edema) children started immediately on HAART against children in whom HAART was administered only after malnutrition was resolved (WHZ of –2, achieved at least 15% weight gain or demonstrated resolution of edema and return of appetite). Children were equally allocated to be either part of the early arm where ART was introduced within 14 days of enrollment or delayed arm where ART was introduced upon nutritional recovery and more than 14 days from enrollment. The study was conducted at King Edward VIII Hospital in Durban South Africa, between June 2012 and December 2015. All children were given the standardized re-feeding for severely malnourished children as recommended by WHO Guidelines. Antiretroviral drugs were provided by the South African National ART program and were dosed according to the the South African national ART guidelines (2012-2015). [110,111] Pharmacokinetic samples were drawn according to the following sampling schedules; on day 1, samples were drawn in the following time windows 1.3–1.8, 3–4, 5–7, and 8–10 hours postdose. On day 14, sample was 30 minutes prior to dosing, and 1.3–1.8, 3–4, 5–7, and 8–10 hours postdose. Abacavir clinical data taken from MATCH was used in the population pharmacokinetics of abacavir in children of abacavir pharmacokinetics in children in chapter 4. Abacavir clinical data taken from MATCH was used in chapter 4 for the population pharmacokinetics meta-analysis of abacavir in children.

2.1.5 SHINE

SHINE (Shorter treatment for minimal TB in children) was an open-label, non-inferiority, multicentre, parallel-group, randomised controlled, two-arm trial conducted in 1200 African and

Indian children with non-severe TB below 16 years with/without HIV infection. The main objective of the trial was to compare efficacy of the standard 6-month regimen with the 4-month regimen using revised WHO dosing guidelines and new FDC tablets. Children were equally allocated between the two arms, with both arms having a 2 months intensive phase with rifampicin, isoniazid, pyrazinamide and ethambutol followed by a continuation phase with rifampicin and isoniazid for 2 months in the shorter arm vs 4 months in the standard arm. The study was conducted in 5 sites in Africa and India: 3 in Africa (Cape Town, South Africa; Kampala, Uganda; Lusaka Zambia) and two in India (Pune and Chennai) between July 2016 and June 2018.[112] Pharmacokinetic samples were collected before drug intake and then at 1, 2, 4, 6, 8 and 12 hours after drug intake. Ethambutol clinical data taken from SHINE was one of the datasets used in the population pharmacokinetics analysis of ethambutol in African children (chapter 5).

2.1.6 DATIC

DATIC (Optimal Dosing of 1st Line Antituberculosis and Antiretroviral Drugs in Children (a Pharmacokinetic Study) was a multicentre, open-label, phase IV, non-randomized trial performed in 200 African children from the age of 1 month to 12 Years, with TB with and without HIV. The main goals of the study were to assess: (i) the pharmacokinetics of first line antituberculosis drugs (isoniazid, rifampicin, pyrazinamide and ethambutol) in paediatrics in Cape Town, South Africa and Blantyre, Malawi (with wide-ranging nutritional status) dosed according to the 2010 WHO/IUATLD dosing guidelines. (ii) the 8-hourly dosing of lopinavir/ritonavir co-administered with rifampicin-based anti-TB treatment in South African children. (iii) the pharmacokinetics of nevirapine in children in Malawi co-administered with rifampicin-based anti-TB treatment. The study was conducted between November 2012 and July 2017 at Red Cross Children's Hospital in

Cape Town and Queen Elizabeth Central Hospital, Blantyre. [70,113] Pharmacokinetic samples were collected at a predose, 1, 2, 4, 6, and 8 hours postdose. Ethambutol clinical data taken from DATIC was one of the datasets used in the population pharmacokinetics analysis of ethambutol in African children (chapter 5).

2.2 Pharmacometric Analyses

This section will give a brief outline, the detailed discussions will be addressed in the following specific chapters

2.2.1 Population Pharmacokinetic modelling

Nonlinear mixed-effects (NLME) modelling was used for analysis of paediatric pharmacokinetics in this thesis. Nonlinear mixed-effects model(s) simultaneously analyse all individual's data using a single pharmacometric model. [114,115] The term 'nonlinear' means the relationship between the dependent variable and the independent variables or model parameters is nonlinear, while the term 'mixed-effects' means the model consists of fixed and random-effects parameters. In a population the fixed effects are constant, whereas random effects differ between individuals. [115–117]

Nonlinear mixed-effects models are made up of 2 major components: (i) structural model, and (ii) statistical model. The structural model (which may or may not contain covariates) describes the central tendencies of the typical dependant variable against the independent variable, i.e. a population's drug concentrations over time**.** Structural models are typically described by compartmental models, these models assume the human body to which the drug distributes as a series of compartments with homogeneity of drug concentration present in each compartment

at any time. The structural model usually consists of a depot compartment (where the drug dose is administered), the central compartment (generally highly perfused parts of the body) and/or the peripheral compartment (s) (generally less perfused parts of the body). [116–118]

The statistical models account for the magnitude of unexplained variability in the data. Various types of variability can be explained based on the data: (i) Between-subject variability (BSV) also known as Inter-individual variability (IIV) describes the differences between individual parameters from the typical model parameters and (ii) Between-occasion variability (BOV), also known as inter-occasion variability (IOV),describes the differences in individual parameters at each occasion from the typical individual model, as well as (iii) the residual unexplained variability (RUV), which refers to the variability between the observed data and the model prediction after controlling for other sources of variability. RUV originates from different types of variability, such as (i) analytical assay error, (ii) inaccurate reporting of data (e.g. imprecise documentation of dosing or sampling time points) or (iii) model misspecifications. Once the variability in the data has been identified, the covariate model aims to explain it using subject specific (e.g. sex, age, weight etc.) or environmental (study, arm, food, formulation etc.) characteristics. This step, which is usually done after the development of the base model is one of the important aspects of pharmacometric modelling, as it allows the integration of knowledge in the model and makes it more predictive. [116–118]

To provide a mathematical formalisation of a model, the *jth* measurement of subject *i* can be described as:

$$Y_{i_j} = f\left(X_{i_j}, \emptyset_i\right) + \varepsilon_{i_j}$$

where $f(\cdot)$ is the individual prediction defined by a nonlinear function with parameter vector $\emptyset i$ and independent variables xij (dose, time). εij is the residual unexplained variability with mean of zero and variance of σ^2, it shows individual deviation from the observed values.

The individual parameters are positive and often right skewed hence a lognormal distribution is assumed as shown:

$$Pij = \theta_j \cdot e^{\eta ijP}$$

where *Pij* is the *jth* pharmacokinetic parameter for the *ith* individual, θ_j is the typical value of the *jth* population parameter, and *ηij* represents a random variable for the *ith* individual in the *jth* parameter(P) distributed with a mean of zero and variance of ω_j^2.

The RUV is usually explored via additive and/proportional models. [114,115] The simplest is the constant error model, also called the additive error model, in which every prediction has the same error regardless of its magnitude. This model means that the lower predictions are more affected by the error than the higher predictions. In the proportional error model, the standard error of the residual error is proportional to the prediction. In this model, the higher predictions are more affected by the error than the ones with lower values. To balance the effect of the error on the magnitude of the prediction, a combined error model can be implemented with both an additive and proportional component as shown:

$$Y_{i_j} = f\left(X_{i_j}, \emptyset_i\right) \cdot (1 + \varepsilon prop) + \varepsilon add$$

Nonlinear mixed-effects modelling utilizes analysis software to implement an estimation method for finding population and individual parameters that best describes the data. In this thesis, NONMEM version 7.3-7.4 (ICON Development Solutions, Ellicott City, MD, USA) was used. NONMEM estimates parameter values by minimizing the minus 2 log likelihood (-2LL) and gives

it as the objective function (OFV) value. The Likelihood for nonlinear mixed-effects models is not easily solved so the OFV has to be numerically approximated .[119] Various estimation methods are available for this purpose. In this thesis, the first-order conditional estimation (FOCE) method with interaction was used. The estimation method returns the population parameters, while the *post-hoc* estimation step returns the individual parameter estimates (Empirical Bayes estimates). The use of NONMEM was supported by auxiliary software. Perl-speaks-NONMEM was used to support in model development and evaluation. Pirana helped in data management and data processing after modelling and R via RStudio interface (R Core Team,2017; RStudio, 2014) aided in graphical analysis.

2.2.2 Model evaluation

Model evaluation is a very vital stage in in the process of selecting the model that best describes the data. Model evaluation tools can be analytical or graphical, and are normally used in combination. Model diagnostic tools are mostly graphical, while, model selection tools are usually analytical.[118] In this thesis, graphical diagnostics were performed using Xpose (version 4.5.0) implemented in R. Diagnostic plots which were consistently used included goodness-of-fit plots, individual plots, residual-based plots and visual predictive check (VPC) plots.[120] Individual plots display individual predicted profiles, population predicted profiles and observed data, they are useful in assessing how well the model describes individual data. Goodness-of-fit plots evaluate how close the model predictions are to the observed data. Typically, the model population predictions (PRED) and individual predictions (IPRED) versus observations are routinely used as goodness-of-fit plots and consistency is checked across the range of prediction values. Residual-based plots such as individual weighted residuals (IWRES) and conditional

weighted residuals (CWRES) are also used commonly as part of goodness-of-fit plots, they provide information on systematic deviation of the model predictions from the observations. Generally, the residual based diagnostics should be normally distributed with mean 0 across any independent variable, most notably time. VPC plots were used to diagnose model adequacy, they are helpful to inform about the appropriateness of the structural model and the random-effects structure.

2.2.3 Model building approach

The model building process basically started with a one-compartment structural model with first-order absorption and elimination, then multi-compartment models with first-order elimination and absorption (with/without an absorption lag time or transit compartments) [121] were evaluated. The statistical model included between-subject, between-occasion and between-visit variability, and were assumed to be lognormally distributed. The additive error for all samples was set to be at least 20% of the lower limit of quantification (LLOQ) of the assay. BLQ concentrations were handled with the M6 method.[122] This means that each series of BLQ values are imputed to half the limit of quantification (LOQ/2), except for consecutive succeeding BQL observations, which are discarded. Additionally, the error for all imputed values was inflated by LLOQ/2. The M6 method employed in the present analysis does not attempt to completely discard the "trailing" BLQ values. Instead these values were removed from the estimation step but retained for VPCs and other simulation-based diagnostics, whose diagnostic power would otherwise be impaired due to the selective exclusion of data (low values) from the observed dataset but not from simulated replicates. This exclusion from the estimation step but not the re-simulation was achieved by including the trailing BLQs assigning a huge additive error and thus

making them virtually irrelevant in the model fit, while retaining them in the dataset for simulation.

Model building was guided by the drop in the objective function value (ΔOFV; proportional to -2 log-likelihood), inspection of goodness-of-fit plots, biological plausibility, VPC and clinical relevance. A decrease in OFV of more than 3.84 between two nested models after the addition of one parameter was considered significant at $P<0.05$. Covariates were included in the model with a step-wise approach. Firstly, they were screened and added one by one based on inspection of parameter versus covariate plots and physiological plausibility. They were retained if they produced a decrease in the -2LL of more than 3.84 for one degree of freedom ($P<0.05$). Then, they were confirmed with a backward elimination step, where each covariate-PK parameter relationship was removed one by one and retained only if an increase greater than 6.64 in -2LL for one degree of freedom ($P<0.01$) was observed. Parameter uncertainty was assessed via sampling importance resampling method (SIR). It was preferred over nonparametric bootstrap method because of shorter computation times.

2.2.4 Advantages of Population pharmacokinetics modelling

Population pharmacokinetics modelling offers a number of advantages over classical analysis methods such as non-compartmental analysis,[123] resulting in increased feasibility of studies and reduction of burden related to drug testing.[124,125] Firstly, population pharmacokinetics modelling enables sparse data analysis without compromising results of the study [126] and predictions of full drug concentration curves can be obtained even when collecting very few samples per patient.[117] Second, population pharmacokinetics models offer a semi-mechanistic platform that allows the inclusion of several concomitant effects on PK parameters (absorption, distribution, elimination),

as opposed to drug concentrations, so they can be used to describe the overlapping effect of weight and age in a cohort of children. Finally, validated models can be utilized in simulations of other sub-populations to test various "what-if" scenarios,[127–129] Simulations can also facilitate treatment optimisation.[130] Use of this approach can contribute towards increased safety of drug testing in children by for example facilitating more informed decisions about dose escalation in early phase clinical trials.[127,130,131] Furthermore, use of pharmacokinetic modelling and simulation can have a significant effect on reduction of number of patients needed in the process of drug testing. [132–134]

2.3 Shiny application

Shiny application is made up of two main sections, the user interface called UI.R and the server file called server.R.

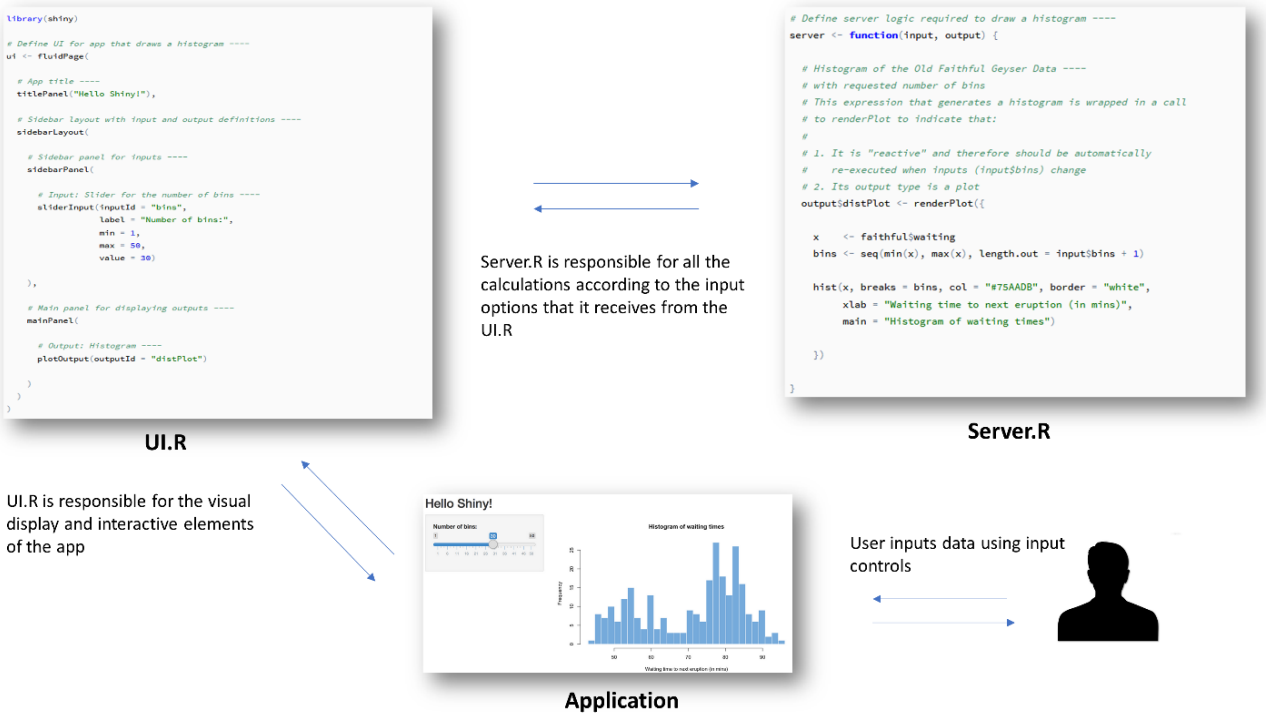

Figure 2.4 Structure of a shiny application

2.3.1 UI section

The UI section of a shiny application defines the overall visual structure of the application, the input controls available to the user, and the content that will be made visible to the user. Shiny translates the R code and shiny functions in this section into html and CSS code that web browsers can read and render into a web application. [104] The layout function is responsible for the outer most visual structure of the Shiny application, it takes the inputs and outputs and arranges them on a page. For example, shiny::fluidPage, which is the layout style used by most apps, creates a web page containing both rows and columns scaled to fill all available browser width. One of the most common application layouts is the sidebarLayout which has a skinny sidebar on the left hand-side (by default) where input controls are usually added and a main panel on the right-hand side which typically displays the results. The input controls also referred to as *control widgets*,

are what the user will use to interact with the application. There are 13 standard control widgets from simple check boxes to sliders, and all widget control functions take at least 2 arguments: the input ID argument, which is needed to access the user input value in the code, and the label argument, which is made to be easily readable by the developer. Outputs from UI.R are linked to the server function, this is one of the main ways the two functions work in cohesion. Outputs have a unique ID similar to inputs. The three main types of outputs are: plots, tables and text.[103,104]

2.3.2 Server section

The server section of a shiny application is where most of the computation takes place. i.e. the code for transforming data or creating visualizations will most likely be in this section. The server utilizes the values users inputted via the control widgets to perform actions such as output plots. These outputs will be saved to a special object called "output" which can later be referenced in the UI section in order to display them. Shiny predominantly utilizes reactive programming in the server section to make the application interactive. With reactive programming, changing an input causes a cascade of reactions from other functions connected to that input. Server functions take two parameters: input and output. The input argument which is basically a list object is named according to the input ID from the user interface. Outputs are also list objects, they use a render function to output plots, tables and texts.[103,104]

2.4 Shiny application building approach

The Shiny app was launched as a separate-file application (UI.R and server.R) for easy testing and management of the application. The UI function is responsible for the visual display and

interactive elements of the app while the server function is responsible for all the calculations according to the input options that it receives from the UI function. Various application layout structures (i.e. sidebarLayout, splitLayout and flowLayout) were tested in the initial building stages of the app. Other additional panels were considered depending on the layout and requirements of the app. Widgets were then included in the UI function, widgets allow the user interface to be interactive. Functionalities based on the UI inputs were then created in the server function. Basic functionalities were included in the early building stages of the app with more complex reactivity functionalities included in the later stages.

Chapter 3: Abacavir exposure in children co-treated for tuberculosis with rifampicin and super-boosted lopinavir-ritonavir

3.1 Abstract

In children requiring co-formulated lopinavir/ritonavir-4:1 and rifampicin, adding ritonavir to achieve a 4:4 ratio with lopinavir (LPV/r-4:4) overcomes the drug-drug interaction. Possible drug-drug interactions within this regimen may affect abacavir concentrations, but this has never been studied.

Children <15 kg needing rifampicin and LPV/r-4:4 were enrolled in a pharmacokinetic study and underwent intensive pharmacokinetic sampling on 3 visits: a) during the intensive and b) continuation phase of anti-tuberculosis treatment with LPV/r-4:4, and c) one month after anti-tuberculosis treatment completion on LPV/r-4:1. Pharmacometric modelling and simulation were used to compare exposures across weight bands with adult target exposures.

Eighty-seven children median (inter-quartile range) age and weight of 19 (4-64) months and 8.7 (3.9-14.9) kg respectively were included in the abacavir analysis. Abacavir pharmacokinetics was best described by a two-compartment model with first-order elimination and transit compartment absorption. After allometric scaling adjusted for the effect of body size, maturation could be identified: clearance was predicted to be fully mature around two years of age and to reach half of this mature value around two months. Abacavir bioavailability decreased 36% during treatment with rifampicin and LPV/r-4:4 but remained within the median adult

recommended exposure, except for the 3-4.9 kg weight-band where exposures were higher. Observed pre-dose morning trough concentrations were higher than the evening values.

Though abacavir exposure significantly decreased during concomitant administration of rifampicin and LPV/r-4:4, it remained within acceptable ranges.

3.2 Introduction

In HIV-positive children younger than 3 years, the World Health Organization (WHO) recommends the nucleoside reverse transcriptase inhibitor (NRTI) abacavir in the first-line antiretroviral therapy (ART) regimen with lamivudine and the protease inhibitor (PI) lopinavir co-formulated with ritonavir in a 4:1 ratio. [135] WHO indicates abacavir for children from 3 months of age at 8 mg/kg twice daily or 16 mg/kg once daily to a maximum of 300 mg per dose twice daily or 600 mg daily. [60,136] In South Africa abacavir is recommended from the age of 1 month and weight above 3 kg. [137] The risk for abacavir hypersensitivity is related to genetic factors and is very low in African children. [67] Abacavir is extensively metabolized by the liver, with less than 2% excreted unchanged in urine. [138] The two major pathways of abacavir metabolism are alcohol dehydrogenase (ADH) and uridine diphosphate glucuronyltransferase (UGT) enzymes, producing inactive carboxylate and glucuronide metabolites.[138] Coadministration with food has no effect on abacavir exposure. [139] Abacavir pharmacokinetic parameters do not appear to be affected by the use of liquid or tablet formulation. [64]

Lopinavir/ritonavir-4:1 (lopinavir co-formulated with ritonavir in a 4:1 ratio) is superior to nevirapine in young infants regardless of nevirapine exposure as part of prevention of mother-to-child- transmission. [140–141] The low dose of ritonavir inhibits cytochrome P450 3A4 (CYP3A4)-mediated metabolism of lopinavir and the P-glycoprotein (P-gp) efflux pump, thereby providing effective lopinavir plasma exposure. [142] Ritonavir may also induce some cytochrome P450 enzymes and various glucuronidases (UGTs) and multidrug transport proteins such as P-glycoprotein. [143–147] Adult data suggests that co-administration of abacavir and

lopinavir/ritonavir-4:1 has no effect on lopinavir pharmacokinetics (PK), but appears to decrease abacavir exposure by approximately 30%.[66] Nevertheless, no dose adjustments are recommended, and the significance of this drug-drug interaction is not known.

The epidemiology of tuberculosis (TB) and HIV are overlapping, particularly in sub-Saharan Africa, and TB infection remains common in HIV-positive children. [148] The short-course regimens for drug-susceptible TB in children consist of daily rifampicin, isoniazid, and pyrazinamide with or without ethambutol or ethionamide for 2 months, followed by isoniazid and rifampicin for 4 months. Rifampicin induces CYP3A4 and is a strong activator of the Pregnane X receptor (PXR), which upregulates many drug metabolizing enzymes and drug transporters, leading to major drug-drug interactions when administered with antiretrovirals metabolized by the same pathways. Thus, rifampicin induces the expression of P-gp and UGT responsible for abacavir metabolism.[149,150] Conversely, rifampicin inhibits hepatic organic anion transporting polypeptides (OATPs). Lopinavir exposure is decreased by up to 90% when administered with rifampicin. [151] To overcome this drug-drug interaction, adding ritonavir to achieve a 4:4 ratio with lopinavir (LPV/r-4:4 also referred to as super-boosting) is a commonly used strategy to overcome the induction by rifampicin, thereby providing effective plasma concentrations of lopinavir. There is no pharmacokinetic data available on the implications of LPV/r-4:4 and rifampicin on abacavir exposure.

We conducted a large pharmacokinetic study to confirm the validity of the LPV/r-4:4 approach in young children with TB and HIV. Within this study, we also investigated abacavir pharmacokinetics during LPV/r-4:4 with rifampicin and standard lopinavir/ritonavir-4:1 after the end of rifampicin treatment.

3.3 Methods

3.3.1 Study design and participants

We conducted a prospective, open-label, one-group one-sequence study at 5 sites in 3 South African provinces: the Family Centre for Research with Ubuntu (FAM-CRU) in the Western Cape; the Empilweni Services and Research Unit (ESRU), Wits RHI Shandukani Research Unit, and the Perinatal HIV Research Units (PHRU) in Gauteng; and the Enhancing Care Foundation in KwaZulu-Natal. Enrolment occurred between January 2013 and November 2015, with the study follow-up completed in July 2016. HIV-positive children with clinician-diagnosed TB, receiving rifampicin-based TB treatment, could enrol if body weight was between 3 and 15 kg, and post-conceptional age beyond 42 weeks. Children could enter regardless of whether TB treatment or ART was initiated first. We excluded children receiving non-standard dosages of TB treatment, those requiring drugs that significantly induce cytochrome P450 enzymes, or children with clinical conditions that could compromise their study participation, such as Division of AIDS (DAIDS) grade 3 alanine aminotransferase (ALT) increase, renal function abnormalities, severe comorbidities, or contraindications to lopinavir/ritonavir.

All drugs, including abacavir (20 mg/mL solution), lopinavir/ritonavir-4:1 (Kaletra® 80/20 mg/mL solution) and ritonavir (Norvir® 80 mg/mL), were supplied through the South African Department of Health ART-program. Drugs were dosed according to the study protocol, See table 4. The original protocol and amendments were reviewed by the Data Safety and Monitoring Board (DSMB) and approved by the human research ethics committees of the Universities of Stellenbosch, Cape Town, the Witwatersrand, and Pharma Ethics in Durban. Parents or legal guardians provided written informed consent. Consents forms were available in English and local

languages including Afrikaans, isiXhosa, and isiZulu. Due to the young age of participants, assent was not sought.

3.3.2 Procedures

As previously described, [152] the children in the study underwent intensive pharmacokinetic sampling on three visits. The first two pharmacokinetic evaluations (PK1 and PK2) were performed during the second and last month of TB and HIV co-treatment, which included LPV/r-4:4. Standard lopinavir/ritonavir-4:1 doses were re-instated 2 weeks after stopping rifampicin and the last sampling visit (PK3) was performed 4-6 weeks thereafter. The day prior to a PK visit, caregivers were reminded to record the evening dose time and to ensure that the child fasted for at least 1 hour prior to arrival at the clinic. Children were administered ART and TB drugs at the clinic and remained fasting for a further hour. Pharmacokinetic samples were drawn before the observed dose and after 1, 2, 4, 6, and 10 hours. The PK was postponed if the participant took an incomplete dose or vomited. Safety, adherence and virological outcomes were also assessed and have been previously reported. [152]

Plasma abacavir concentrations were determined with a validated liquid chromatography-tandem mass spectrometry (LC-MS/MS) assay developed in the Division of Clinical Pharmacology, University of Cape Town. Samples were processed with a protein precipitation extraction method using abacavir-d4 as the internal standard, followed by high-performance liquid chromatography with MS/MS detection using an AB Sciex API 3200 instrument. The calibration curves fit quadratic (weighted by 1/concentration) regressions over the range of 0.0243–6.21 µg/mL for abacavir. The accuracies for the abacavir assay were 104.5%, 100.6%, and 101.6% at the low, medium, and

high-quality control levels, respectively, during inter batch validation. The lower limit of quantification (LLOQ) was 0.0243 µg/mL.

3.3.3 Statistical analysis

Population pharmacokinetic model development

The concentration-time data was analysed using nonlinear mixed-effects modelling implemented in the software NONMEM version 7.4.3 [153] with ancillary software (PsN, Pirana and Xpose). [120] The first-order conditional estimation method with eta-epsilon interaction (FOCE-I) was used to estimate pharmacokinetic parameters. Model building was guided by ΔOFV; proportional to -2 log-likelihood, inspection of goodness-of-fit plots, VPC, biological plausibility, and clinical relevance. A decrease in ΔOFV of more than 3.84 between two nested models after the addition of one parameter was considered significant. Several structural models were evaluated, including one and two compartment disposition, first-order absorption and elimination with or without an absorption lag time or transit compartments. Between-subject (BSV), -occasion (BOV) and -visit variability (BVV) of random effects were tested on pharmacokinetics parameters and were assumed as lognormally distributed. BVV and BSV were tested for disposition parameters (clearance and volume parameters), while BOV was tested for absorption parameters. Each dose was treated as a separate occasion, while consecutive evening and morning doses were grouped within the same visit. To account for the uncertainty regarding the accuracy of the reported timing of dosing on the evening preceding the pharmacokinetic visit, we tested the estimation of an additional delay in absorption for the evening dose. A combined proportional and additive error model was used to describe the residual unexplained variability. The additive error for all samples was bound to be at least 20% of the lower limit of quantification (LLOQ).

BLQ concentrations were handled with the M6 method as described by Beal. [122] Briefly, the first BLQ value after the peak (or the last in a series of BLQ values before the peak) was imputed to half the lower limit of quantification (LLOQ/2) and included in the fit with their additive error inflated by LLOQ/2, while any subsequent BLQ values (or preceding if before the peak) were excluded from the fit and only considered for visual predictive check diagnostics. Allometric scaling was included to account for the known effect of body size on pharmacokinetics with exponents fixed to 3/4 for clearance parameters and 1 for volumes of distribution. [154] TBW and FFM [155] were evaluated as alternative size descriptors on each of the disposition parameters. To account for maturation, a postmenstrual age guided function was used (Equation 1).

$$maturation = \frac{PMAGE^{\gamma}}{(PMAGE_{50}^{\gamma} + PMAGE^{\gamma})} \quad \text{(Equation 1).}$$

where PMAGE denotes postmenstrual age, $PMAGE_{50}$ is the value of PMAGE at which 50% of the maturation is complete, and γ is a parameter changing the shape of the relationship. Since no information on the actual gestational age of the children was available, the postmenstrual age was assumed to be the postnatal age plus 9 months. Other candidate covariates were screened based on inspection of parameter versus covariate plots and then tested in the model for inclusion and retained based on statistical significance (using 3.84 points drop as significant at p=0.05 for the inclusion of a single parameter) and physiological plausibility. The precision of the final parameter estimates was evaluated by sampling importance resampling method (SIR). [156]

3.3.4 Abacavir dosing simulations

Monte Carlo simulations using the final model were used to simulate paediatric abacavir exposures (AUC0-12) during the treatment with standard lopinavir/ritonavir-4:1 and LPV/r-4:4 in

children between 3 to 24.9 kg under South African weight band dosing. Simulations were performed using 15000 in-silico patients, 100 males and 100 females at each 1-month age interval from 0 to 17 years of age. The age-weight combinations were generated from a weight-for-age model developed based on values from children with TB and hence consistent with the population for whom the dosing guidelines are designed. [157] All in silico children were assumed born at term and dosed 12-hourly with abacavir. Additionally, a dataset with weights between 25 and 59.9 kg was used to simulate abacavir exposures of adolescents and adults. Once daily dose of 600 mg was used and dividing AUC_{0-24} by 2 to get AUC_{0-12}. All simulated exposures were compared to the recommended 12-hour adult median AUC of 6.02 mg·h/L as suggested by the European Medicines Agency

https://www.ema.europa.eu/en/medicines/human/EPAR/ziagen#product-information-section

Other adult AUC values from Yuen et al.,[158] Moyle et al.,[66] Mcdowell et al.,[138] and Weller et al.[159] were also used for comparison.

3.4 Results

Between January 2013 and November 2015, we enrolled 96 children into the main study. [109] However, not all children received abacavir and/or completed the study. Eighty-seven children were included in the abacavir analysis, with 86 PK profiles in the first PK visit, 74 in the second, and 71 in the third PK visit. A total of 1,344 measured drug concentrations were available for analysis, 18 samples were excluded from the analysis due to unclear dosage history or concentrations incoherent with the recoded dosing. The patient characteristics are shown in Table 1. The median age and weight (range) at enrolment were 19 (4-64) months and 8.7 (3.9-

14.9) kg respectively. Children younger than 12 months were well represented in this cohort with 11% (8/72) of the children still below 12 months at the third PK visit. The majority of patients at each PK visit were between 5 and 9.9 kg. At the first PK, 7 (8%) patients were in the 3- 4.9 kg weight group.

Abacavir pharmacokinetics was best described by a two-compartment disposition model (difference in objective function value, ΔOFV = -728 when compared to a one-compartment model, $P<10^{-6}$) with first-order elimination and transit compartments describing absorption (ΔOFV = -148, $P<10^{-6}$, when compared with simple first-order absorption). The model fitted the data well, as evident from the visual predictive checks (VPC) shown in Figure 1 All parameter estimates are shown in Table 2.

The inclusion of allometric scaling with total body weight (TBW) improved the model fit (ΔOFV = -38) and using fat-free mass (FFM) instead did not provide any further meaningful improvements. After adjusting for body size, we identified a maturation effect on abacavir clearance (ΔOFV = -14, $P<10^{-3}$), which was predicted to reach to full maturation by around 2 years of age and half of its mature value at around 2 months, as shown in Figure 4.

The typical abacavir clearance of a 9.4-kg child co-treated with LPV/r at standard 4:1 dose was estimated at 9.67 L/h. Importantly, a 36% decrease in bioavailability (and thus overall exposure) of abacavir was noted during co-administration of rifampicin and LPV/r-4:4 (ΔOFV = -44, $P<10^{-6}$). Since co-administration of rifampicin coincides with ritonavir super-boosting in our dataset, we tried to use ritonavir exposure (we calculated individual AUC values with non-compartmental analysis techniques) as an alternative predictor to explain the decrease in abacavir bioavailability (results not shown). Ritonavir exposure was very variable and, although the concentration during

super-boosting dose were indeed larger, there was a wide overlap with the exposure while on standard LPV/r 4:1. However, not only did using ritonavir exposure not improve the model fit compared to using the categorical covariate rifampicin co-administration, but the model unintuitively identified a weak positive correlation between the exposure of abacavir and ritonavir, which is the contrary of what would be expected if larger increasing RTV AUC is responsible for the lower bioavailability of abacavir.

Additionally, we found that the observed morning pre-dose concentrations (C_0) were larger than expected if assuming a perfect 12-hour steady-state scenario. In fact, observed morning pre-dose concentrations were larger than the observed concentration at 10 hours (C_{10}), as shown in Table 3. To account for this, an absorption delay parameter was included in the model for the unobserved doses given to the children on the evening before the PK visit. This improved the model fit significantly (ΔOFV = -127, $P<10^{-6}$) and adjusted for this difference.

Dosing simulations

The simulated paediatric exposures, which were compared to the target recommended 12-hour adult median exposure (AUC_{0-12}) of 6.02 mg·h/L, are shown in Figure 3. When co-treated with LPV/r-4:4, the simulated exposures in most children's weight groups were in line with the adult target, with the exception of the 3-4.9 kg weight group, where the exposures were significantly higher than other weight groups. When treated with standard doses of LPV/r-4:1, all paediatric weight groups had higher exposures than the recommended adult median exposure, with the same trend of even higher exposure in the 3-4.9 kg weight group.

The model was also used to simulate the predicted concentrations in adolescents and adults by using weights 25 to 59.9 kg and the currently recommended 600-mg once-daily adult dose. AUC_{0-24} was divided by 2 to obtain a value comparable with AUC_{0-12} used in children. The model predicted that adults 40-59.9 kg achieve exposure in line with most of the children 6-24 kg, but due to the fact that all adults receive the same dose, the subjects with weights 25-39.9 kg had substantially higher exposures.

Summarising, all children achieved values in line or larger than the recommended target. When comparing the children and the extrapolated adult exposures from our model, we can then conclude that most children 5-24.9 kg achieve exposure in line with adults 40-59.9 kg, while both young children 3-4.9 kg and young adults 25-39.9 kg achieve higher concentrations.

3.5 Discussion

We developed a population PK model of abacavir in children characterising the effects of weight and age. Our model identified a significant 36% reduction in abacavir exposure when the children were co-treated with rifampicin and LPV/r-4:4. In the parent study, we have shown that super-boosting from LPV/r-4:1 to LPV/r-4:4 achieves similar lopinavir concentrations, [152] so it is unclear whether the decreased exposure was due to extra ritonavir added to boost LPV/r-4:4 or rifampicin co-treatment. Both ritonavir and rifampicin induce UGT and p-glycoprotein. However, when ritonavir exposure was tested as alternative predictor in the model to explain the lower bioavailability of abacavir, it could not explain the observed effect. This suggests that the effect is probably related to rifampicin, but further investigation is needed to confirm this.

Co-administration of abacavir and LPV/r 4:1 does not affect lopinavir plasma concentrations but is thought to reduce abacavir levels by approximately 30%, presumably through increased glucuronidation, as in other protease inhibitors. [160] In adults, the clinical significance of this drug-drug interaction is not known. However, in children there was some early indication that stavudine and LPV/r-4:1 based regimens may outperform abacavir LPV/r-4:1 based regimens and that this could be due to this drug-drug interaction, but subsequent data did not confirm this finding. [105] In this cohort of children, co-treatment with abacavir and LPV/r-4:1 did not lead to unexpected abacavir levels as shown in Figure 2, but we did not compare the level achieved to children on non-nucleoside reverse transcriptase inhibitors or integrase inhibitors.

The simulations show, that although children co-treated with LPV/r-4:4 and rifampicin had reduced abacavir exposure, $AUC_{0\text{-}12}$ is comparable to the adult target, as well as exposures seen in other studies conducted in children. [128,161–163] Young infants are predicted to achieve even higher exposures, due to immature metabolic pathways. Although abacavir is now the first-line treatment for most young children in low-resource settings, it is currently not licensed in children below the age of 3 months. In South Africa it is used in children over 1 month of age despite lack of data. Our abacavir PK model showed that a dose of 8 mg/kg twice daily is adequate for children co-treated with LPV/r-4:4 and rifampicin from 3 kg to maintain clinically relevant exposure and is higher in children co-treated with abacavir and LPV/r-4:1. The results in the 3-4.9 kg weight band should be interpreted with caution. Only 7 study subjects were in this weight band, and their AUC was very variable, with some very low observed values. Besides the effect of maturation of clearance, other factors may introduce variability in drug concentrations in these small children, including difficulties with drug administration. Better characterization of pharmacokinetics in

children below 3 months is needed to determine a dose with more certainty and consequently allow incorporation into neonatal and infant treatment protocols. We had very few young children, so the characterisation of maturation has limited precision, see figure 4. Additionally, information on weight band approaches to dosing in the smallest and youngest infants is also lacking.

The observed abacavir C_0 were higher than the observed C_{10}. A diurnal effect with higher modelled morning trough lopinavir concentrations was also shown in this cohort. [152] Similarly, in a study by Van Heeswijk et al., LPV/r given in the evening or in the morning had the same AUC (thus not much difference in Clearance), but the profile was delayed, with C_{12} higher when the drug was given in the evening. [162] This phenomenon could be due to a delayed night dose timing, a delayed absorption due to coadministration with food, or diurnal variation. Co-administration of abacavir with food has no effect on abacavir overall exposure (AUC), but delays abacavir absorption. [164] Diurnal variation is a possible reason for nelfinavir, ritonavir, and nevirapine morning C_0 being higher than the evening C_{10}. [165–168] The effects of the diurnal variation could be due to a decreased blood pressure and a slower pulse rate during sleep, which reduces hepatic blood flow, thereby slowing the rate of drug absorption and reducing drug metabolism. [169] Since only a single pre-dose sample was available in our study, the data was not able to reliably discriminate between the possible different options outlined above to explain the larger pre-dose values, so we decided to use the delayed absorption, which both fit the data very well and was a plausible explanation.

Our analysis has several weaknesses. Although our model can predict drug levels in the lower weight bands based on the estimated maturation effect, we had no children younger than 3

months in this study. Therefore, drug concentration in infants require confirmation in further studies. Additionally, the antiviral effect of abacavir is due to its intracellular anabolite, carbovir triphosphate, not measured in this study. A linear association was previously described in adults, with the intracellular levels having a longer half live. While it is unknown whether this relationship holds in children, it suggests that using abacavir levels as a proxy is an acceptable and conservative approach. [170]

To conclude, the proposed model successfully characterised the PK of abacavir, including the effect of body weight and age**.** Abacavir exposure was decreased by concomitant administration of rifampicin and LPV/r-4:4, but the resulting exposures were still in line with adult values, thus seemingly not requiring a dose adjustment. Higher trough concentrations were observed in the mornings, suggesting slower absorption at night (possibly due to coadministration with food) or diurnal variation. PK data in neonates and infants younger than 3 months are needed to confirm with more certainty the dose in these.

Declaration of interests

HR has received funding from the Drugs for Neglected Diseases initiative (DND*i*) to do this study and is part of a US National Institutes of Health funded research unit. HM is funded by the Wellcome Trust (206379/Z/17/Z). HR, MFC, HM, TJ, and PD are supported by the National Research Foundation (NRF) of South Africa. HR, TJ and PD are supported by the NRF and Swedish Foundation for International Cooperation in Research and Higher Education collaboration. All other authors declare no competing interests.

Data sharing

The data underlying the results of this study are available upon request because it contains potentially sensitive information. Interested researchers may contact the Drugs for Neglected Diseases Initiative (DNDi), commissioner of this study, for data access requests via email at CTdata@dndi.org. Researchers may also request data by completing the form available at www.dndi.org. In this, they confirm that they will share data and results with DNDi and will publish any results open access.

Acknowledgments

This study was sponsored by the Drugs for Neglected Diseases initiative (DNDi), and DND*i* is developing easier to use combination antiretroviral drugs for infants and children. DND*i* thanks the Agence Française de Développement, UBS Optimus Foundation, and Unitaid for funding this study. We thank Jennifer Norman for oversight of the laboratory procedure; support staff at DND*i*, PHPT and the study sites; the members of the Data Safety and Monitoring Board. Mahmoud Abdelwahab for assisting with the charts. Drugs were provided by the South African Department of Health. Lastly, we thank the study participants and their parents.

Role of the funding source

This study was sponsored by the Drugs for Neglected Diseases *initiative* (DND*i*). DND*i* developed the idea, co-ordinated the protocol development, supported laboratory analysis, data management, and analysis. DND*i* obtained funding for this study from the Agence Française de Développement (AFD), France; UBS Optimus Foundation, Switzerland; and Unitaid, Switzerland. These funders had no role in study design, data collection, data analysis, data interpretation, or

writing of this paper. For its overall mission, DND*i* also receives financial support from Médecins sans Frontières (MSF) International.

Table 3.1 Clinical characteristics of patients at each pharmacokinetic visit.

	PK visit 1	PK visit 2	PK visit 3
Number of patients in analysis/males (%)	86/37 (43)	74/29 (36)	71/27 (39)
Number of samples in analysis/ BLQ (%)	504/84 (17)	436/59 (13)	404/45 (11)
Number of samples per patients [b]	6 (4-6)	6 (4-6)	6 (4-6)
Age (months)	19 (4-64)	23 (8-68)	26 (10-70)
Age <1y (%)	25 (30)	13 (17)	6 (8)
Weight (kg)	8.7 (3.9-14.9)	9.6 (5.7-15.9)	10.2 (6.8-15.9)
3–4.9 kg band	7 (8)	NIL	NIL
5–9.9 kg band	51 (59)	40 (54)	35 (50)
10–13.9 kg band	24 (28)	26 (35)	26 (36)
14-19.9 kg band	4 (5)	8 (11)	10 (14)
Weight-for-age Z-score [a]	-2.43 (-5.19-1.34)	-1.93 (-4.84-1.55)	-1.50 (-4.86-1.51)
Weight-for-height Z-score [a]	-2.02 (-4.14-2.25)	-1.80 (-3.68-4.28)	-1.12 (-3.74-4.31)
Abacavir dose (mg/kg) BID	9.52 (7.84-12.8)	9.72 (7.62-16.3)	9.60 (7.79-13.2)
Rifampicin dose (mg/kg) OD	14.6 (10.2-15.0)	11.9 (11·6-13·6)	NIL
Lopinavir dose (mg/kg) BID	14.5 (11.5-23.1)	13.8 (11.0-21.1)	13.5 (11.4-18.5)
Ritonavir total dose (mg/kg) BID	15.1 (11.7-24.2)	14.2 (11.0-22.1)	3.3 (2.86-4.62)

median (IQR), n (%), OD = Once a day, BID = Twice a day

[a] Z-scores calculated according to WHO growth chart

[b] median (range)

Table 3.2 Final Parameter estimates for abacavir population pharmacokinetic model.

	Typical value		Variability	
Model Parameter	**Value**	**95% CI**	**% CV**	**95% CI**
Clearance (L/h) [a]	9.67	8.27-10.6	14.4 (BSV) 18.4 (BVV)	10.9-18.5 14.4-21.4
Central volume of distribution (L) [a]	8.76	6.99-9.94		
Absorption rate constant, ka (1/h)	2.22	1.82-2.80	55.5 (BOV)	47.0-72.0
Bioavailability	1 FIXED		44.8 (BOV)	32.9-45.9
Peripheral volume of distribution (L) [a]	3.32	2.82-3.98	29.0 (BSV)	19.2-33.6
Inter-compartmental clearance (L/h) [a]	1.35	1.09-1.67	13.5 (BSV)	12.4-19.9
y [b]	4.35	3.23-5.50		
PMAGE50 [b] (months from conception)	10.7	10.5-11.0		
Absorption mean transit time (min) [c]	3.60	2.64-6.54	175 (BOV)	141-205
Number of transit compartments	1.03	0.901-1.20		
Proportional error (%)	23.0	21.2-25.0		
Additive error (µg/L)	0.310	0.0661-0.400		
LPV/r-4:4 + rifampicin effect on bioavailability (%)	-36.0	-38.7— -32.9		
Delay in absorption for night dose (h)	2.62	2.23-2.90	9.90 (BVV)	9.52-15.4

Between-subject (BSV), -visit (BVV), and -occasion (BOV) variabilities were assumed as lognormally distributed and are reported as %CV.

[a] All clearances and volumes of distribution were allometrically scaled and the typical values reported here refer to a child weighing 9.4 kg, the median value in the dataset.

[b] $PMAGE_{50}$ is the postmenstrual age at which 50% maturation is reached, while y is the shape factor in the sigmoidal maturation function

[c] The absorption mean transit time is the average time the drug spends travelling from the first transit compartment to the absorption compartment**.**

The 95% confidence interval of parameter estimates was obtained with sampling importance resampling (SIR; n = 1,000) of the final model.

Table 3.3 Abacavir exposures and pre-dose concentrations in each PK visit.

	PK visit 1	PK visit 2	PK visit 3
Model-predicted $AUC_{0\text{-}12}$ (mg·h/L)	6.36 (1.28-14.2)	7.01 (1.46-16.5)	10.2 (2.08-25.6)
Model-predicted C_{max} (mg/L)	3.32 (0.741-6.29)	3.34 (1.44-7.05)	4.93 (1.75-11.1)
Observed C_{max} (mg/L)	2.52 (0.462-6.07)	2.95 (0.274-8.12)	4.87 (0.551 11.5)
Observed C_0 (mg/L) [%BLQ] [a]	0.0282 (BLQ-0.181) [44.6]	0.0433 (BLQ-0.480) [35.6]	0.0444 (BLQ-0.641) [23.8]
Observed C_{10} (mg/L) [%BLQ] [a]	BLQ (BLQ-0.162) [56.1]	0.026 (BLQ-0.195) [41.6]	0.0308 (BLQ-0.195) [40.3]

The data is reported as median (IQR).

[a] In square brackets, the percentage of observed values below the limit of quantification

Table 3.4 Antiretroviral drug dosing for children weighing ≥3 kg to <16 kg

Weight (kg)	Abacavir (mg) Twice daily	Lopinavir/ritonavir (mg) Twice daily	Ritonavir *(mg) Twice daily	Rifampicin (mg) Once a day
3-3.9	40	80/20	64	45
4-4.9	40	80/20	64	60
5-5.9	60	120/30	96	60
6-6.9	60	120/30	96	90
7-7.9	80	120/30	96	90
8-8.9	80	120/30	96	120
9-9.9	80	120/30	96	120
10-10.9	120	160/40	120	120
11-11.9	120	160/40	120	120
12-12.9	120	160/40	120	180
13-13.9	120	160/40	120	180
14-14.9	160	200/50	160	180
15-15.9	160	200/50	160	210

*Additional ritonavir used for super-boosting during rifampicin co-treatment and until 2 weeks after rifampicin was stopped.

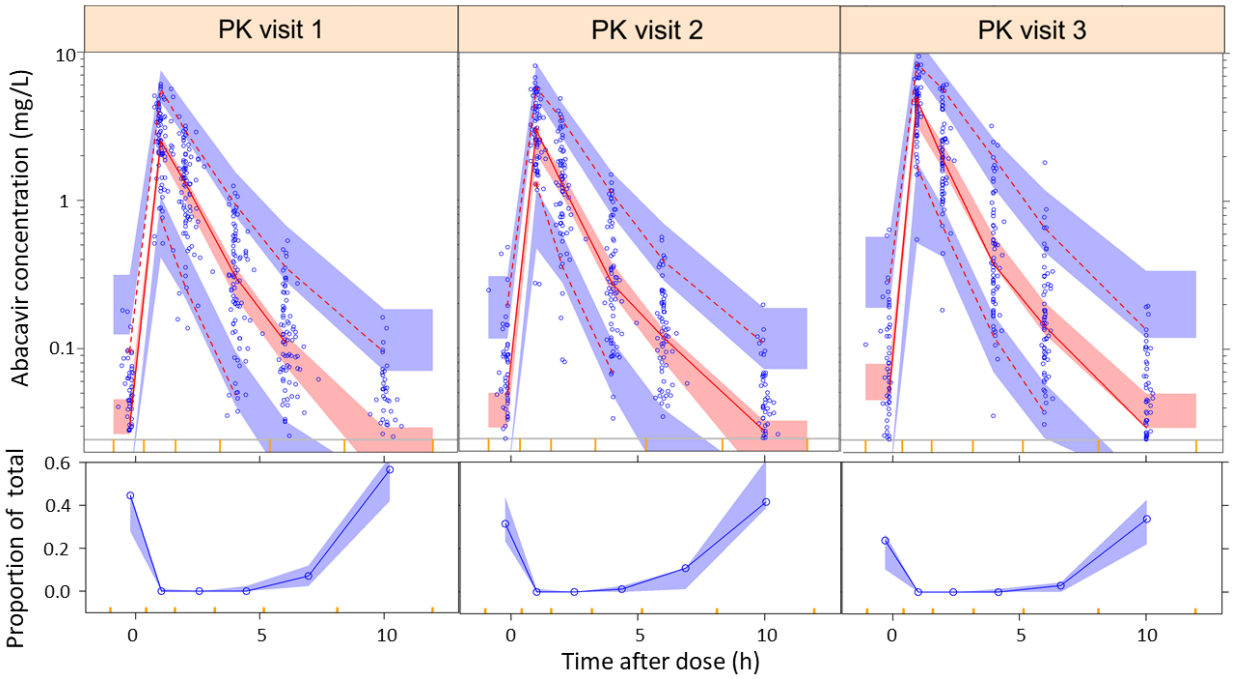

Figure 3.1 Visual Predictive Check of abacavir concentration versus time after dose, stratified by PK visit. PK visit 1 is the intensive phase of anti-tuberculosis treatment with LPV/r-4:4, PK visit 2 is the continuation phase of anti-tuberculosis treatment with LPV/r-4:4, and PK visit 3 represents one month after anti-tuberculosis treatment completion on LPV/r-4:1. The solid and dashed lines represent the 50th , 5th, and 95th percentiles of the observed data, while the shaded areas represent the model-predicted 95% confidence intervals for the same percentiles. The dots are the observed concentrations. The yellow ticks on the x-axis are bin boundaries. The dots at the bottom of the VPC are BLQ values. The lower panels refer to the proportion of LLOQ values vs. time after dose: the solid blue line represents the observed proportion, while the blue shaded area is the 90% confidence interval for the same proportion, as predicted by the model.

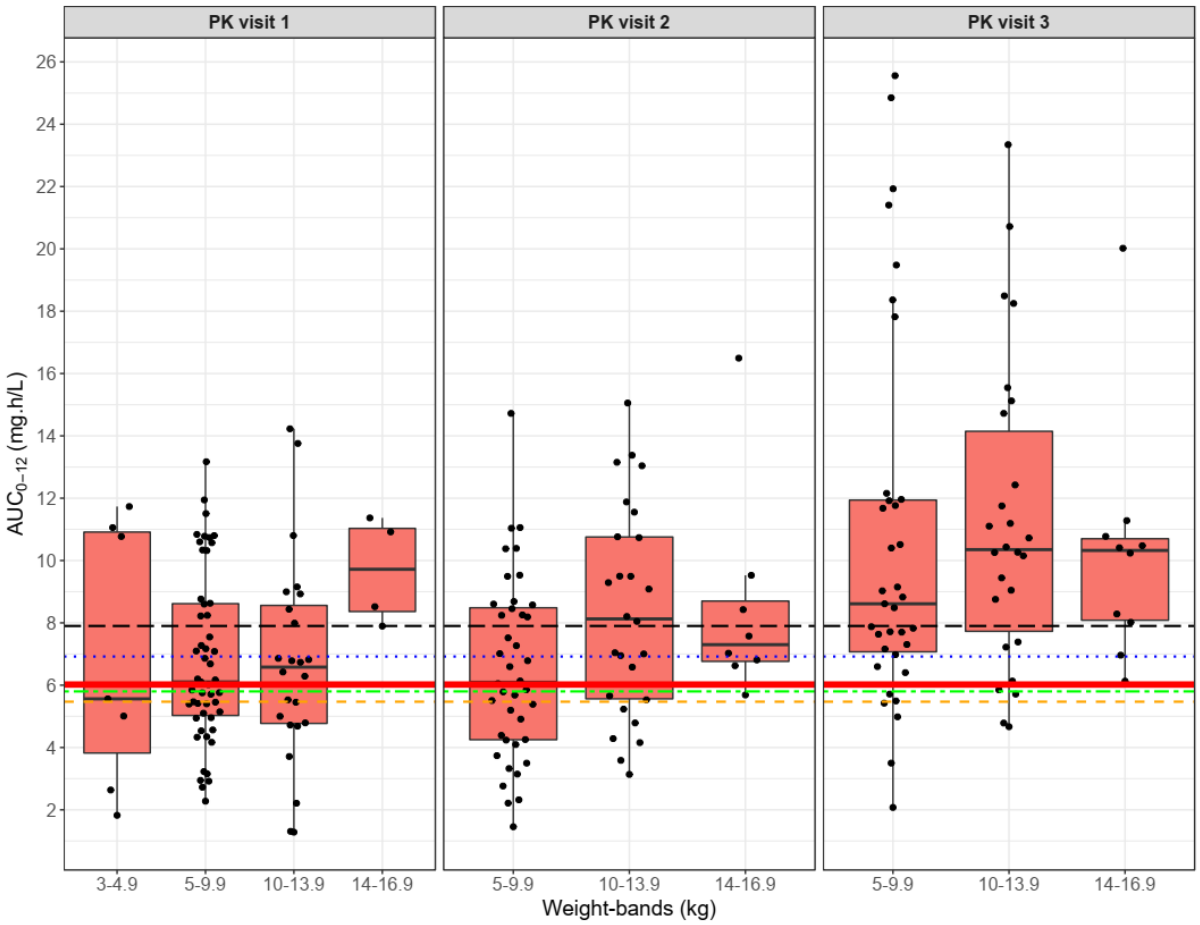

Figure 3.2 Summary of model-predicted abacavir AUC0-12 versus weight-bands in each pharmacokinetic visit. The box indicates the inter-quartile range, while the whiskers denote the 2.5th and the 97.5th percentiles. Each dot represents an individual AUC. PK visit 1 is the intensive phase of anti-tuberculosis treatment with LPV/r-4:4, PK visit 2 is the continuation phase of anti-tuberculosis treatment with LPV/r-4:4 and PK visit 3 represents one month after anti-tuberculosis treatment completion on LPV/r-4:1. The red horizontal solid line represents reference median AUC, while the broken lines represent adult AUC values from literature: Yuen et al. (dashed orange line), Moyle et al. (long dashed black line), Mcdowell et al. (dot-dash green line), Weller et al. (dotted blue line).

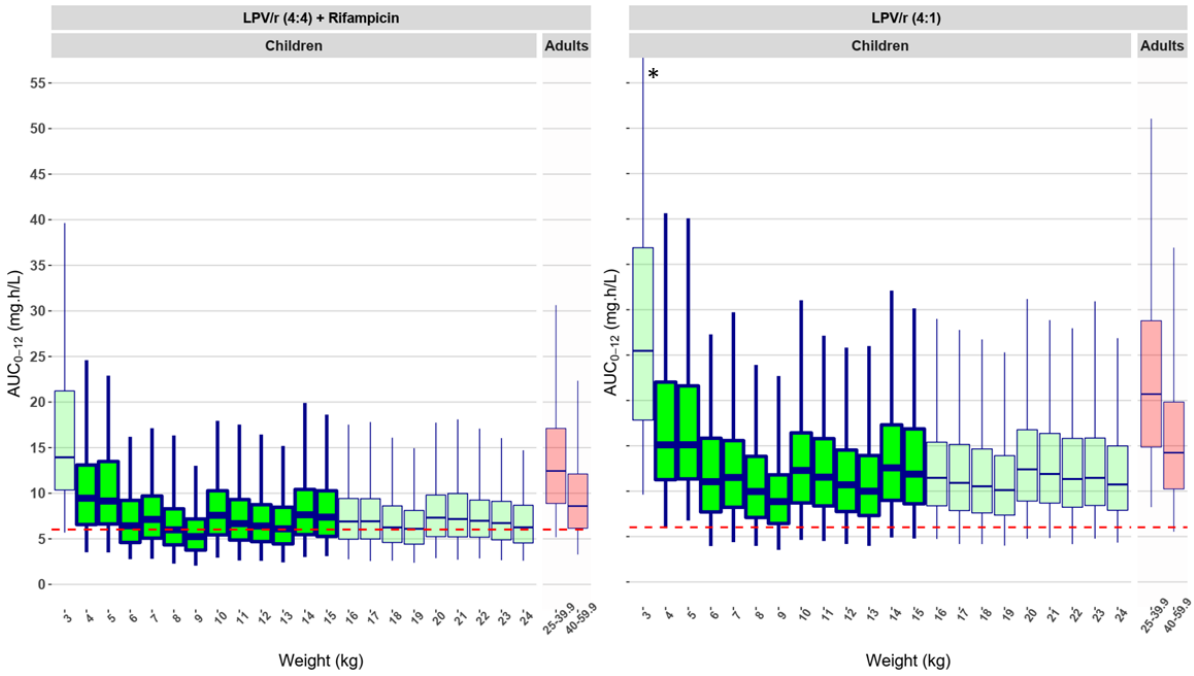

Figure 3.3 Simulated steady-state abacavir AUC0-12 versus body weight.The left panel shows exposures during co-treatment with super-boosted LPV/r 4:4 and rifampicin, while the right panel refers to co-treatment with un-boosted LPV/r-4:1. The box indicates inter-quartile range, while the whiskers denote the 2.5th and the 97.5th percentiles. The green boxplots show the exposures of children from 3 to 24.9 kg receiving the current paediatric dosing as shown in Table 4, while the red boxplots show the predicted exposure in adults 25-39.9 kg and 40-59.9 kg, both receiving a dose of 600 mg once daily. Adult AUC_{0-24} has been divided by 2 to obtain a value comparable to AUC_{0-12} to compare to children' s exposures. The red horizontal dashed line represents the recommended median adult exposure (6.02 mg·h/L). The children in this study population were mostly in the range from 4 to 16 kg; all the results outside this weight range (boxes with faint colour) were extrapolated using maturation and allometric scaling. *To improve the readability of the chart, the y-axis was cut; the 97.5th predicted AUC for children in the 3-kg weight-band reaches 67 mg·h/L.

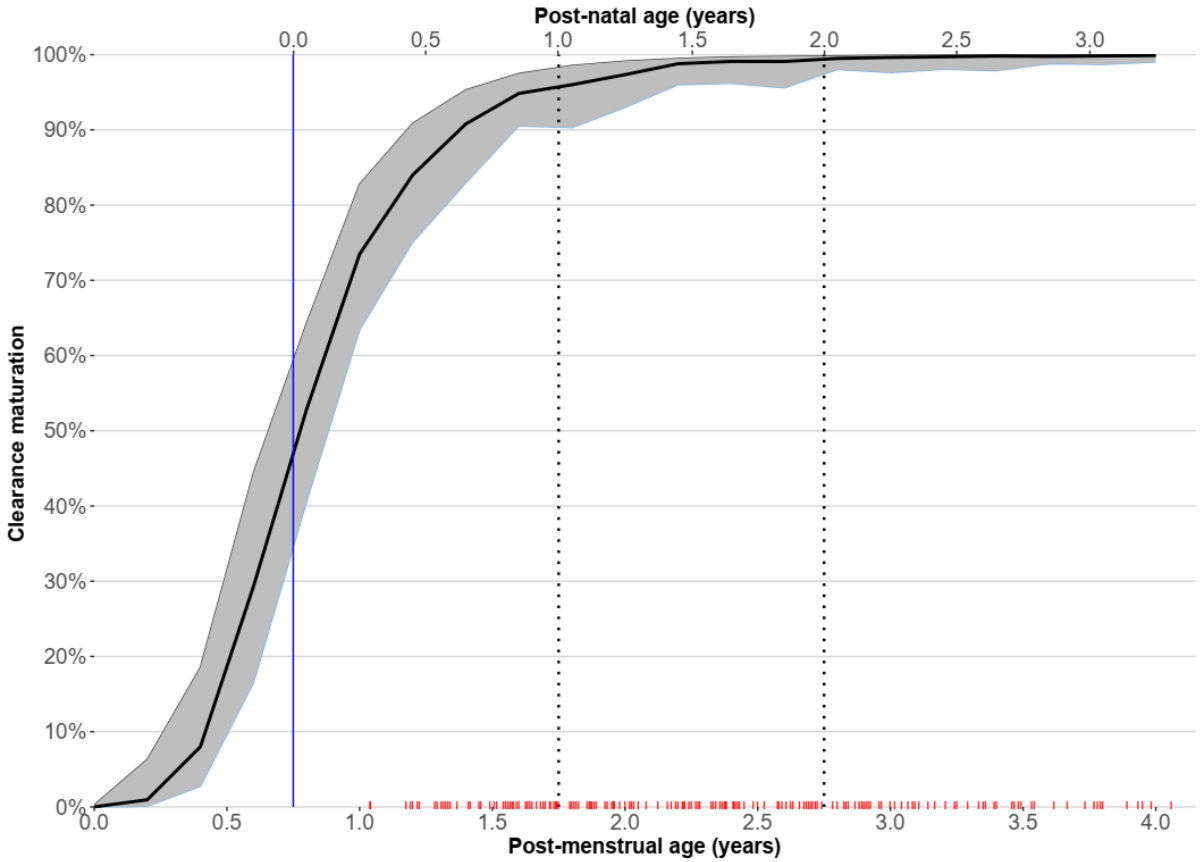

Figure 4: Maturation function of abacavir clearance vs. post-menstrual age (bottom x-axis), or post-natal age (top x-axis, assuming average gestation of 9 months), after adjusting for weight. The solid vertical blue represents birth, while the dashed vertical lines represent 1 year and 2 years post-natal age respectively. The red ticks on the lower x-axis represent the post-menstrual age values available in our data.

Chapter 4: Abacavir pharmacokinetics in African children living with HIV: a pooled analysis describing the effects of age, malnutrition and common concomitant medications.

4.1 Abstract

Abacavir is part of WHO-recommended regimens to treat HIV in children under 15 years of age. In a pooled analysis across four studies, we describe abacavir population pharmacokinetics to investigate the influence of age, concomitant medications, malnutrition and formulation.

A total of 230 HIV-infected African children were included, with median (range) age of 2.1 (0.1-12.8) years and weight of 9.8 (2.5-30.0) kg. Abacavir pharmacokinetics was best described by a two-compartment model with first-order elimination, and absorption described by transit compartments. Clearance was predicted around 50% of its mature value at birth, reaching 99% of full maturation by 3 years. The estimated typical clearance at steady state was at 10.7 L/h in a child weighing 9.8 kg co-treated with lopinavir/ritonavir, and was 12% higher in children receiving efavirenz. During co-administration of rifampicin based antituberculosis treatment and super-boosted lopinavir in a 1:1 ratio with ritonavir, abacavir exposure decreased by 29.4%**.** Malnourished children living with HIV had higher abacavir exposure initially, but this effect waned with nutritional rehabilitation. An additional 18.4% reduction in clearance after the first abacavir dose was described, suggesting induction of clearance with time on lopinavir/ritonavir-based therapy. Finally, absorption of the fixed dose combination tablet was 24% slower than the abacavir liquid formulation. In this pooled analysis we found that children on lopinavir/ritonavir

or efavirenz had similar abacavir exposures, while concomitant TB treatment and super-boosted lopinavir gave significantly reduced abacavir concentrations.

4.2 Introduction

In 2018, 84,000 children from eastern and southern Africa acquired HIV.[171] Approximately 940,000 of 1.7 million children under 15 years living with HIV, were receiving combination antiretroviral treatment (ART) in 2018. The World Health Organization (WHO) recommends two nucleoside reverse transcriptase inhibitors (NRTI's), abacavir and lamivudine, in first-line ART for children younger than 15 years. In children younger than 3 years, the third component is lopinavir co-formulated with ritonavir (LPV/r in a 4:1 ratio). In children older than 3 years of age, the non-nucleoside reverse transcriptase inhibitor (NNRTI) efavirenz which was previously recommended, has recently been replaced by dolutegravir.[55,135] HIV is often complicated by associated conditions such as malnutrition and co-infections. Despite its wide use in children, knowledge of abacavir pharmacokinetics is limited, with scant information to guide improved dosing in children of various age groups in the context of malnutrition, drug-drug interactions and other covariates.

Abacavir is indicated for children over 3 months of age at 8 mg/kg twice daily or 16 mg/kg once daily.[136,172] Abacavir is extensively metabolized by the liver, with less than 2% excreted unchanged in urine .[138] The two major pathways of abacavir metabolism involve alcohol dehydrogenase (ADH) and uridine diphosphate glucuronyltransferase (UGT) enzymes, producing inactive carboxylate and glucuronide metabolites.[138] Previous studies report that coadministration with food and formulation has no effect on abacavir exposure.[59,173] However, abacavir solution has been associated with an 11% higher peak serum concentration (C_{max}) than the tablet formulation.[164] Its binding to plasma proteins is about 50%.[59]

Many physiological systems are not functioning optimally in children with malnutrition. Total body water is increased, plasma albumin is decreased, Phase I and II metabolic reactions are considerably reduced as the severity of malnutrition increases.[29–31] These physiological alterations may either directly or indirectly influence the pharmacokinetics of abacavir. [174]

Drug-drug interactions among antiretrovirals and anti-tuberculosis drugs are common. When adults on abacavir are co-administered LPV/r, abacavir exposure decreases by approximately 30%.[66] In patients co-treated for TB with a rifampicin-based regimen, lopinavir would decrease by up to 90% with the standard LPV/r 4:1 dosing, so additional ritonavir is administered to achieve a 4:4 ratio with lopinavir (super-boosted lopinavir) to counteract the interaction. We previously showed that abacavir exposure is reduced by 36% when children were co-treated with rifampicin and super-boosted lopinavir.[175] Cohort studies in children raised concern that some abacavir-containing regimens may be less effective than regimens with a different nucleoside reverse transcriptase inhibitor backbone.[176,177] Drug-drug interactions with companion NNRTIs or protease inhibitors (PIs) resulting in reduced abacavir exposures could potentially contribute to such findings.

The purpose of this pharmacokinetic meta-analysis was therefore to pool several available abacavir clinical datasets to take advantage of the increased sample size and perform a more robust analysis to investigate the consequence of differences in body size, age, concomitant TB co-medications, malnutrition, and drug formulation on abacavir pharmacokinetics in children

4.3 Methods

4.3.1 Clinical studies and data

This pooled analysis used data from ARROW (Uganda and Zimbabwe),[106] CHAPAS-3 (Uganda and Zambia),[105] DNDi (South Africa),[152] and MATCH (South Africa).[110] Briefly, the objectives in regards to PK of the three individual studies were: in ARROW, to compare the pharmacokinetics of once daily *vs*. twice daily dosing of abacavir and lamivudine when given together with nevirapine or efavirenz; in CHAPAS-3, to compare abacavir, stavudine, or zidovudine as dual- or triple fixed-dose-combination paediatric tablets with lamivudine and nevirapine or efavirenz; in DNDI, to test whether adding extra ritonavir to co-formulated lopinavir/ritonavir (4:1) would overcome the effect of rifampicin on lopinavir exposures; and in MATCH, to describe the pharmacokinetics of antiretrovirals in paediatric patients with severe acute malnutrition as defined by the WHO. In all the studies, abacavir was administered orally and the sample profiles were intensively-sampled on separate visits, the detailed distribution of patients and their characteristics across study visits are provided in Table 4. Of the 230 children available for analysis, in 227 children, pharmacokinetic sampling was performed during twice daily dosing. Forty-one of these children also underwent pharmacokinetic evaluation while receiving once daily doses, while 3 children received daily doses only. One hundred and fifty-four children were on concomitant lopinavir/ritonavir and 76 were on efavirenz. Rifampicin-containing anti-TB treatment was administered to 104 children, of these, 101 were on super-boosted lopinavir/ritonavir (4:4) and 3 on efavirenz. Malnourished children, characterized in this analysis as having weight-for-age and height-for-age Z-score less than -2.0 were 115. The majority of children in our analysis received abacavir with LPV/r (4:1) and therefore were the reference group in the model.

4.3.2 Analytical methods

The analytical methods have previously been described in depth in the original published articles for each analysis. Plasma abacavir concentrations from DNDI, CHAPAS and MATCH studies were determined with a validated liquid chromatography-tandem mass spectrometry (LC-MS/MS) assay developed in the Division of Clinical Pharmacology, University of Cape Town. The lower limit of quantification (LLOQ) was 0.0243 µg/mL for DNDI, and .0238 µg/mL for CHAPAS and MATCH. The Plasma concentrations of abacavir from the ARROW study was determined using validated mass spectrometry and HPLC by GlaxoSmithKline (Research Triangle Park, NC, USA). The lower limit of quantification for abacavir was 0.0243 µg/mL.

4.3.3 Population pharmacokinetic analysis

Data from each study were explored separately and added one by one starting from those with more intensive data, as suggested in Svensson et al..[178] After the inclusion of each dataset, the model fit was reassessed, and modified if necessary.

The population pharmacokinetics of abacavir was described using nonlinear mixed-effects modelling (NONMEM 7.4.4) with auxiliary software (PsN, Pirana and Xpose) which were used for automation and diagnostics during the model-building process.[120] The first-order conditional estimation with eta-epsilon interaction (FOCE-I) was used to estimate pharmacokinetic parameters.

Single- and multi-compartment models with first-order elimination and absorption (with or without an absorption lag time or transit compartments) were evaluated. Between-subject (BSV), between-visit (BVV), and between-occasion variability (BOV) of random effects were tested on pharmacokinetics parameters and were assumed as lognormally distributed. Each dose was

treated as a separate occasion, while consecutive evening and morning doses were grouped within the same visit. BVV and BSV were tested on clearance and volume of distribution, while BOV was tested on absorption parameters. [179]

The additive error for all samples was set to be at least 20% of the lower limit of quantification (LLOQ) of the assay, study specific LLOQ can be found in table 1. BLQ concentrations were handled with the M6 method as described by Beal.[122] Briefly, the first BLQ value after the peak (or the last in a series of BLQ values before the peak) was imputed to half the lower limit of quantification (LLOQ/2) and included in the fit with their additive error inflated by LLOQ/2, while any subsequent BLQ values (or preceding if before the peak) were excluded from the fit and only considered for visual predictive check diagnostics.

Model building was guided by the drop in the objective function value (ΔOFV; proportional to -2 log-likelihood), inspection of goodness-of-fit plots, visual predictive check (VPC), biological plausibility, and clinical relevance. A decrease in OFV of more than 3.84 between two nested models after the addition of one parameter was considered significant at $P<0.05$.

4.3.4 Investigating factors that influence abacavir pharmacokinetics

Allometric scaling by total body weight was introduced on all clearance and volume parameters to account for the known effect of body size on pharmacokinetics with exponents fixed to 3/4 for elimination and intercompartmental clearance and 1 for volumes of distribution.[177,180,181] Total body weight (TBW) and fat free mass (FFM) [182] were evaluated as alternative size descriptors on both disposition parameters. To account for maturation, a sigmoidal function of postmenstrual age was used (Equation 1):

$$maturation = \frac{PMAGE^{\gamma}}{(PMAGE_{50}^{\gamma}+PMAGE^{\gamma})}, \qquad \text{Equation 1}$$

where PMAGE denotes postmenstrual age, $PMAGE_{50}$ is the value of PMAGE at which 50% of the maturation is complete, and γ is a parameter determining the shape of the relationship. Since no information on the actual gestational age of the children was available, it was assumed to be 9 months.

After inclusion of weight and age in the model, additional covariates were screened based on inspection of parameter versus covariate plots and physiological plausibility and retained based on statistical significance at $P<0.01$. To describe the time-changing effect of malnutrition that resolves with days on nutritional supplementation, an exponential function was used (Equation 2).

$$Malnutrition = MAL_0 \cdot e^{-\frac{\lambda_{MAL} \cdot time}{logn\,(2)}} \qquad \text{Equation 2}$$

Where MAL_0 is the initial value of the malnutrition effect at day 0 (before start of supplementation), λ_{MAL} is the half-life of the process (in days) and time is the duration of the nutritional supplementation treatment (in days). The precision of the final parameter estimates was evaluated by sampling importance resampling method (SIR). [156]

4.3.5 Simulations

Using the parameter estimates from the final model, Monte Carlo simulations were performed to generate steady-state abacavir $AUC_{0\text{-}12}$ during co-treatment with standard LPV/r (4:1), efavirenz, or rifampicin plus super-boosted lopinavir. A 12-hourly dosing and a target dose of 8mg/kg based on the South African weight-band guidelines (weights from 3 – 35.9 kg) were used to simulate exposure in 57,014 *in silico* patients weighing 3 to 35.9 kg. The age-weight combinations were generated from a weight-for-age model developed based on values from children with TB and hence consistent with the population for whom the dosing guidelines are

designed.[157] All simulated exposures were compared to the recommended 12-hour adult median AUC of 6.02 mg·h/L as suggested by the European Medicines Agency.[183]

4.4 Results

4.4.1 Data summary

Four studies contributing 2760 plasma concentrations from 230 children living with HIV were used in this pooled analysis. Of these, 285 plasma concentrations (10.3%) were below the lower limit of quantification (LLOQ) of which most were drawn pre-dose. The median (range) age and weight were 2.1 (0.1-12.8) years and 9.8 (2.5-30.0) kg, respectively. The detailed patient and study characteristics and their distributions in each study are in Table 1.

4.4.2 Population Pharmacokinetics

The population pharmacokinetics of abacavir was best described by a two-compartment disposition model (difference in objective function value, ΔOFV = -671 when compared to a one-compartment model, $P<10^{-6}$) with first-order elimination and transit compartments describing absorption (ΔOFV = -122, $P<10^{-6}$, when compared with simple first-order absorption). To adjust for differences in body size, allometric scaling of TBW was included for all disposition parameters and improved the model fit (ΔOFV = -268). Using fat-free mass (FFM) instead of TBW did not provide any significant improvements. After adjusting for body size, the effect of age on clearance was captured using a maturation function (ΔOFV = -15, $P<10^{-3}$). Clearance was predicted to be at 54% of its mature value at birth and at 99% of full maturation by 3 years, the maturation function of abacavir clearance with confidence intervals is shown in Figure 3. The apparent clearance

(CL/F) for a typical 9.8 kg child co-treated with standard LPV/r 4:1 at steady state was estimated at 10.7 L/h.

Clearance of the first abacavir dose was 18.4% lower (ΔOFV = -11.5, $P<10^{-4}$) than clearance for a typical child on standard LPV/r 4:1 for over 7 days. Co-administration with anti-TB treatment plus super-boosted lopinavir decreased abacavir bioavailability by 29.4% (ΔOFV = -48, $P<10^{-6}$). An increase in clearance of 12% was seen in children on efavirenz (ΔOFV = -10.9, $P<10^{-4}$). Malnourished children had higher and more variable exposures compared to a non-malnourished typical child. The model captured this additional exposure by estimating that malnourished children have 115% higher bioavailability and 64% decreased clearance at the start of nutritional rehabilitation, but their exposure gradually normalized to that of the general population with a plasma half-life of 12.2 days as their nutrition recovered (ΔOFV = -70.3, $P<10^{-6}$). Additionally, BOV on bioavailability (ΔOFV = -67, $P<10^{-6}$) and BOV on clearance (ΔOFV = -74, $P<10^{-6}$) was 1.39-fold and 3.35-fold larger for malnourished children compared to a typical child, respectively.

Abacavir plus lamivudine fixed-dose combination tablets had a 24.9% slower absorption than abacavir liquid formulation (ΔOFV = -19, $P<10^{-5}$). For the children on twice-daily dosing, the morning observed pre-dose concentrations were often higher than the corresponding observed concentration at 8-10 hours after the morning dose administration. This was explained by an average delay of 2.52 hours in absorption for the evening dose, which led to significant model fit improvement (ΔOFV = -194, $P<10^{-6}$). The final parameter estimates with uncertainty are presented in Table 2 and a VPC stratified by study and visit is shown in Figure 1.

4.4.3 Simulations

Simulated abacavir AUC_{0-12} based on the South African weight-band dosing recommendations were compared to the adult recommended AUC_{0-12} of 6.02 mg·h/L, shown in Figure 2. With co-administration of LPV/r (4:1) or efavirenz, abacavir AUC_{0-12} was higher than the recommended adult AUC_{0-12}, while the values were within the adult AUC_{0-12} range when abacavir was co-administered with super-boosted lopinavir and rifampicin-based TB treatment. Higher exposures were observed in the 3.0 to 4.9 kg weight group, likely due to incomplete maturation of clearance. Similarly, the heavier children in the 25 to 35.9 kg group receiving the adult dosage also achieved higher exposures. In contrast, low exposures were seen in 7 to10 kg weight group.

4.5 Discussion

A pooled individual participant data population analysis was performed to describe abacavir pharmacokinetics in children and characterized the effect of body size, organ maturation, malnutrition and concomitant medications. The pooling of data from different studies allowed us to re-evaluate and characterize drug-drug interactions and other covariate effects on abacavir exposure more robustly and reliably than in any single study. Allometric scaling with total body weight explained the effect of body size on the disposition parameters, while a sigmoidal function of age captured the effect of developmental change and organ maturation in the younger children. The maturation estimates were in line with previous reports,[176,177] with this effect reaching near maturity before two years of age, as shown in Figure 3.

Co-administration of abacavir with LPV/r (4:1) in the absence of rifampicin was shown by Waters et al. to reduce abacavir exposure by 30% in adults.[66] Decreased abacavir exposures was also

seen in studies where abacavir was co-administered with protease inhibitors, as shown in Table 3. In our analysis, we observed low abacavir clearance in children on the first day of treatment, resulting in 22% increased exposures. This could be explained by the absence of ART-driven induction, which is generally attained within 1 to 4 weeks.[184,185] Even though most children were severely malnourished during the first day of treatment, the size of this effect is lower than that of Waters et al., but they compared abacavir as a single drug against abacavir co-administered with LPV/r (4:1) at steady-state, while in our analysis, abacavir and LPV/r (4:1) were administered together from the first day of treatment. The induction effect of efavirenz was 12% stronger than LPV/r (4:1) at steady state, consistent with previous data that efavirenz is a known inducer of UGT.[186]

A 29.4 % decrease in abacavir exposure was identified in children treated with rifampicin-based anti-TB treatment and super-boosted lopinavir. Ritonavir and rifampicin both upregulate the pregnane X receptor (PXR), which induces several Phase II enzymes including UGT, a primary enzyme involved in abacavir metabolism.[143,145,146] It is uncertain to which extent rifampicin, ritonavir, and/or lopinavir contributed to the effect. We previously reported that the lopinavir concentrations were similar during anti-TB treatment and super-boosting,[152] likely excluding a lopinavir contribution. Moreover, when we attempted to correlate the individual values of ritonavir exposure to the decrease in abacavir concentrations, the model fit was worse when ritonavir was used instead of the categorical effect encompassing anti-TB treatment and super-boosting. Therefore, the estimated decrease is mostly due to rifampicin. We expected a similar effect in children on efavirenz and rifampicin. However, this effect could not be confirmed, as only 3 children received this treatment combination. Importantly, we expect higher abacavir

exposure when co-administered with drugs such as dolutegravir that has lower potential for drug interactions.

Malnourished children experienced higher abacavir exposure, which was best described in the model with an apparent increase in bioavailability and decrease in clearance. The reason for the higher exposure may be due to decreased functionality of metabolizing enzymes or altered protein levels. Indeed, total protein levels on the first day of treatment (65.0 [56.8–73] g/dL) were lower than after 14 days of treatment (77 [64–84] g/dL).[174] At the same time, malnutrition alters the functionalities of many body-systems, making it difficult to identify all factors impacting abacavir pharmacokinetics. It is worth mentioning that although malnutrition does affect plasma protein composition, its impact is very minimal compared to its combined effect with inflammation.[187–189] Subsequently, inflammation is also associated with decreased hepatic expression of drug metabolizing enzymes such CYP and UGT enzymes.[190,191] Introduction of ART is linked with reduction of inflammation and improvement of malnutrition. The effect of malnutrition on abacavir pharmacokinetics appears to recover faster than children's weight gain. This is evident in the MATCH study, where PK between visit 1 and 2 was different while there was a small improvement in WAZ, see table 4. This may explain the lack of association between malnutrition and PK in DNDi study of children co-treated with rifampicin where, although some patients were malnourished, the first study visit was at least 1 month after treatment initiation. Despite including all the above-mentioned covariates, high variability in bioavailability and clearance was still observed in the MATCH study compared to the other studies, possibly reflecting the variability in the severity of malnutrition within the cohort.

In our analysis, abacavir when formulated in fixed-dose combination tablets with lamivudine (and co-administered with efavirenz) had slower absorption than the liquid formulation, which was co-administered with LPV/r (4:1). This is consistent with prior reports that associated the liquid formulation with an 11% higher C_{max} than the tablet formulation, although the difference was deemed as clinically unimportant.[164] In all the studies in this analysis, food was given at least 2 hours after dose administration, making food an unlikely cause of the observed difference.

The observed abacavir pre-dose concentrations (mostly 12 hours after the previous evening's self-reported time of dose) were often higher than the concentrations observed at 8-12 hours after observed dose intake. This could possibly be due to the night dose being given later than documented, slower absorption due to coadministration with food, or diurnal variation.

In Table 3, we summarize published abacavir pharmacokinetic analyses, for comparison with our results. For each study, we included details on the study population and the dose received, the reported values of AUC and clearance. We also use allometry and the median value of body weight in each population to apply allometric scaling to clearance and allow for easier comparison of AUCs across studies. In general, AUC_{0-12} of abacavir during co-administration with efavirenz or lopinavir/ritonavir with or without rifampicin was comparable to the adult target, as well as exposures seen in other studies conducted in children, the exception being in the severely malnourished children whose exposures were variable and higher compared to their counterparts.

Our analysis suffers from limitations arising from data pooling from diverse studies. These include unequal distribution of covariates between studies, such as, first-dose abacavir concentrations only being available in the dataset of malnourished children, and use of liquid formulations were

used more frequently in younger children and with lopinavir/ritonavir. Also, although the abacavir assay was performed by different laboratories, both laboratories participate in international quality assurance and proficiency testing schemes and should have comparable standards, with systematic differences between assays addressed in the PK model. We believe that these challenges have been well handled in our analysis with the use of nonlinear mixed-effects modelling which was specifically developed to account for the concomitant effect of multiple factors.

To conclude, the findings from this pooled analysis present robust abacavir parameter estimates and characterization of the effect of relevant covariates such as body size, age, and concomitant medications, since the results are based on a large number of participants from different settings. There was a decrease in abacavir exposure from first dose to steady state when co-administered with LPV/r, being even more pronounced for efavirenz. Abacavir exposures were decreased by concomitant administration of rifampicin and super-boosted LPV/r. On the contrary, malnourished children had high and variable exposures, but the exposure normalized as the nutritional status resolved. In spite of reductions in abacavir with repeated doses of ART (slightly greater effect with EFV than with LPV/r), abacavir concentrations in children on WHO-recommended weight-band doses are higher on average than adults. Moreover, this analysis confirmed our earlier finding that children with TB on super-boosted LPV/r plus rifampicin had reduced ABC exposures but these were still similar to those reported in adults. Thus, although there are significant drug-drug interactions with concomitant ARVs and TB treatment, our findings do not support adapted dosing in these groups. Abacavir concentrations should however

be confirmed in TB/HIV coinfected children on EFV-based ART with rifampicin-based TB treatment.

Acknowledgments

Mahmoud Abdelwahab for the helpful discussions in relation to the charts and tables.

Funding

SH was partly supported as Experienced Research Fellow for by the Alexander von Humboldt Foundation, Germany, during this project.

Table 4.1 Clinical characteristics of patients and demographics in studies included in the analysis.

	ARROW[22]	CHAPAS-3[23]	DND*i*[24]	MATCH[25]	COMBINED
Patients in analysis (N)	41	27	87	75	230
Males (N)	17	13	38	41	109
Samples in analysis (N)	598	204	1338	620	2760
Samples per patient (N) median (range)	7 (2-8)	8 (2-8)	6 (4-6)	4 (4-5)	7 (2-8)
Lower limit of quantification (ug/mL)	0.0243	0.0238	0.0243	0.0238	-
Age (Years) median (IQR)	7.6 (4.0-12.6)	4.7 (2.1-12.8)	1.9 (0.3-5.8)	1.4 (0.2-10.9)	2.1 (0.2-12.8)
Age<1 year (%)	0	0	28.7	42.7	24.8
Weight (kg) median (IQR)	20.5 (14.0-30.0)	15.4 (10.7-27.9)	9.5 (3.9-15.9)	7.4 (2.5-25.0)	9.8 (2.5-30.0)
Abacavir formulation	FDC	FDC	Liquid	Liquid	-
Concomitant medication (N) [b]					
3TC+ EFV	41	24	0	8	73
3TC+ EFV + RIF	0	3	0	0	3
3TC+LPV/r (4:1)	0	0	71	58	129
3TC+LPV/r (4:4) + RIF	0	0	87	15	101
Weight-for-age Z-score [a] **median (IQR)**	-1.13 (-3.09-0.544)	-0.952 (-3.94-1.15)	-1.46 (-5.19-1.55)	-3.19 (-6.29-0.323)	-1.71 (-6.30-1.55)
Malnourished (N (%)) [c]	6 (14.6)	3 (11.1)	45 (51.7)	61 (81.3)	115

ABC=abacavir, EFV=efavirenz, 3TC=lamivudine, LPV/r (4:4) = super-boosted Lopinavir/ritonavir, LPV/r (4:1) = standard lopinavir/ritonavir, RIF=rifampicin, N=number

BID = Twice a day, FDC = fixed-dose combination

[a] Z-scores calculated according to WHO (<10years) and CDC (>10 years) growth charts

[b] Values reflect the numbers of children on the drugs at PK evaluation

[c] weight-for-age and height-for-age z-score <2.0

Table 4.2 Final parameter estimates with uncertainty for abacavir

Model Parameter estimates	Typical value		Variability	
	Value	95% CI	% CV	95% CI
Clearance (L/h) [CL][a]	10.7	9.87; 11.5	14.5 (BSV) 15.3 (BVV)	11.7; 16.4 13.3; 17.1
Central volume of distribution (L) [a]	11.0	10.2; 11.7		
First-order absorption rate constant (1/h) [Ka]	2.29	1.99; 2.56	77.3 (BOV)	69.1; 83.3
Relative oral bioavailability ( ) [F]	1 FIXED		39.2 (BOV)	35.1; 43.1
Peripheral volume of distribution (L) [a]	3.33	2.97; 3.64	44.6 (BSV)	38.6; 49.4
Inter-compartmental clearance (L/h) [a]	1.10	0.97; 1.21		
y_maturation function [b] ( )	2.57	1.84; 3.18		
$PMAGE_{50}$ [b] (months)	8.10	6.30; 9.53		
Mean absorption transit time (mins)	6.24	4.96; 7.50	132 (BOV)	116; 145
Number of absorption transit compartments ( )	11.9	8.66; 14.8		
Proportional error (%)	23.8	22.2; 25.0		
Additive error (µg/L)	2.01	1.51; 2.56		
Change in F when on rifampicin + super-boosted lopinavir	-29.4	-35.8; -24.3		
Change in CL for first abacavir dose (%)	-18.4	-32.2; -7.50		
Change in CL when on EFV (%)	+12.0	+2.57; +20.1		
Change in F of malnourished children at start of supplementation (%)	+115	+67.4; +150		
Change in CL of malnourished children at start of supplementation (%)	-64.0	-75.4; -53.3		
Malnutrition effect half-life [d](/day)	12.2	-16.8; -9.87		
Change in speed of absorption for FDC tablets (%)	-24.9	-36.8; -17.2		
Delay in absorption for night dose (h)	2.52	2.10; 2.76		
Extra BOV BIO in MATCH (fold change)	1.39	1.13; 1.62		
Extra BVV CL in MATCH (fold change)	3.35	2.77; 3.85		

Between-subject (BSV), -visit (BVV), and -occasion (BOV) variabilities were assumed as lognormally distributed and are reported as %CV (sqrt(omega)*100)

[a] All clearances and volumes of distribution were allometrically scaled and the typical values reported here refer to a child weighing 9.8 kg on LPV/r (4:1) at steady state, the median value in the dataset.

[b] $PMAGE_{50}$ is the postmenstrual age at which 50% maturation is reached, while y_maturation function is the shape factor in the sigmoidal maturation function

[c] The absorption mean transit time is the average time the drug spends travelling from the first transit compartment to the absorption compartment**.**

[d] Malnutrition function denotes the amount of change in clearance and bioavailability per time.

[e]FDC= Fixed dose combinations

Table 4.3 Comparison of populations and AUCs between present pooled analysis and previous abacavir publications

Author	Study	Study arm	n	Location	Median Weight [kg] (range)	median Age [yrs] (range)	Dose (mg/kg) per day	Formulation	Other ARVs	AUC_12	original CL/F (L/h)	Allometry CL/F (L/h/ 70 kg [e])
Pooled ABC	ARROW, CHAPAS, DNDI, MATCH	LPV/r (4:1)	230	South Africa, Uganda, Zambia, Zimbabwe	9.8 (2.5-30.0)	2 (0.2-12.8)	16	Liquid, tablet	3TC	10.2	10.7	46.8
		EFV								10.4	12.0	52.3
		LPV/r (4:4) +TB								6.66	7.55	33.2
		EFV +TB								7.58	12.0	52.3
Waters 2007		Control	24	UK	83.6	43.0 (31.0-62.0)	8	Tablet	3TC, ZDV	9.31	32.2	28.2
		ATV/r								7.57	39.6	34.7
		Control								7.57	39.6	34.7
		LPV/r (4:1)								5.24	57.3	50.2
Jackson 2012		Control	19	UK		45.0 (37.0-53.0)	8	Tablet	3TC, ZDV	6.77	44.3	38.8
		DRV/r								4.94	60.7	53.2
		RAL								6.99	43.0	37.6
Cella [a,b] 2011	PENTA-13	Children	70		23.8 (13.7–60.5)	5.9 (2.1–12.8)	16	Liquid, tablet	3TC, ZDV, NVP, EFV, LPV/r	6.96	33.2	74.6
	PENTA-15	infants	70		12 (7.4–15.9)	1.8 (0.3-2.9)		Liquid		7.03	13.4	50.3
Zhao 2013	PENTA-13 &15, ARROW	infants	21	Uganda, Zimbabwe	17.6 (7.6-60.9)	5.7 (0.4-12.8)	16	Liquid, tablet	3TC, ZDV, NVP, EFV, LPV/r	6.10	20.1	56.6
		Children	48							8.70		
Sleasman[c] 2009	P1018	<18 years	15	USA	62.8 (37.6-89.2)	15.9 (13.7-17.6)	9.8	Tablet	3TC, ZDV, PIs, NNRTIs	7.01	42.8	46.4
		≥18 years	15		71.6 (44.1-122.7)	21.5 (18.5-24.3)	8.4			6.59	45.5	44.7
Jullien [d] 2004			105	France	25 (2.5-84.0)	8.5 (0.1-16.0)	16	Liquid, tablet	NRTI+ PIs or NNRTI	8.5	23.7	51.3

ABC = abacavir, EFV = efavirenz, TB = rifampicin-based TB treatment, LPV/r = Lopinavir/ritonavir, 3TC lamivudine, ZDV zidovudine, ATV/r = atazanavir/ritonavir DRV/r = darunavir/ritonavir, RAL = raltegravir, NVP = Nevirapine, CL/F = apparent clearance, ARV = anti-retroviral, UK = United Kingdom, USA = United States of America,

[a] Simulated patient were added to the original PENTA 13 (14 children) and PENTA 15 (23 infants), [b]Prior from adult distribution used for model for children

[c] NRTI, NNRTIs and PIs drug names for not provided

[d] Drug names for NRTI,NNRTIs and PIs not provided

[e] Original clearance values scaled to a 70 kg individual to allow for easier comparison of AUCs across studies

Table 4.4 Distribution of patients and their characteristics across study visits in the analysis.

	Participants (samples)	Weight (kg)	Age (years)	WAZ [b]	TB co-infected (n) [a]
ARROW					
VISIT 1 (ABC + EFV) BID	39 (272)	19.5 (14.0; 29.5)	7.4 (4.0; 12.5)	-1.15 (-3.23; 0.54)	0
VISIT 2 (ABC + EFV) OD	41 (326)	20.5 (14.0; 29.5)	7.7 (4.1; 12.6)	-1.12 (-3.01; 0.20)	0
CHAPAS-3					
VISIT 1 (ABC + EFV) BID	24 (180)	15.7 (10.7; 27.9)	4.7 (2.1; 12.8)	-1.04 (-3.94; 1.15)	3
VISIT 2 (ABC + EFV) OD	3 (24)	14.4 (13.2; 19.7)	3.8 (3.3; 4.7)	-0.83 (-0.97; 0.78)	
DNDI					
VISIT 1 (ABC + LPV/r + RIF)	85 (497)	8.8 (3.9; 14.9)	1.6 (0.3; 5.3)	-1.93 (-5.19; 1.39)	85
VISIT 2 (ABC + LPV/r + RIF)	74 (436)	9.5 (4.9; 15.9)	1.9 (0.3; 5.7)	-1.38 (-4.84; 1.56)	74
VISIT 3 (ABC + LPV/r)	71 (405)	10.0 (6.8; 15.9)	2.1 (0.8; 5.8)	-1.39 (-4.86; 1.51)	0
MATCH					
VISIT 1, delay in initiation of ART (ABC + LPV/r)	34 (135)	7.5 (2.6; 11.7)	1.2 (0.2; 3.7)	-2.80 (-5.63; -0.37)	6
VISIT 2, delay in initiation of ART (ABC + LPV/r)	30 (146)	7.6 (3.3; 12.2)	1.4 (0.3; 3.2)	-2.05 (-4.71; 0.32)	6
VISIT 1, delay in initiation of ART (ABC + EFV)	5 (20)	12.0 (9.8; 19.0)	3.6 (3.4; 8.4)	-2.48 (-3.25; -2.13)	0
VISIT 2, delay in initiation of ART (ABC + EFV)	4 (19)	17.3 (11.2; 19.0)	7.8 (3.7; 8.5)	-2.58 (-2.73; -2.54)	0
VISIT 1, early initiation of ART (ABC + LPV/r)	33 (132)	6.2 (2.5; 17.0)	0.8 (0.2; 10.8)	-3.59 (-6.29; -1.03)	4
VISIT 2, early initiation of ART (ABC + LPV/r)	30 (145)	6.8 (3.3; 23.5)	0.9 (0.2; 10.9)	-3.31 (-6.29; 0.17)	7
VISIT 1, early initiation of ART (ABC + EFV)	2 (8)	16.6 (13.6; 19.6)	8.6 (6.5; 10.7)	-3.71 (-3.72; -3.69)	0
VISIT 2, early initiation of ART (ABC + EFV)	3 (15)	15.5 (14.5; 25.0)	9.9 (6.6; 10.7)	-3.89 (-4.55; -3.25)	0

The data is reported as median (range).
ABC = abacavir, EFV = efavirenz, TB drugs = rifampicin-based TB treatment, LPV/r = Lopinavir/ritonavir

BID = twice daily, OD = once daily

[a] Additional ritonavir used for super-boosting lopinavir during rifampicin-based TB treatment

[b] Z-scores calculated according to WHO (<10years) and CDC (>10 years) growth charts

PK in ARROW, CHAPAS-3 and DNDI was taken at least 1 month after treatment start. Visit 2 in MATCH was on average after 14 day

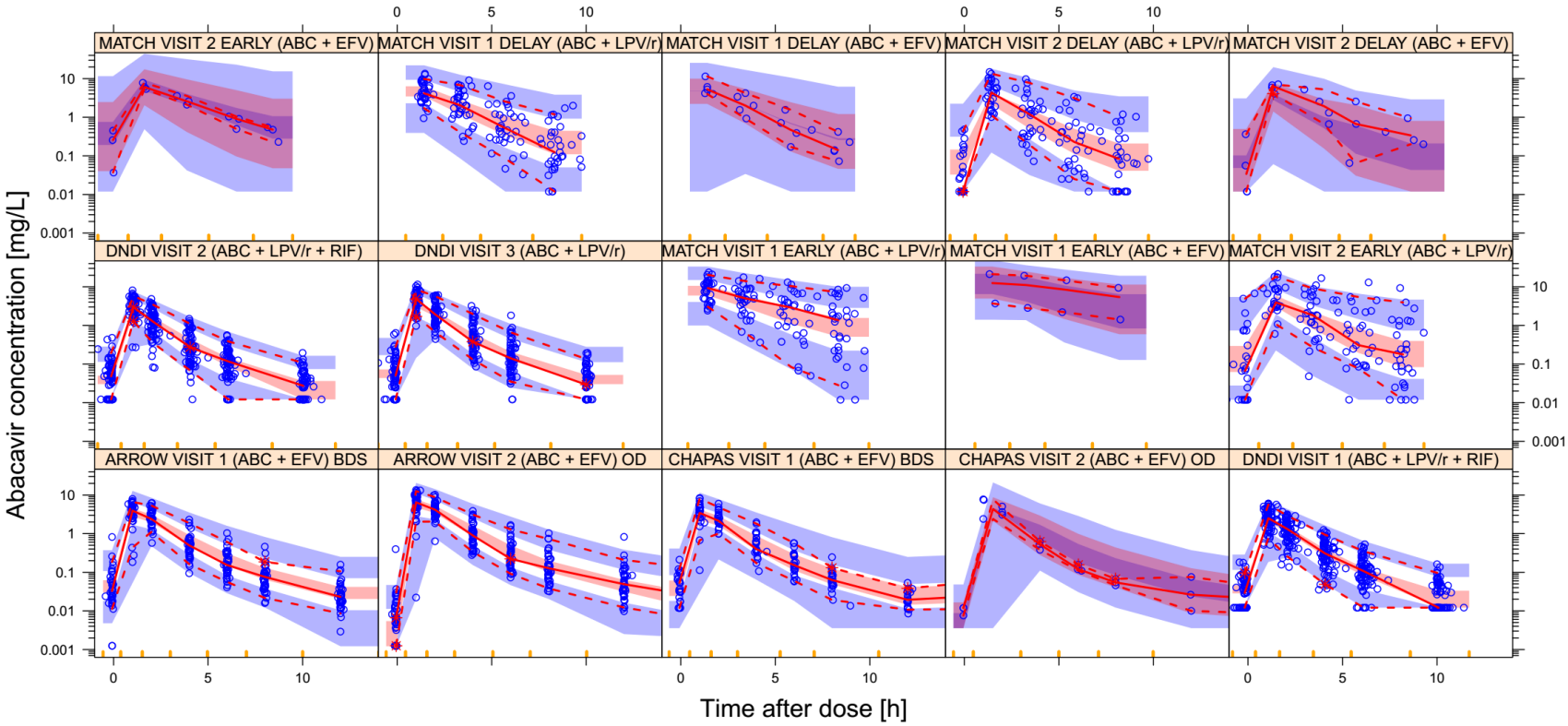

Figure 4.1 Visual Predictive Check of abacavir concentration versus time after dose, stratified by study and PK visit. For an explanation of the meaning of each visit, please refer to Table 4. The solid and dashed lines represent the 5th, 50th, and 95th percentiles of the observed data, while the shaded areas represent the model-predicted 90% confidence intervals for the same percentiles. The dots are the observed concentrations. The yellow ticks are bin boundaries. The dots at the bottom of the VPC are BLQ value. ABC = abacavir, EFV = efavirenz, RIF = rifampicin, LPV/r = Lopinavir/ritonavir, BDS = twice daily, OD = once daily.

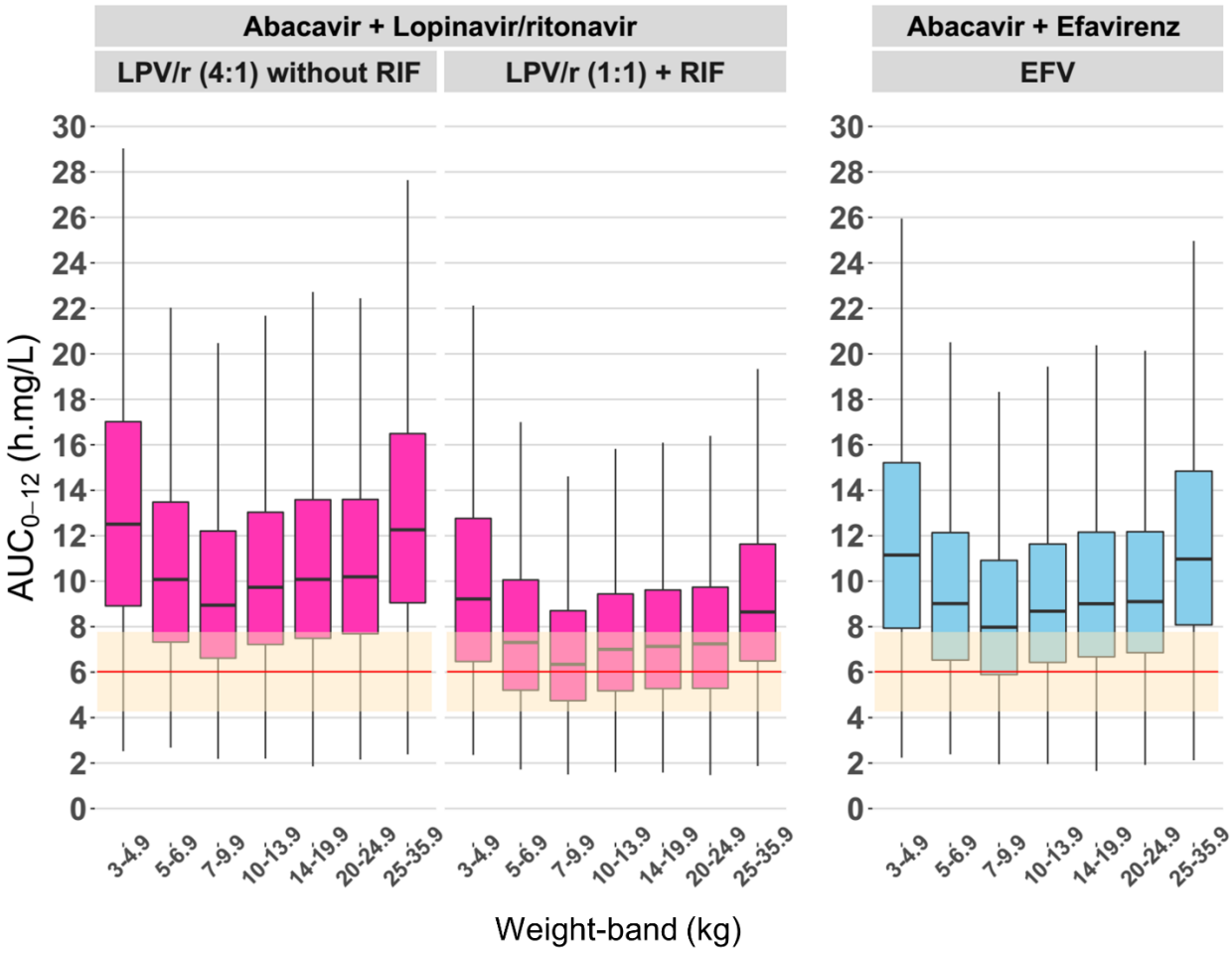

Figure 4.2 Simulated steady-state of 8 mg/kg abacavir AUC0-12 versus body weight, by concomitant antiretrovirals with or without TB treatment. The left panel shows exposures during co-treatment with standard LPV/r (4:1). The middle panel shows exposures in children on super-boosted lopinavir during rifampicin (RIF)-based TB treatment, while the right panel shows exposures in children on efavirenz (EFV). The box indicates inter-quartile range, while the whiskers denote the 2.5th and the 97.5th percentiles. The red horizontal red line represents the recommended median adult exposure (6.02 mg·h/L).

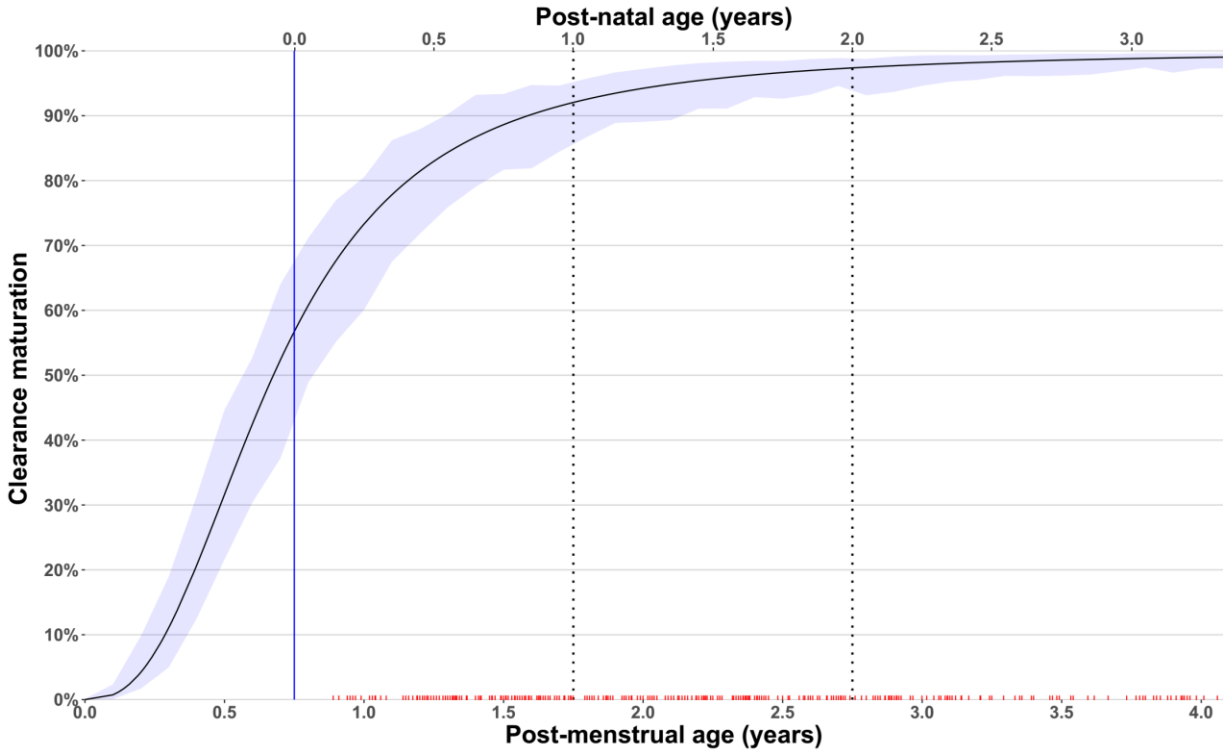

Figure 4.3 Maturation function of abacavir clearance vs. post-menstrual age (bottom x-axis), or post-natal age (top x-axis, assuming average gestation of 9 months), after adjusting for weight. The shaded area represents the 90% confidence intervals. The solid vertical blue represents birth, while the dashed vertical lines represent 1 year and 2 years post-natal age respectively. The red ticks on the lower x-axis represent the post-menstrual age values available in our data.

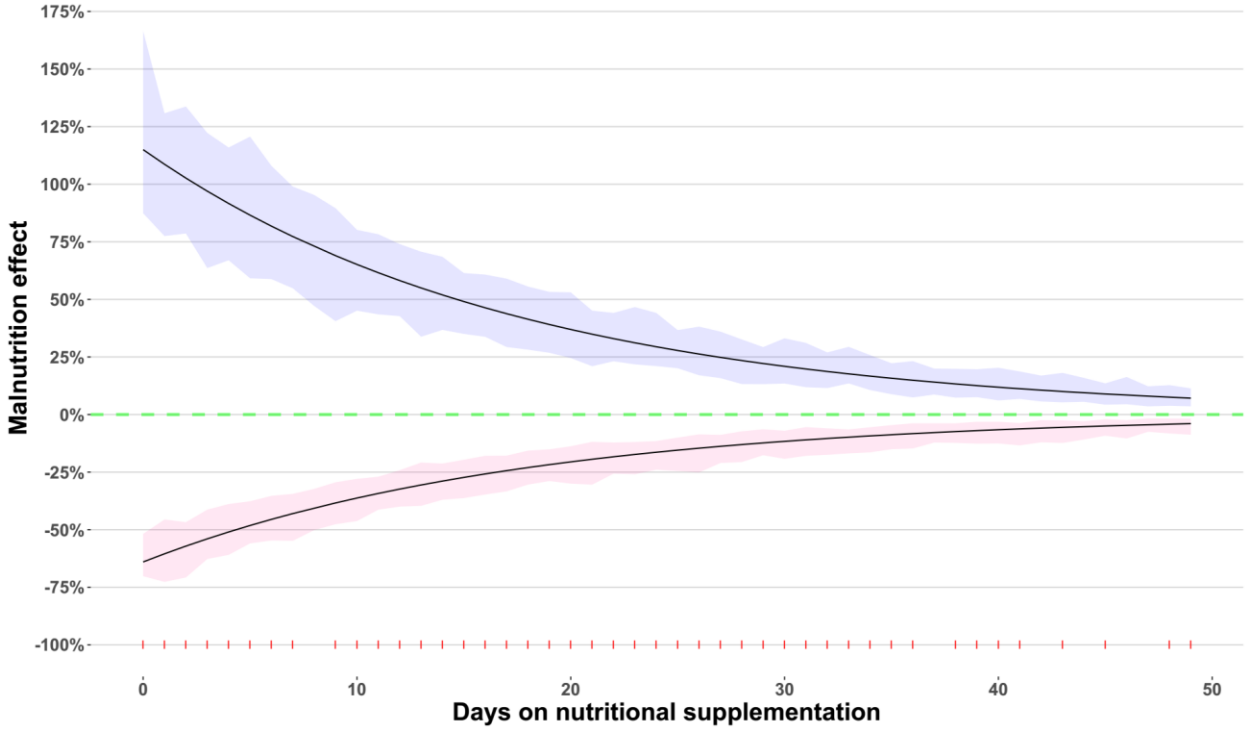

Figure 4.4 Effect of malnutrition on abacavir bioavailability (purple) and clearance (pink) vs. days on nutritional supplementation. The shaded areas represent the 90% confidence intervals. The y-axis value of 0% (dotted green line) represents the values of a typical child co-treated with standard LPV/r 4:1 at steady state after the resolution of malnutrition. The red ticks on the lower x-axis represent the days on nutritional supplementation available in our data.

Chapter 5: Population Pharmacokinetics of Ethambutol in African children: a pooled analysis

5.1 Abstract

Ethambutol protects against the development of resistance to co-administered drugs in the intensive phase of first-line tuberculosis treatment in children. It is especially relevant in settings with a high prevalence of HIV or isoniazid resistance. We describe the population pharmacokinetics of ethambutol in children with tuberculosis to guide dosing in this population.

We pooled data from 188 intensively sampled children from the DATiC, DNDi and SHINE studies, who received 15-25 mg/kg ethambutol daily according to WHO guidelines. The median (range) age and weight of the cohort were 1.9 (0.3-12.6) years and 9.6 (3.9-34.5) kg, respectively. Children with HIV (HIV+; n=103) received antiretroviral therapy (lopinavir/ritonavir in 92%). Ethambutol pharmacokinetics was best described by a two-compartment model with first-order elimination, and absorption transit compartments. Clearance was estimated to reach 50% of its mature value by 2 months after birth and 99% by 3 years. Typical steady-state clearance in a 10 kg child was 15.9 L/h. In HIV+ children on lopinavir/ritonavir, bioavailability was reduced by 32% (median [IQR] steady-state C_{max} 0.882 [0.669-1.28] mg/L vs 1.66 [1.21-2.15] mg/L). In young children, bioavailability correlated with age. At birth, bioavailability was 69.2% that in children 3.2 years or older.

To obtain exposure within the 2-6 mg/L recommended range for C_{max}, paediatric doses require doubling the current doses (tripling with HIV+ children on lopinavir/ritonavir). This raises concerns regarding the potential for ocular toxicity, which requires evaluation.

5.2 Introduction

Ethambutol is included in the intensive phase of first-line treatment of tuberculosis (TB) in areas of high HIV prevalence or isoniazid resistance.[69,192] It inhibits bacterial growth by preventing mycobacterial cell wall synthesis, but its primary inclusion in the first-line anti-TB therapy is for protection against resistance to co-administered first line anti-TB drugs and for treatment of extensive disease.[68] Despite the extensive use of ethambutol in children, knowledge of its pharmacokinetics is limited and more information is required to characterize the impact of factors such as age, weight, HIV infection, and drug-drug interactions to better guide management.

Current recommended ethambutol paediatric dosing is 15-25 mg once daily.[70] Its oral bioavailability is approximately 80% with plasma protein binding around 70–80%. [193] Ingesting food at the same time decreases the rate of ethambutol absorption but not its overall bioavailability. [68,69] Peak plasma ethambutol concentrations are between 2–4 hours after dose. A peak concentration (C_{max}) of 2 to 6 mg/L for a mean ethambutol dose of 25 mg/kg has been proposed as a therapeutic target in adults.[70,80] Ethambutol is mostly excreted unchanged in urine, around 50 to 70% of oral doses are collected unchanged in healthy subjects. Alcohol dehydrogenase is responsible for the breakdown of ethambutol to an aldehyde intermediate and dicarboxylic acid. [71,72]

HIV and TB co-infections are very common in sub-Saharan Africa.[148] Children living with HIV (HIV+) receive antiretroviral therapy (ART) and often require co-treatment for TB, increasing the chance of drug–drug interactions. The commonly reported drug-drug interactions are between rifampicin and either protease inhibitors (PIs) or non-nucleoside reverse transcriptase inhibitors (NNRTIs).[194] Limited data is available about drug-drug interactions between ethambutol and ART, particularly in children. Another consequence of TB and HIV co-infections are drug-disease interactions. One aspect of drug-

disease interactions is malabsorption due to intestinal malfunction. Decrease in absorption of antibacterial agents is linked with progressive immunodeficiency.[195]

Pharmacokinetic studies are often small with limited power to detect important covariates. Pooling of data from different studies increases the power to detect covariates through nonlinear mixed-effects modelling. The aim of the present study was therefore to pool pharmacokinetic data and characterize the population pharmacokinetics of ethambutol in African children, both with and without HIV, treated for TB. The purpose was to identify factors impacting ethambutol pharmacokinetics in order to guide dosing.

5.3 Methods

5.3.1 Clinical studies and data

This analysis was performed with plasma concentration data obtained from 188 intensively sampled patients from 3 clinical studies. These included three studies in South Africa: the pharmacokinetics of lopinavir when super-boosting with ritonavir in Infants and Young Children co-infected With HIV and TB sponsored by the Drugs for Neglected Diseases initiative (DNDi);[109] DATiC (Optimal Dosing of 1st line Antituberculosis and Antiretroviral Drugs in Children) [70,113] which also included children in Malawi; and Shorter treatment for minimal TB in children (SHINE) which included children in Zambia. [112] The main objectives of these studies were: in DATiC, to assess: (i) the pharmacokinetics of first line anti-TB drugs, and the 8-hourly dosing of lopinavir/ritonavir co-administered with rifampicin-based anti-TB treatment; in the super-boosting study, to test whether boosting with additional ritonavir added to co-formulated lopinavir/ritonavir (4:1) to achieve a 4:4 ratio would overcome the rifampicin effect on lopinavir exposures; in SHINE, to compare efficacy of the standard 6-month regimen with the 4-month

regimen using revised WHO dosing guidelines and new fixed drug combination (FDC) tablets. All children received the recommended 15-25 mg/kg/day ethambutol dose according to WHO guidelines. Ethambutol was administered as 400 mg (Sandoz Pharmaceuticals Ltd) or 100 mg (RIEMSER Pharma GmbH, or Macleods Pharmaceuticals Ltd) tablets, or for children weighing ≥25 kg, in FDC with rifampicin, isoniazid and pyrazinamide with 275 mg per tablet (Macleods Pharmaceuticals Ltd). Children from the DNDi study were administered Sandoz tablets while those in SHINE received Macleods tablets. In DATiC, 89% of children received RIEMSER and the remainder received Sandoz tablets. Younger children received crushed tablets due to inability to ingest the full tablet. Ninety-three percent of the latter were below 5 years of age, and all children (n=15) administered ethambutol through a nasogastric tube (NGT) were below 1 year.

5.3.2 Analyses

Ethambutol concentrations were determined at the Clinical Pharmacokinetic Laboratory at the University of Cape Town. The assay was validated over the concentration range of 0.0844 to 5.40 mg/L using a validated liquid chromatography mass spectrometry assay.[196]

5.3.3 Population pharmacokinetic analysis

Nonlinear mixed-effects modelling implemented in NONMEM version 7.4.4 (ICON Development Solutions, Ellicott City, MD, USA) was used to describe ethambutol plasma concentration data. The first-order conditional estimation with eta-epsilon interaction (FOCE-I) was employed to estimate population pharmacokinetic parameters of ethambutol. Data visualization and evaluation of NONMEM output was conducted with PsN, Pirana and R Package xpose4 [120] during the model development process.

Ethambutol was administered as ethambutol dihydrochloride (molecular weight = 277.23 g/mol)[197] and the dose was expressed as mg of this salt in all studies. To obtain the equivalent dose of ethambutol (molecular weight = 204.31 g/mol)[198], the active compound measured in the assays, the dose of ethambutol dihydrochloride was multiplied by 0.737.

Data from each study was explored separately and included in the model consecutively based on the most intensive data, as suggested by Svensson et al. [199] With inclusion of each dataset, the model fit was reassessed, and adjusted based on the general principles of model development outlined below.

Single- and multi-compartment models with first-order absorption and elimination were evaluated to identify the model which best described ethambutol concentration data. Lag time and transit compartments [121] were evaluated for the modelling of absorption. Between-subject variability (BSV) and between-occasion variability (BOV) of random effects were assumed to have log-normal distributions and were modelled using an exponential error term.[179] The estimates of BSV and BOV were provided as percentage coefficient of variation (%CV). A combined additive and proportional error model was used to describe residual unexplained variability, with the additive error for all samples set to at least 20% of the LLOQ. Censored plasma concentration values were handled with the M6 method[122], whereby the last censored value in a series during the absorption phased and the first censored value in a series in the terminal phase were imputed to half of the censoring threshold, while the other censored values in a series were excluded from the model fit and only included in diagnostic plots. To account for the larger level of uncertainty in the imputed censored values, their additive error was inflated by half the censoring threshold. In DNDI and SHINE the censoring threshold was LLOQ, whereas in DATiC it was the imputed LOD (which is 30% of LLOQ).

Model building was guided by the drop in the objective function value (ΔOFV; proportional to -2 log-likelihood), inspection of goodness-of-fit plots, VPC, biological plausibility, and clinical relevance. A decrease in OFV of more than 3.84 between two nested models after the addition of one parameter was considered significant (corresponds to P<0.05).

5.3.4 Investigating factors that influence ethambutol pharmacokinetics

The effect of body size on pharmacokinetics of ethambutol was introduced by allometrically scaling all clearance and volume parameters. Exponents were fixed to 3/4 for clearance and 1 for volume of distribution parameters. [180,181,200] Fat-free mass (FFM) and total body weight (TBW) [182] were assessed as possible size descriptors on disposition parameters. After allometric scaling was included, the enzyme maturation process and its effect on clearance was evaluated according to the approach previously described by Anderson and Holford.[200] Maturation was calculated as:

$$maturation = \frac{PMAGE^{\gamma}}{(PMAGE_{50}^{\gamma} + PMAGE^{\gamma})} \qquad \text{(Equation 1)},$$

where PMAGE denotes postmenstrual age, $PMAGE_{50}$ is PMAGE at which 50% of the maturation is complete, and γ is a parameter determining the shape of the relationship. Gestational age was used to calculate PMAGE, when unavailable, a gestational age of 39 weeks was used. To stabilize the parameter estimates of the model, we included informative priors[101] (10% uncertainty) for PMAGE (47.7 post-menstrual weeks) and γ (3.40), based on a published human renal function maturation model[176]. After inclusion of weight and age in the model, additional covariates were screened based on the range of covariate values in the dataset, physiological plausibility and inspection of parameter versus covariate plots and retained based on statistical significance at p<0.01.

Different methods of drug administration were used in the studies due to inability of younger children to ingest solid dosage forms, age was then tested on absorption parameters. For categorical covariates identified, the fractional change in the typical parameter value was determined. The precision of the final parameter estimates was then evaluated by sampling importance resampling method (SIR). [156]

5.3.5 Simulations

Using Monte Carlo simulations, the final model was used to simulate AUC_{0-24} and C_{max} achieved by each weight band under different dose administrations, including the current recommended 15-25 mg/kg dose, and these were compared to the proposed therapeutic C_{max} of 2 to 6 mg/L and AUC_{0-24} of 16 to 29 h·mg/L taken from previously published ethambutol studies in adults.[75,78,201] The exposures were simulated using an *in-silico* population (*n* = 50,959) weighing 3 to 35.9 kg with combinations of weight and age previously reported in TB-infected children. [157] The children were dosed every 24 hours.

5.4 Results

The available data consisted of 1012 ethambutol plasma concentrations from 188 children receiving a median (range) dose of 20.2 (12.5-25.0) mg/kg. The median (range) age and weight were 1.9 (0.3-12.6) years and 9.6 (3.9-34.5) kg, respectively. A total of 121 (12%) plasma concentrations (mostly trough samples) were below the limit of quantification. Of 188 children in the analysis, 103 (54.8%) were HIV+ on ART. Ninety-two percent of the children on ART were on lopinavir/ritonavir, with 88% on super-boosted lopinavir and 12% on 3 times daily standard lopinavir. The detailed patient demographics of each study are provided in Table 1.

5.4.1 Structural model and parameter estimates

A two-compartment disposition model with first-order elimination proved superior to a one-compartment disposition model with first-order elimination (ΔOFV = -110, $p<10^{-6}$). The absorption phase was described successfully by a transit compartment model with five transit compartments (ΔOFV = -43.5, $p<10^{-6}$ when compared to simple first-order absorption). The final parameter estimates with uncertainty are presented in Table 2 and a VPC showing suitable fit is shown in Figure 2.

Inclusion of allometric scaling improved the model fit. Using fat-free mass instead of total body weight provided significant improvements (ΔOFV = -7.1, $P<10^{-3}$). The effect of age on clearance was captured using a maturation function, its inclusion improved the model fit (ΔOFV = -22.5, $P<10^{-5}$). However, the parameter estimates for the maturation profile were not well determined and went well into ages that are widely expected to be fully mature. The use of the prior improved both the stability of the model and produced more reasonable values for the maturation profile. Clearance was predicted to reach 50% of its mature value at around 2 months after birth and 99% of full maturation by around 3 years. The estimated typical ethambutol apparent clearance at steady state assuming full maturation was 15.9 L/h in a child weighing 10 kg not co-treated with lopinavir/ritonavir. Of note, to compare the value of the apparent clearance (and other disposition parameters) from this analysis with previous reports that may not have accounted for dose conversion from ethambutol dihydrochloride to ethambutol, it is necessary to multiply by 1.357.

Amongst the examined covariates after the inclusion of allometric scaling and maturation, children on lopinavir/ritonavir had 32% lower ethambutol bioavailability and thus lower overall exposure (ΔOFV = -31.4, $P<10^{-6}$). Children from the DNDi and SHINE studies exhibited a 23.6 % slower ethambutol absorption in comparison to the DATiC study (ΔOFV = -13.4, $P<10^{-4}$). The effect of age on absorption

parameters was tested using a "hockey-stick" model, in which the relationship was linear from birth up to a certain cut-off (breakpoint) age, beyond which the absorption parameter value remained constant. Using this approach, the model predicted bioavailability to decrease by 8.5 % per year below 3.2 years (breakpoint) (ΔOFV = -9.3, $P<10^{-3}$). The estimate of the additive error hit the stipulated lower boundary (20% of LLOQ), so it was fixed to this value. A 1.37-fold larger BOV in bioavailability in the pre-dose concentrations (ΔOFV = -7.7, $P<10^{-3}$) was observed.

5.4.2 Monte Carlo simulations

Model-based simulations were used to explore the exposure obtained with the WHO-recommended weight-based dosing. As seen in Figure 3, most children treated with these guidelines are not predicted to achieve the range of AUC_{0-24} and C_{max} observed in adults. To obtain those target exposures, the model predicts that children not on lopinavir/ritonavir will require an average of 50 mg/kg/day, whereas children co-administered with lopinavir/ritonavir will require an average of 84 mg/kg/day. Overall, children in the lower weight-bands receiving ethambutol will require higher doses compared to children in the upper weight-bands. Further details are given in Figure 4 and Table 3.

5.5 Discussion

In this population pharmacokinetic meta-analysis of ethambutol in children, the effects of weight, age, and HIV infection were explored. The observed ethambutol concentrations were lower than the suggested adult target concentrations, i.e. 2-hour C_{max} of 2-6 mg/L.[3] In children receiving a median ethambutol dihydrochloride dose of 20.2 mg/kg, the model-predicted median (IQR) steady-state C_{max} was 1.66 (1.21-2.15) mg/L at 2.74 hours for children not taking lopinavir/ritonavir, while the value was 0.882 (0.669-1.28) mg/L at 3.0 hours for children co-treated with lopinavir/ritonavir. The predicted

ethambutol concentrations were comparable to those from other paediatric studies which are also low, ranging from 0.78 to 2.1 mg/L when dosing at 10 to 20 mg/kg . [70,73,202,203] It is worth noting that direct comparison of C_{max} values between these pharmacokinetic studies is challenging, since different types of assays for measurement of drug concentration, sampling schedules, and types of formulations were used. These variations can heavily influence C_{max} and T_{max}, and may account for the apparently faster rate of absorption (resulting in shorter T_{max} and higher C_{max}) we found in DATiC compared to the other studies.

The model identified a 32% reduction in ethambutol exposure in HIV+ children on lopinavir/ritonavir. Although the currently available studies are conflicting in their results, HIV+ patients have been shown to achieve somewhat lower concentrations of ethambutol. [70,73,78,196,204] In noncompartmental analyses of ethambutol pharmacokinetics in paediatrics, the HIV+ groups had lower area under the concentration-time curve (AUC) than HIV-negative groups. [70,196,204] Two of these studies also reported significant reduction of C_{max} in the HIV+ group compared to the HIV-negative group. [70,196] The children in these studies were dosed according to the WHO 2010 guidelines and included children on ART without lopinavir/ritonavir. The exact mechanism causing the low ethambutol concentrations in HIV+ patients is unclear. While anti-TB drugs, particularly rifampicin, through activation of pregnane-X-receptor, cause significant interactions with PIs and NNRTIs, there is currently limited evidence describing potential drug-drug interactions between ethambutol and ART. Ethambutol is a substrate of the P-glycoprotein efflux pump,[205] and ritonavir through activation of pregnane-X-receptor induces P-glycoprotein. [143,206,207] Another explanation for low concentrations in advanced HIV infection is malabsorption, which has been suggested as a potential reason for low plasma concentrations of anti-TB drugs in HIV+ patients. [208–210] The association of HIV with reduced concentrations has been noted

to be more profound for ethambutol and rifampicin than other first-line drugs.[211] In our analysis, the majority of children on lopinavir/ritonavir were administered ethambutol formulations different to our reference child, so it is also possible that the reduced exposure observed in children on lopinavir/ritonavir is due to the type of formulation this group used. However, when testing this effect of lopinavir/ritonavir on ethambutol exposure only within the DATiC study, where all children received the same formulation, the reduced ethambutol exposure was still observed. Whether the decreased ethambutol exposures seen in children with super-boosted lopinavir are indeed associated with HIV-related malabsorption, drug-drug interaction or formulation (or study) differences could not be established with certainty in this analysis, the exact mechanism driving this effect and its clinical relevance needs further investigation.

The decreased bioavailability observed in children below 3 years of age could be related to the drug administration methods used in these age groups. While older children could swallow tablets or capsules, this is not always the case for the younger children, who require tablets to be split or crushed. The problem with this method is ensuring the correct dose is measured and given to the child by the caregiver, such methods increase the variability in the dose administered.[212] One limitation in our analysis is the lack of information on the method of administration in some children. For the DNDi study, the method of administration was imputed based on age. Both age and method of administration were tested in the model to explain the observed lower ethambutol bioavailability. Age performed better and was therefore retained in the final model.

The simulations predict that paediatric patients treated according to the currently recommended 15-25 mg/kg/day will achieve concentrations lower than the target AUC and C_{max} values. For the majority of children to obtain exposure within the target range, the doses require doubling if not on

lopinavir/ritonavir, and tripling if on lopinavir/ritonavir. However, adjusting ethambutol dosages as suggested above, raises the concern of ocular toxicity. Although uncommon, ocular toxicity has been reported in adults on daily ethambutol doses of 15–25 mg/kg, with more common occurrences at doses greater than 50 mg/kg. In children, ocular toxicity has not been reported at daily ethambutol dose of 15-30 mg/kg in most studies,[79] possibly due to low ethambutol exposures achieved in children compared to adults. Further studies are needed to substantiate whether the currently recommended doses in children offer sufficient exposure to protect companion drugs against resistance or whether increased ethambutol doses would be required.

Our analysis has several limitations. Incomplete information on creatinine values, which were not collected for all children, limited our ability to assess whether renal function could explain some of the variability in clearance. HIV+ patients were on ART so we could not distinguish whether the observed decreased bioavailability was due to treatment or disease. Similarly, as most children on ART received lopinavir/ritonavir, we could not robustly compare with the other antiretrovirals. However, the impact of the other ART regimens on ethambutol exposure was also tested in the model

To conclude, ethambutol doses of 15 to 25 mg/kg/day, as advised in the current WHO guidelines, resulted in C_{max} and AUC values lower than those reported in adults. Moreover, exposures were 32% lower in children co-treated with lopinavir/ritonavir. Decreased bioavailability was also seen in children below 3 years. Considerably higher ethambutol doses are needed in children to match adult exposures, but concerns about the potential for ocular toxicity limits this approach. The consequences of failing to achieve sufficiently high ethambutol concentrations in children needs further investigation. With a wider range of drugs for TB available now, a fourth drug with better risk-benefit profile should be

considered, particularly for children, given the difficulty of detecting the ocular toxicity in this population group.

Table 5.1 Clinical characteristics of patients and demographics in studies included in the analysis

	DATiC	DNDi	SHINE	COMBINED
Number of all patients/males	79/33	84/36	25/16	188/85
Number of PK samples	368	471	173	1012
Number of samples per patient	5 (3-6)	6 (4-6)	7 (6-7)	6 (3-7)
Age (Years)	2.6 (0.3-11.6)	1.6 (0.3-6.8)	3.1 (0.3-12.6)	1.9 (0.3-12.6)
Weight (kg)	11.1 (4.2-26.7)	8.8 (3.9-14.9)	11.8 (6.4-34.5)	9.6 (3.9-34.5)
Fat-free mass (kg)	9.1 (3.5-22.6)	6.8 (3.3-13.6)	9.2 (4.6-29.2)	7.7 (3.3-29.2)
EMB formulation (n) [a]				
Fatol®	70	0	0	70
Sandoz®	9	84	0	93
Macleods®	0	0	25	25
Form of administration				
Whole tablet	27	Not recorded [b]	12	41
Crushed and swallowed	23	Not recorded [b]	13	117
Crushed and syringe	14	0	0	14
Crushed and NGT	15	0	0	15
HIV+	19	84	0	103
Absolute CD4 count (cells/mm^3) [c]	576 (214-1318)	893 (463-1730)	0	848 (418-1716)
Viral load (log10 copies/mL) [c]	4.36 (3.11-5.72	5.68 (4.65-6.24)	0	5.51 (4.20-6.21)
Concomitant antiretrovirals				
LPV/r + ABC + 3TC	11	84	0	95
NVP + ZDV + 3TC	3	0	0	3
EFV + ZDV + 3TC	3	0	0	3
EFV + ABC + 3TC	2	0	0	2

Median (range)

3TC lamivudine, ABC abacavir, ZDV zidovudine, EFV efavirenz, LPV/r lopinavir/ritonavir, NVP nevirapine.

[a] Number of children on the formulation on the day of the PK visits

[b] Whole tablet was imputed for children older than 5 years, while crushed tablet was imputed for children younger than 5 years

[C] Median (IQR)

Table 5.2 Parameter estimates of the final model of ethambutol

Model Parameter	Typical value		Variability	
	Value	95% CI [d]	% CV	95% CI
Clearance - CL (L/h) [a]	15.9	14.8; 17.3	11.6 (BSV)	7.12; 15.3
Central volume of distribution (L) [a]	44.3	37.2; 51.1		
Relative oral bioavailability - F ( )	1	FIXED	33.1 (BOV)	30.1; 36.1
First-order absorption rate constant - ka (1/h)	1.43	1.10; 1.84	63.7 (BOV)	51.3; 77.5
Mean absorption transit time - MTT (mins)	40.4	35.3; 46.1	48.5 (BOV)	41.2; 56.9
Number of absorption transit compartments - NN (n)	4.82	3.70; 6.32		
Inter-compartmental clearance (L/h) [a]	11.5	10.1: 13.2		
Peripheral volume of distribution (L) [a]	86.2	73.6; 102		
$PMAGE_{50}$ (months) [b]	10.8	9.66; 11.7		
y- shape of maturation function ( ) [b]	3.25	2.76; 3.77		
Change in speed of absorption in DNDi and SHINE (%) [e]	-23.6	-31.6; -14.4		
Change in F when on LPV/r (%)	-32.0	-38.9; -23.8		
Breakpoint for age effect on F (years)	3.17	2.18; 4.14		
Age on F, fractional change (/year)	+0.0853	+0.0463; +0.130		
Scaling of BOV in F for unobserved doses (fold change)	1.36	1.12; 1.65		
Additive error (µg/L) c	16.8	FIXED		
Proportional error (%)	17.7	16.5; 19.1		

Between-subject (BSV) and -occasion (BOV)

[a] All clearances and volumes of distribution were allometrically scaled and the typical values reported here refer to a child weighing 10 kg (at fully mature clearance) not co-treated with lopinavir/ritonavir.

[b] $PMAGE_{50}$ is the postmenstrual age at which 50% maturation is reached, while y is the shape factor in the sigmoidal maturation function. The parameters were supported by prior information.

[c] Additive error was fixed to 20% of LLOQ.

[d] The 95% confidence interval of parameter estimates was obtained with sampling importance resampling (SIR; n = 1,000) of the final model.

[e] $Ka = \theta_{Ka} \times \theta_{Changeinspeedofabsorption}$; MTT =$\theta_{MTT} \div \theta_{Changeinspeedofabsorption}$

Of note, to compare the value of all disposition parameters from this analysis with previous reports that may not have accounted for dose conversion from ethambutol dihydrochloride to ethambutol, it is necessary to multiply by 1.357.

Table 5.3 Doses used in simulation of ethambutol hydrochloride exposures

Weight band (kg)	Recommended WHO dosing in mg (mg/kg)	Ethambutol optimised dosing in mg (mg/kg)	
	All children	No LPV/r-based ART	LPV/r-based ART
3-3.9	75 (19-25)	200 (51-67)	300 (77-100)
4-5.9	100 (17-25)	300 (51-75)	500 (85-125)
6-7.9	150 (19-25)	400 (50-66)	800 (100-133)
8-11.9	200 (17-25)	600 (50-75)	800 (66-99)
12-14.9	300 (20-25)	800 (53-67)	1200 (80-100)
15-19.9	400 (20-26)	800 (40-53)	1600 (80-106)
20-24.9	400 (16-20)	800 (32-40)	1600 (64-80)
25-35.9	600 (20-24)	1200 (40-48)	1600 (43-64)

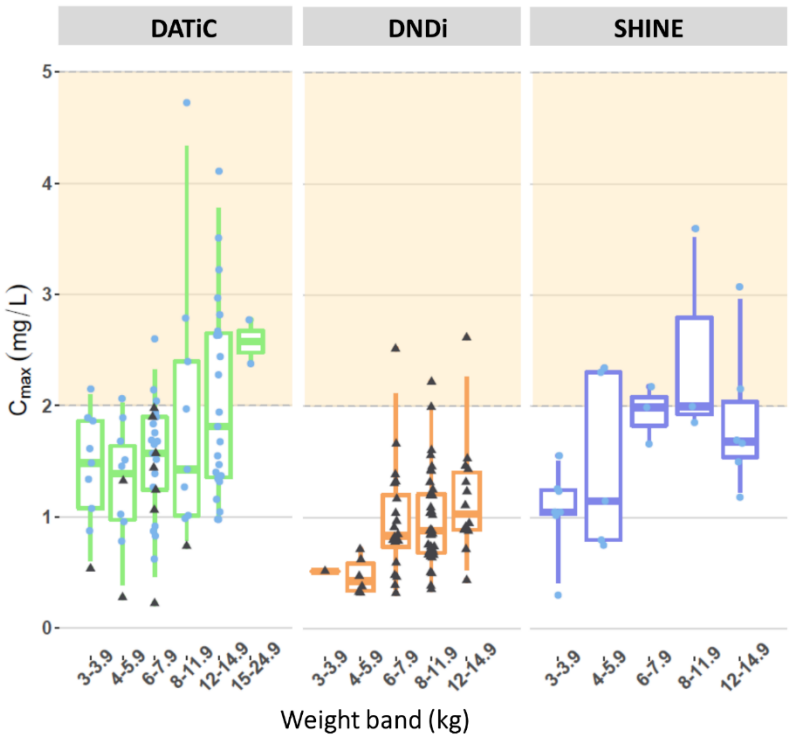

Figure 5.1 Summary of model-predicted ethambutol Cmax versus body weight for DATiC (left), DNDi (middle), and SHINE (right). The orange shaded area from 2 to 6 mg/L represents the recommended thresholds. Each dot represents an individual C_{max}, the black triangular dots represent patients who also received lopinavir/ritonavir. While the blue dots represent coadministration without lopinavir/ritonavir. The box indicates inter-quartile range, while the whiskers denote the 2.5th and the 97.5th percentiles

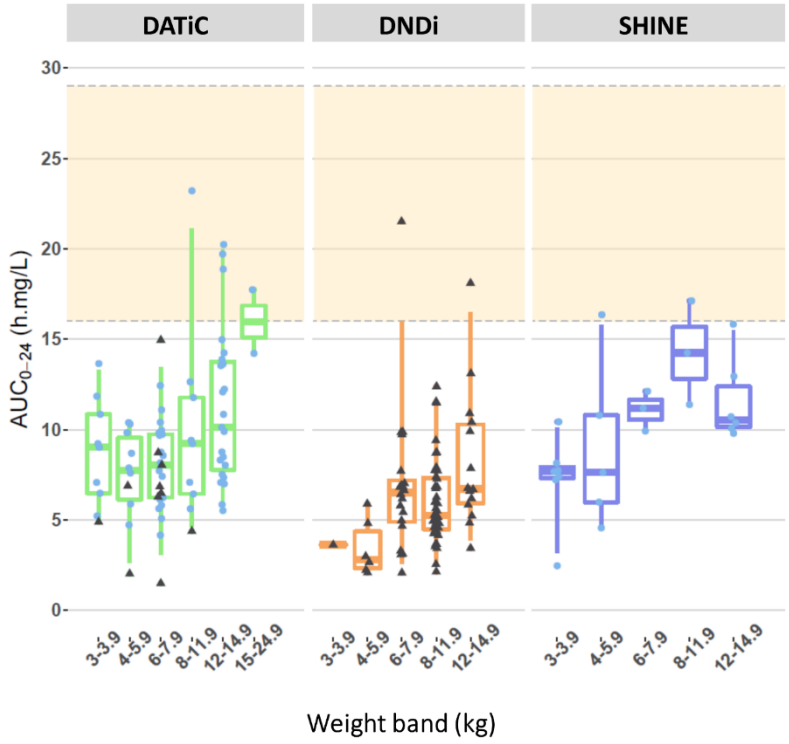

Figure 5.2 Summary of model-predicted ethambutol AUC from time 0 to 24 h (AUC0–24) versus weight for DATiC (left), DNDi (middle), and SHINE (right). The orange shaded area from 16 to 29 h·mg/L represents the range of reported adult $AUC_{0\text{-}24}$. Each dot represents an individual AUC, the black triangular dots represent patients who also received lopinavir/ritonavir, while the blue dots represent coadministration without lopinavir/ritonavir. The box indicates inter-quartile range, while the whiskers denote the 2.5th and the 97.5th percentiles.

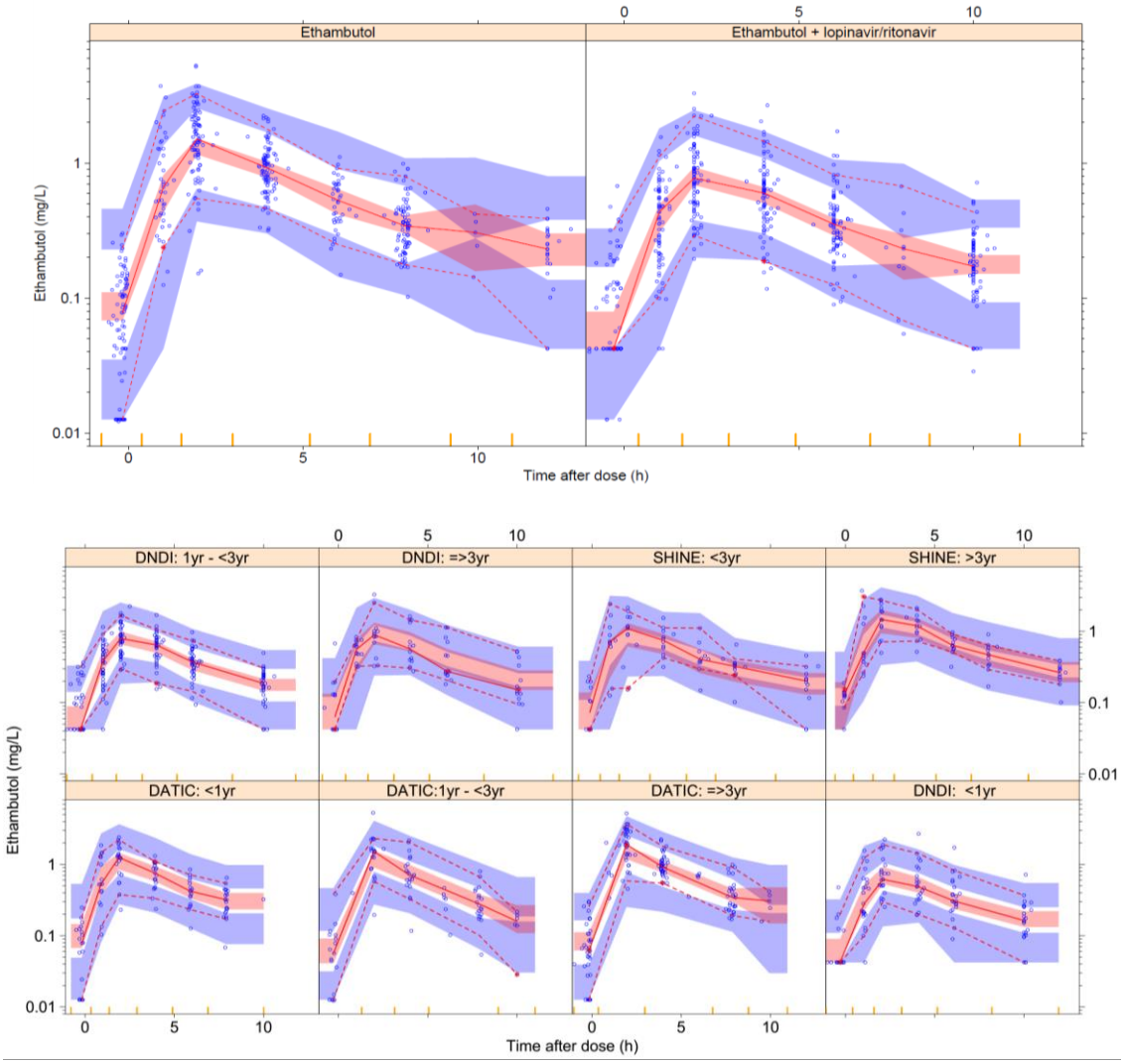

Figure 5.3 Visual Predictive Check of ethambutol concentration versus time after dose, stratified by HIV treatment (top) and age (bottom). The solid and dashed lines represent the 5th, 50th, and 95th percentiles of the observed data, while the shaded areas represent the model-predicted 95% confidence intervals for the same percentiles. The dots are the observed concentrations.

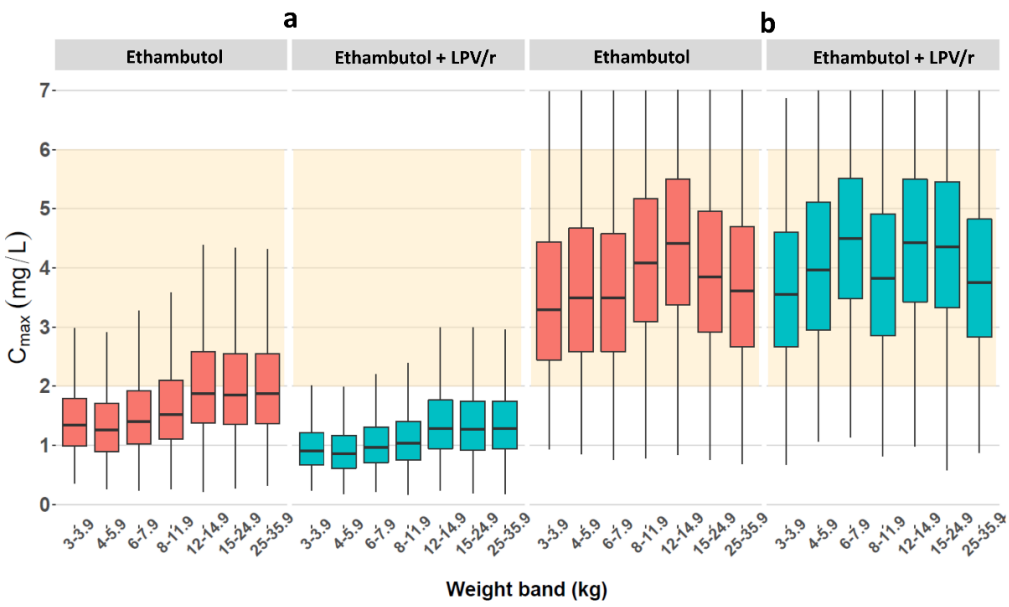

Figure 5.4 Simulated ethambutol Cmax versus body weight, with the concentrations achieved with the WHO-recommended weight-based dosing ("**a**") and the suggested optimized dosing (**"b"**). The red boxes represent patients on ethambutol without coadministration of lopinavir/ritonavir while the blue boxes represent patients whom ethambutol was coadministered with lopinavir/ritonavir. The orange shaded area from 2 to 6 mg/L represents the recommended range. The box indicates inter-quartile range, while the whiskers denote the 2.5th and the 97.5th percentiles

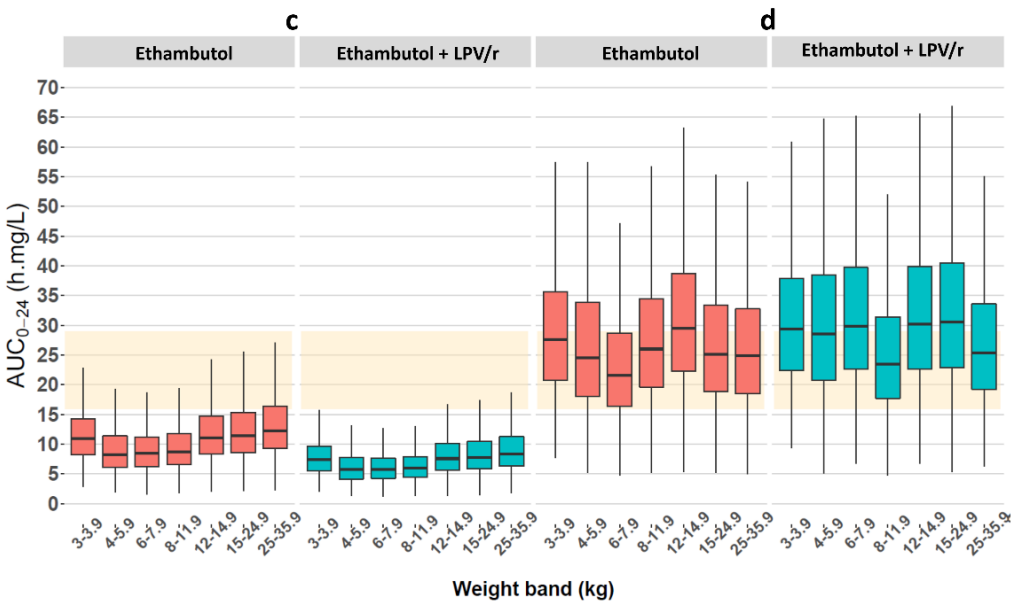

Figure 5.5 Simulated ethambutol AUC from time zero to 24 h (AUC0–24) versus body weight, with the concentrations achieved with the WHO-recommended weight-based dosing (**"c"**) and the suggested optimized dosing (**"d"**)**.** The red boxes represent patients on ethambutol without coadministration of lopinavir/ritonavir while the blue boxes represent patients whom ethambutol was coadministered with lopinavir/ritonavir. The orange shaded area from 16 to 29 h·mg/L represents the reported adult median $AUC_{0\text{-}24}$. The box indicates inter-quartile range, while the whiskers denote the 2.5th and the 97.5th percentile

Chapter 6: An open-source R shiny based tool to predict dose exposure in paediatrics for anti-infective drugs.

6.1 Introduction

Comprehensive pharmacokinetic and pharmacodynamic evaluations in paediatrics are complicated by the fact that a small number of clinical studies are conducted in this population group.[213] For this reason, paediatric dosing regimens are often extrapolated from adult data, without direct observation of drug concentrations in children. Dose-finding studies in children are often an afterthought post-registration for novel drugs and they are not common even for older drugs, thus delaying access or preventing children from receiving optimal treatment. For this reason, the ability to predict an accurate "best guess" dose when designing a paediatric dose-finding can aid tremendously in quickly identifying a safe and effective dose for children.

In infectious disease pharmacotherapy, it is assumed that both adults and children have a comparable disease progression and drug response.[214] Therefore, the commonly used assumption in paediatric dose optimization is a similar PK/PD relationship to adults. [130,215] The resulting strategy is therefore to target the same exposures proven to be effective in adults while monitoring safety in children. In the absence of paediatric clinical data, the widely used approach to achieve adult exposures in children is to use the same mg/kg dose as adults. This constant mg/kg approach implicitly assumes a linear relationship between pharmacokinetic parameters and body weight, but this is an approximation. The relationship between body size and PK has

widely been studied using the principles of allometric scaling. Where, the volume of distribution is scaled linearly with an exponent of 1, and clearance is scaled nonlinearly with an exponent of ¾.[17] Linear approximation may not have significant consequences when scaling the dose for older children and adolescents, but it results in systematic under-exposure in smaller children compared to adults.

Allometry alone works well for children older than 2 years of age, but in the younger paediatric subgroups, age-related maturational changes of enzymes, organs, and drug transporters also impact pharmacokinetic processes.[181,215] These age-related differences may alter drug clearance and overall drug exposure in paediatrics leading to suboptimal dosing. To adjust for the age-related differences, a maturation function is normally used. The time course of maturation is drug specific and most processes that affect pharmacokinetics are fully mature at ~2 years.[215]

Using allometric scaling and maturation has been shown to be more accurate and reliable than constant mg/kg. Strong evidence suggests that constant mg/kg causes low dosing in children whom maturation is complete. Despite this, constant mg/kg dosing is still widely used. The possible reason for the persistent use of the incorrect approach is likely the fact that the nonlinear relationships underpinning allometry and maturation are more complex to understand and difficult to implement than the linear relationship. To try and fill this gap between theory and implementation, the WHO Paediatric Anti-retroviral Working Group (PAWG) [216] created a generic paediatric dosing tool based on a spreadsheet in Microsoft Excel specifically designed to aid the devising of paediatric dosing regimens from adult exposures incorporating allometric scaling and maturation principles.[217] The tool shows expected area under the curve (AUC) of different weight bands in relation to the reference adult. It accomplishes this through the use of

allometric scaling of total body weight and maturation of clearance, if the drugs maturation parameters are known. While helpful, the spreadsheet tool has limitations, in that it only compares overall AUC, it can still be confusing with its multiple sheets and complex formulae and has limited scope in creating detailed visualizations.

Interactive visualizations provide users with the ability to quickly and effectively explore data in real time. Trends in the data can be found quicker, thus speeding up analysis and decision making. Interactive visualizations are especially helpful for people without a background of statistical analysis. Creating interactive visualizations requires extensive knowledge of web technologies like CSS, HTML and JavaScript. The addition of Shiny package [218] to the data analysis and statistical language R,[219] enabled it to handle interactive visualizations and reports.[104,220]

Shiny app provides a set of user interface (UI) functions that generate CSS, HTML and JavaScript. Therefore, prior knowledge of web technologies is not required. Users can explore and visualize their data or perform their own analyses using pre-developed methods. Shiny app can display any kind of data generated in R, and the language R also features packages such as MlxR,[221] which can perform pharmacometric model simulations and it has successfully been used in the drug development world. The combination of these advanced R packages provides a platform for interactive visualization and sophisticated reports for pharmacometric result, such as dose-exposure in children.

The objective of this project is (1) to improve the spreadsheet-based generic tool by re-implementing it with an open-source graphical user interface and (2) add additional functionalities, including drug-specific pharmacokinetic models, the effect of other covariates, and random variability between subjects for simulation of exposures.

6.2 Methods:

Shiny app is made up of two main sections, the user interface called UI.R and the server file called server.R. The UI section of a shiny application defines the overall visual structure of the application, the input controls available to the user, and the content that will be made visible to the user. Shiny app translates the R code and shiny app functions in this section into html and CSS code that web browsers can read and render into a web application. Outputs from UI.R are linked to the server function. The server section of a shiny application is where most of the computation takes place. i.e. the code for transforming data or creating visualizations will most likely be in this section. The server section utilizes the values users inputted via the control widgets to perform actions such as output plots.[103,104]

The paediatric dosing tool (Pedi-dose) is developed as a Shiny app using the R software. It uses allometric scaling and maturation principles as well as longitudinal data simulation to devise paediatric dosing regimens from adult exposures and published PK models. The app can be accessed on the following website http://shiny.webpopix.org/host/test_tool/. While functional, the current shiny app is a prototype and this is a temporary link.

Pedi-dose contains two major sections. 1) the 'generic module' which is designed similarly as the Microsoft Excel spreadsheet tool, 2) a 'drug-specific module' containing a library of published population pharmacokinetic models that allows for simulation of between-subject and –occasion variability as well as other important drug-specific covariates.

In the 'generic module', the user can explore the expected overall exposure (AUC) relative to the reference adult for a generic drug. This module uses allometric scaling to adjust for the effect of body size on clearance, and if maturation parameters are known, also the effect of age on

clearance. The 50th percentile from the WHO growth charts was used to represent age of children. The effect on clearance is then used to obtain exposure (AUC), which is used to compare between children and adults. The module assumes similar bioavailability between children and adults and first-order elimination, i.e., the clearance is constant within the relevant concentration range, with no significant saturable elimination processes.

In the 'drug-specific module', the software is used to simulate the entire pharmacokinetic profile (concentration over time after dose) at steady state by using a published drug-specific population pharmacokinetic model implemented in MlxTran, which can include covariates and between-subject and –occasion variability. The stochastic simulations are performed with the mlxR package with input parameters specified by the user. The simulations can be performed using different in silico population data, such as the standard WHO/CDC growth charts, or a specific population (e.g. malnourished children, or custom data). The population pharmacokinetic models can be loaded from the available library.

6.3 Results

A typical workflow in Pedi-dose starts with the user selecting the desired module (generic or drug-specific) and then providing the required input parameter values, i.e., the weight and daily dose administered to a reference adult patient, the strength of the paediatric formulation and the number of tablets required in each weight-band and the acceptable exposure range. Clicking the "update chart" button after the user is satisfied with the input parameters, will commence the calculation/simulation process which will generate outputs as tables and plots containing the

final results. The user can scroll between the different outputs by clicking on the tabs inside each module.

Once the user enters the input parameters and then clicks the “update chart” button, the outputs will be shown as follows depending on the module selected: For the generic module, the output will be displayed as, (i) the plot of the expected AUC per weight-band relative to the values achieved for the reference adult, (ii) summary table of the output grouped by weight-band presented in a tabulated format. If the maturation profile of the drug is known, a plot that shows the maturation profile can be displayed. The variability observed in each weightband in the generic module comes from weight of the largest and smallest child. Figure 6.1 shows an example of the output from the generic module. For the drug-specific module, the output can be displayed as, (i) a plot of the simulated concentration-time profile of a typical child in a selected weight-band, this allows the user to also consider potentially risky peak concentrations and explore alternative scenarios with different dosing frequency (e.g. twice daily), (ii) a plot of simulated exposures (AUC, C_{max} and C_{min}) achieved by each weight band, the user can then compare the values with an absolute target exposure of that drug (iii) summary table of the simulated output grouped by weight-band presented in a tabulated format. The variability in the drug-specific module comes from Between subject variability. Figure 6.2 shows output of the drug-specific module. After completion of the analysis, a pdf report can be generated by clicking on the “Generate Report” button .This report has a heading and the date of the analysis as well as all the information related to the analysis including all the input parameters entered and all output plots and table.

The tool has been validated by evaluating some of the current paediatric dosing regimens recommended by WHO for anti-infective drugs. The predicted exposures of the 'generic module' are closely in line with results from population pharmacokinetic modelling, and generally in keeping with those found in confirmatory clinical trials. Most importantly, the doses predicted using the tool achieve exposures closer to the target and more even across weight-bands than those obtained with the constant mg/kg approach.

6.4 Discussion

We developed a clinical decision support software tool that provides paediatric dosing suggestions from available adult data. This tool builds on the Microsoft Excel spreadsheet tool that uses allometric scaling- and maturation-based predictions. Similar to previous tool; It incorporates allometric scaling and maturation, but also includes the possibility to perform drug specific predictions thanks to the available library of published drug specific population pharmacokinetic models. With this tool, we emphasised greatly on implementing an intuitive user-friendly interface which reactively and quickly provides real time feedback on the required dosing. We believe that this tool will provide the necessary clinical support and could be an important addition in the 'first guess' paediatric dosing in clinical research settings.

At present, there are some limitations to the tool. The tool requires internet access to perform its basic functionalities, therefore, in settings with no internet access the tool is inaccessible. Also, the tool depends highly on the quality of population pharmacokinetic models and only one population pharmacokinetic model is currently implemented, with the option to include more

models in future. Moreover, pharmacodynamic information which can be of interest to some users is not available with the current interface

Future integration of the tool can allow for wider implementation of population pharmacokinetic models with many more covariates and a wider range of patient population. This could improve dosing predictions for paediatrics as the tool would better describe PK of the various paediatric subgroups, meaning, the tool can also be used for other population groups other than paediatrics too. Although not implemented, the current version of the tool is capable of handling more population pharmacokinetic models. This tool can also be implemented as a mobile app, making it usable in instances where internet connectivity is unavailable. In the future updates, the tool can be able to support more sophisticated models such as physiologically-based PK models.

In summary, we present Pedi-dose, a shiny app implementation of the PAWG paediatric dosing tool which is user-friendly and can be accessed online with a web-browser. While the tool is only meant to be used as a first step in the design of clinical trials for paediatric dosing and not as a substitute to confirmatory studies, it represents a significant step forward with respect to using the constant mg/kg paradigm.

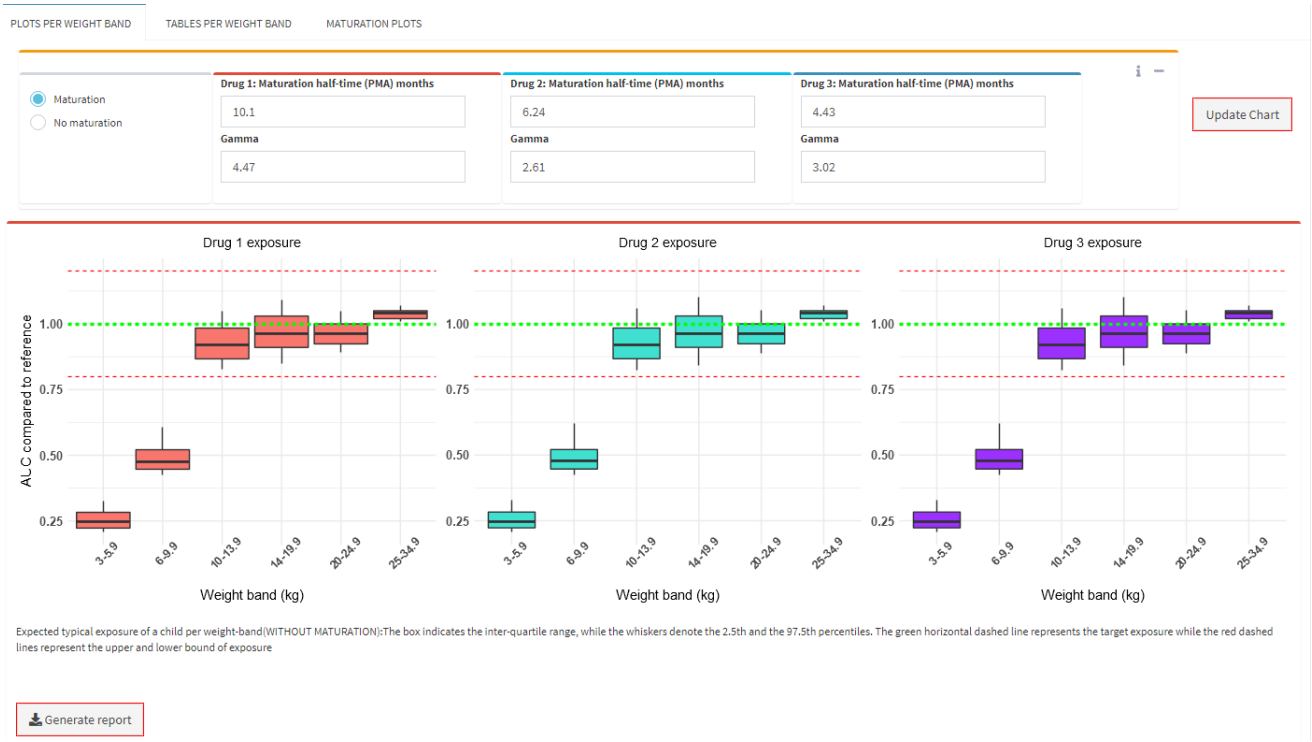

Figure 6.1 Screenshot of the generic module showing expected exposure of a typical child per weight-band in relation to the reference adult. Each box indicates the smallest and largest child in that particular weightband

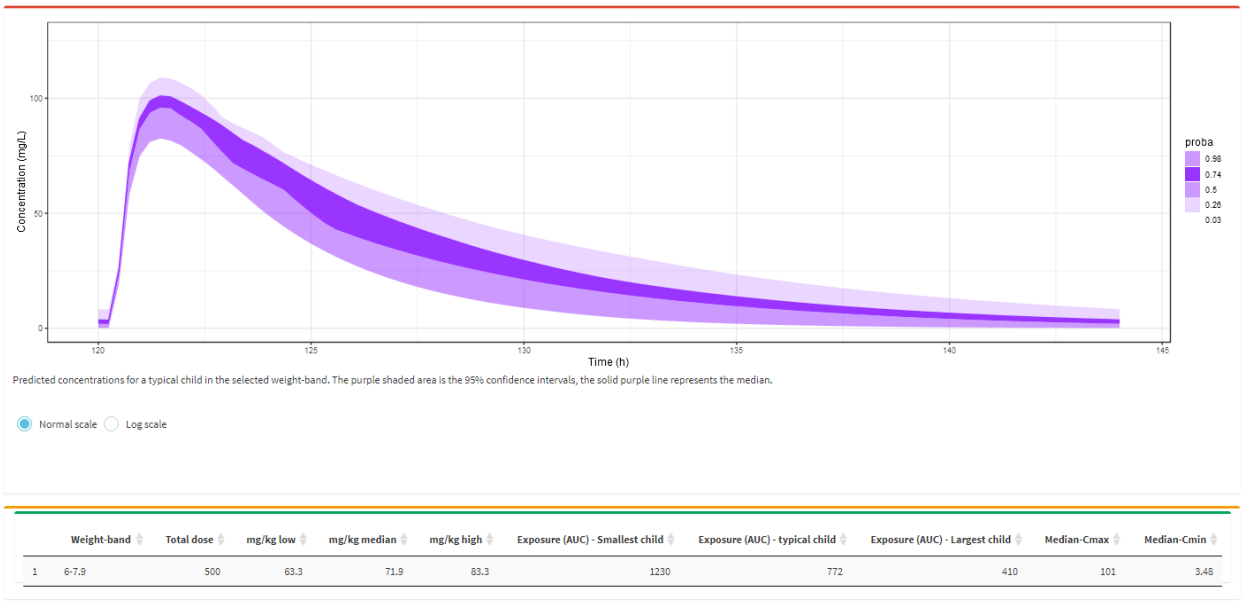

Figure 6.2 Screenshot of the drug specific module showing predicted concentration of a typical child in a selected weight-band.

Chapter 7: Conclusions

HIV and TB are amongst the leading causes of death worldwide. HIV and TB co-infection is highest in the African Region with 50% of infections and deaths occurring in Southern Africa. Introduction of antiretroviral and antituberculosis drugs has drastically improved HIV and TB mortality, but successful treatment in paediatrics remains a challenge largely due to the lack research performed in this population group. In order to optimize doses in paediatrics, demographic differences in patients, such as age, weight, and the biological changes must be considered, together with the identification and management of drug-drug interactions. The need for accurate methods that can capitalize on the limited available paediatric data is thus crucial.

In this dissertation, these challenges were addressed by efficient use of observational data through the development of non-linear mixed effects models that were used to describe the pharmacokinetics of drugs less well studied, like the first-line antiretroviral drug abacavir and antituberculosis drug ethambutol, which is used in selected cases for paediatric TB. Nonlinear mixed-effects modelling with pooling of data from different studies makes it possible to detect covariates with more power. The research presented here contributes to the knowledge of antituberculosis and antiretroviral drugs in paediatrics in an African setting. The patients from the studies involved in this dissertation received drug regimens and combinations based on standard regimens used in most parts of the world, hence the findings maybe applicable beyond Africa. Another aim of this dissertation was to develop a web-based paediatric dosing tool utilizing R shiny. The tool is meant to be used as a first step in the design of paediatric dosing.

7.1 Abacavir exposure in children co-treated for tuberculosis with rifampicin and super-boosted lopinavir-ritonavir

Co-administration of rifampicin-based antituberculosis regimen and antiretroviral drugs can result in drug-drug interaction. One such drug-drug interaction occurs when lopinavir is administered with rifampicin, where lopinavir exposures are decreased by up to 90%. In children requiring co-administration of LPV/r-4:1 and rifampicin, adding extra ritonavir to achieve a 4:4 ratio with lopinavir (LPV/r-4:4) overcomes this drug-drug interaction. However, the impact of extra ritonavir and rifampicin on abacavir PK has not been explored. The abacavir model in chapter 3 identified a significant reduction in abacavir exposure when the children were co-treated with rifampicin and LPV/r-4:4. The model could not distinguish the contribution of each drug. As lopinavir concentrations were similar during standard dosing without rifampicin, and during TB treatment with superboosting, lopinavir is unlikely to have caused the change in abacavir exposure. Ritonavir exposure was tested as alternative predictor in the model to explain the lower bioavailability of abacavir, but it could not explain the observed effect. This suggests that the drug driving the reduction in abacavir exposures is most likely rifampicin. Despite the decreased exposures observed in children co-treated with rifampicin and LPV/r-4:4, the resulting exposures were still in line with adult values, thus the model showed that a dose of 8 mg/kg twice daily is adequate for children co-treated with LPV/r-4:4 and rifampicin to maintain clinically relevant exposure. The model included allometric scaling with total body weight to explain the effect of body size on the disposition parameters, while a sigmoidal function of age was used to capture the effect of developmental change and organ maturation in the younger children. Young

infants are predicted to achieve even higher exposures than older children due to immature. metabolic pathways. Although our model can predict drug levels in the lower weight bands, we had no children younger than 3 months in this study, so the characterisation of maturation has limited precision.

7.2 Abacavir pharmacokinetics in African children living with HIV: a pooled analysis describing the effects of age, malnutrition and common concomitant medications.

The reduced abacavir exposure observed when children were co-treated with rifampicin and LPV/r-4:4 was further confirmed by the abacavir model in chapter 4, we expected a similar effect in children on efavirenz and rifampicin. However, this effect could not be confirmed, as only 3 children received this treatment combination. The pooling of data from different sources in chapter 4 allowed us to re-evaluate and characterize covariate effects and drug-drug interactions more robustly than in a single study. Increased abacavir clearance (and thus decreased overall exposure) was observed after 7 days on ART treatment compared to the first day of ART treatment. This could be explained by the absence of protease inhibitors lopinavir/ritonavir driven induction, which is generally attained within 1 to 4 weeks. Waters et al also reported decreased abacavir exposure in adults on protease inhibitors lopinavir/ritonavir. The effect we observed was less pronounced compared to that of Waters et al. It is worth noting that they compared abacavir as a single drug against abacavir co-administered with LPV/r (4:1) at steady-state, while in our analysis, children were malnourished and abacavir and LPV/r (4:1) were

administered together from the first day of treatment. Malnourished children had high and variable exposures which normalized as the nutritional status resolved. The exact mechanism responsible for the higher exposure in malnourished children could not be identified with certainty. However, malnutrition affects the function of many body-systems, it is therefore possible that malnutrition alters abacavir PK via multiple effects on ADME processes, for example, by decreasing functionality of metabolic enzymes and alteration of protein levels. In spite of reductions in abacavir with repeated doses of ART (slightly greater effect with EFV- than with LPV/r-containing regimens), abacavir concentrations in children on WHO-recommended weight-band doses were higher on average than adults. Similar to the abacavir model in chapter 3, allometric scaling with total body weight explained well the effect of body size on the disposition parameters, while a sigmoidal function of age captured the effect of developmental change and organ maturation in the younger children. The maturation estimates from chapter 3 and 4 were in line with previous reports, where children below 3 years are predicted to have higher exposures than older children above 3 years. However, our findings do not support adapted dosing in these groups.

7.3 Population Pharmacokinetics of Ethambutol in African children: a pooled analysis

Ethambutol is a commonly used drug in the treatment of TB, it is added in the intensive phase of first-line treatment for children in settings with a high prevalence of HIV or isoniazid resistance, and in cases of extensive tuberculosis (TB). It is used in combination with isoniazid, rifampicin, and pyrazinamide, to protect against the development of resistance to the co-administered

drugs. Despite its wide use, there is limited information on ethambutol pharmacokinetics in paediatrics. In chapter 5, we explored the pharmacokinetics of ethambutol with the aim of characterizing the impact of factors such as age, weight and drug-drug interactions to better guide the management of paediatrics. Allometric scaling with fat free mass was used to explain the effect of body size on the disposition parameters, and the effect of age on clearance was captured using a maturation function. The recommended ethambutol doses of 15 to 25 mg/kg/day resulted in exposures (C_{max} and AUC) lower than those reported in adults. However, these exposures were comparable to those reported in other paediatric studies. The exposures were further reduced in HIV coinfected children on lopinavir/ritonavir. The exact mechanism behind the much lower ethambutol concentrations in HIV-infected patients on lopinavir/ritonavir is unclear, and could be due to a number of reasons, including drug-drug interactions between ethambutol and lopinavir/ritonavir, though there is little evidence in literature to support this notion. It is worth noting that, the majority of children on lopinavir/ritonavir were administered ethambutol formulation that is different to that of the other children, therefore it is possible that the reduced exposure is due to formulation diffrences. Another possible explanation could be malabsorption due to HIV infection. Although the pooled analysis allowed for exploration of covariates with more power, the unequal distribution of covariates between studies hindered us to fully explore the exact mechanism driving this effect and its clinical relevance. Further investigations are required, particularly since the currently available studies show conflicting results on the impact of HIV on ethambutol concentrations. Also, Children who took ethambutol split or crushed had decreased bioavailability, most of these children were below 3 years of age. In order to archive the proposed therapeutic exposures, considerably higher ethambutol doses

optimised across weight will be needed. However, the concern with these higher ethambutol doses is the potential for ocular toxicity. Moreover, the significances of failing to achieve sufficiently high ethambutol concentrations particularly in children are not well documented and need further investigation before any dose adjustment suggestions can be made. Alternative drugs with better risk-benefit profile should be considered

7.4 An open-source R shiny based tool to predict dose exposure in paediatrics for anti-infective drugs.

The selection of paediatric doses is generally aimed at achieving safe and equivalent exposure compared to licensed adult doses. Predicting the pharmacokinetic consequences of multiple developmental changes in paediatrics is generally very challenging. However, in children over 2 years of age the effect of body size alone is the main source of pharmacokinetic differences between adults and children. The effect of body size on pharmacokinetics is very similar across the majority of drugs and can be predicted with reasonable accuracy. Allometric scaling has been shown predict doses better than mg/kg, however mg/kg is still commonly used. In chapter 6, we designed an open-source Shiny application that provides an easy platform to design and evaluate paediatric dosing regimens based on adult exposures. The tool is based on allometric scaling and maturation principles, it also utilizes published non-linear mixed effects models. The advantage of this tool over the previous tool is its ability to utilize the complex nonlinear relationships and display them in a simple manner, making it an ideal tool for clinicians or researchers involved in dose optimization in children. The tool contains two major sections. 1) the 'generic module' which is designed similarly as the Microsoft Excel spreadsheet tool, 2) a library of published 'drug-

specific module' that allows for stochastic simulations of between-subject and –occasion variability with the mlxR package. We believe that this tool will provide the necessary clinical support and could be a major step forward in the 'first guess' paediatric dosing in clinical research settings. Though functional, the tool has limitations, it requires internet access to perform its basic functionalities and only one population pharmacokinetic model is currently implemented, even though the current version of the tool is capable of handling more population pharmacokinetic models. The app can be accessed freely on the following temporary link http://shiny.webpopix.org/host/test_tool/.

7.5 Overall summary

This thesis describes the PK properties of ethambutol and abacavir, two commonly used drugs in the management of HIV and TB but with limited PK knowledge in paediatrics. This thesis also introduces a Shiny application that designed to be used as 'first guess' in paediatric dose predictions.

For abacavir, the thesis shows that co-treatment of abacavir + LPV/r-4:4 with rifampicin or abacavir + efavirenz results in reduced abacavir exposures, co-treatment of abacavir + LPV/r 4:1 also results in decreased abacavir exposures, but to a lesser degree to the above mentioned. Also, malnutrition results in higher and variable abacavir exposures. However, in spite of the above mentioned, abacavir concentrations in children on WHO-recommended weight-band doses were higher on average than adults, thus based on the results from this thesis, abacavir dose adjustment is not required. The thesis also confirmed that the current recommended ethambutol doses result in lower exposures than those of adults, the exposures were even lower

in HIV positive children on lopinavir/ritonavir and in young children due to reduced bioavailability from tablets being split or crushed. For the majority of children to obtain exposure within the target range, ethambutol doses would need to be increased. A paediatric dosing tool designed to be used as a first guess in dose predictions by researchers and clinicians was developed.

References

1. Organization WH. WHO | Global tuberculosis report 2019. *World Heal Organ* 2020. Available at: http://www.who.int/tb/publications/global_report/en/.

2. UNAIDS. *UNAIDS data 2019 annual report*. 2019.

3. Venturini E, Turkova A, Chiappini E, Galli L, de Martino M, Thorne C. Tuberculosis and HIV co-infection in children. *BMC Infect Dis* 2014; **14 Suppl 1**: S5.

4. WHO. *Cascade Data Use Manual To Identify Gaps in Hiv and Health Services for Programme Improvement Hiv Strategic Information for Impact User Manual*. 2018.

5. Dodd PJ, Prendergast AJ, Beecroft C, Kampmann B, Seddon JA. The impact of HIV and antiretroviral therapy on TB risk in children: A systematic review and meta-analysis. *Thorax* 2017; **72**: 559–75.

6. Waalewijn H, Turkova A, Rakhmanina N, *et al.* Optimizing Pediatric Dosing Recommendations and Treatment Management of Antiretroviral Drugs Using Therapeutic Drug Monitoring Data in Children Living with HIV. *Ther Drug Monit* 2019; **41**: 431–43.

7. Nachman SA, Lindsey JC, Moye J, *et al.* Growth of human immunodeficiency virus-infected children receiving highly active antiretroviral therapy. *Pediatr Infect Dis J* 2005; **24**: 352–7.

8. Storm DS, Boland MG, Gortmaker SL, *et al.* Protease inhibitor combination therapy, severity of illness, and quality of life among children with perinatally acquired HIV-1 infection. *Pediatrics* 2005; **115**.

9. Nacro B, Zoure E, Hien H, *et al.* Pharmacology and immuno-virologic efficacy of once-a-day HAART in African HIV-infected children: ANRS 12103 phase II trial. *Bull World Health Organ*

2011; **89**: 451–8.

10. Obimbo EM, Mbori-Ngacha DA, Ochieng JO, *et al.* Predictors of early mortality in a cohort of human immunodeficiency virus type 1-infected african children. *Pediatr Infect Dis J* 2004; **23**: 536–43.

11. Broder S. The development of antiretroviral therapy and its impact on the HIV-1/AIDS pandemic. *Antivir Res 2010;* **85**:1–38.

12. Szczech LA, Winston JA. The impact of antiretroviral therapy on HIVAN. *Kidney Int* 2004; **65**: 1114–5.

13. Jahn A, Floyd S, Crampin AC, *et al.* Population-level effect of HIV on adult mortality and early evidence of reversal after introduction of antiretroviral therapy in Malawi. *Lancet* 2008; **371**: 1603–11.

14. Schaaf HS, Garcia-Prats AJ, Hesseling AC, Seddon JA. Managing multidrug-resistant tuberculosis in children: review of recent developments. *Curr Opin Infect Dis* 2014; **27**: 211–9.

15. UNICEF. Paediatric Treatment and Care - UNICEF DATA. Available at: http://data.unicef.org/topic/hivaids/paediatric-treatment-and-care/.

16. Geneva, Switzerland. Technical consultation on the use of pharmacokinetic analyses for paediatric medicine development. 2009.

17. Anderson BJ, Holford NHG. Understanding dosing: children are small adults, neonates are immature children. *Arch Dis Child* 2013; **98**: 737–44.

18. Penazzato M, Gnanashanmugam D, Rojo P, *et al.* Optimizing research to speed up availability of pediatric antiretroviral drugs and formulations. *Clin Infect Dis* 2017; **64**: 1597–603.

19. Rose K, Stötter H. ICH E 11: Clinical investigation of medicinal products in the paediatric population. In: *Guide to Paediatric Clinical Research*., 2006; 33–7.

20. Eidelman C, Abdel-Rahman SM. Pharmacokinetic considerations when prescribing in children. *Int J Pharmacokinet* 2016; **1**: 69–80.

21. Batchelor HK, Marriott JF. Paediatric pharmacokinetics: Key considerations. *Br J Clin Pharmacol* 2015; **79**: 395–404.

22. Fernandez E, Perez R, Hernandez A, Tejada P, Arteta M, Ramos JT. Factors and mechanisms for pharmacokinetic differences between pediatric population and adults. *Pharmaceutics* 2011; **3**: 53–72.

23. Allegaert K, Verbesselt R, Naulaers G, *et al.* Developmental pharmacology: Neonates are not just small adults... *Acta Clin Belg* 2008; **63**: 16–24.

24. van den Anker J, Reed MD, Allegaert K, Kearns GL. Developmental Changes in Pharmacokinetics and Pharmacodynamics. *J Clin Pharmacol* 2018; **58**: S10–25.

25. Richey RH, Shah UU, Peak M, *et al.* Manipulation of drugs to achieve the required dose is intrinsic to paediatric practice but is not supported by guidelines or evidence. *BMC Pediatr* 2013; **13**: 81.

26. Melander A. Influence of Food on the Bioavailability of Drugs. *Clin Pharmacokinet* 1978; **3**: 337–51.

27. McLeod HL, Relling M V, Crom WR, *et al.* Disposition of antineoplastic agents in the very young child. In: *British Journal of Cancer*. Vol 66., 1992; 23–9.

28. Anderson GD. Children versus adults: Pharmacokinetic and adverse-effect differences. In: *Epilepsia*. Vol 43. John Wiley & Sons, Ltd, 2002; 53–9.

29. Oshikoya KA, Sammons HM, Choonara I. A systematic review of pharmacokinetics studies in children with protein-energy malnutrition. *Eur J Clin Pharmacol* 2010; **66**: 1025–35.

30. Oshikoya KA, Senbanjo IO. Pathophysiological changes that affect drug disposition in protein-energy malnourished children. *Nutr Metab* 2009; **6**: 50.

31. Krishnaswamy K. Drug Metabolism and Pharmacokinetics in Malnourished Children. *Clin Pharmacokinet* 1989; **17**: 68–88.

32. De Wildt SN, Johnson TN, Choonara I. The effect of age on drug metabolism. *Paediatr Perinat Drug Ther* 2003; **5**: 101–6.

33. Fernandez E, Perez R, Hernandez A, Tejada P, Arteta M, Ramos JT. Factors and mechanisms for pharmacokinetic differences between pediatric population and adults. *Pharmaceutics* 2011; **3**: 53–72.

34. Strolin M, Whomsley R, Baltes EL. Differences in absorption, distribution, metabolism and excretion of xenobiotics between the paediatric and adult populations. *Expert Opin Drug Metab Toxicol* 2005; **1**: 447–71.

35. Benedetti MS, Whomsley R, Canning M. Drug metabolism in the paediatric population and in the elderly. *Drug Discov Today* 2007; **12**: 599–610.

36. Neumann E, Mehboob H, Ramírez J, Mirkov S, Zhang M, Liu W. Age-dependent hepatic UDP-glucuronosyltransferase gene expression and activity in children. *Front Pharmacol* 2016; **7**.

37. Seitz R. Human Immunodeficiency Virus (HIV). *Transfus Med Hemotherapy* 2016; **43**: 203–22.

38. Arts EJ, Hazuda DJ. HIV-1 antiretroviral drug therapy. *Cold Spring Harb Perspect Med* 2012; **2**.

39. Swanstrom R, Coffin J. HIV-1 pathogenesis: The virus. *Cold Spring Harb Perspect Med* 2012; **2**.

40. U.S. Department of Health and Human Services. The HIV Life Cycle | Understanding HIV/AIDS | AIDSinfo. *AIDSinfo* 2019: 2.

41. Naif HM. Pathogenesis of HIV infection. *Infect Dis Rep* 2013; **5**: 26–30.

42. Houben ENG, Nguyen L, Pieters J. Interaction of pathogenic mycobacteria with the host immune system. *Curr Opin Microbiol* 2006; **9**: 76–85.

43. Flynn JL, Chan J. Tuberculosis: Latency and reactivation. *Infect Immun* 2001; **69**: 4195–201.

44. Ulrichs T, Kaufmann SHE. New insights into the function of granulomas in human tuberculosis. *J Pathol* 2006; **208**: 261–9.

45. Henderson RA, Watkins SC, Flynn JL. Activation of human dendritic cells following infection with Mycobacterium tuberculosis. *J Immunol* 1997; **159**: 635–43.

46. Giacomini E, Iona E, Ferroni L, *et al.* Infection of Human Macrophages and Dendritic Cells with Mycobacterium tuberculosis Induces a Differential Cytokine Gene Expression That Modulates T Cell Response. *J Immunol* 2001; **166**: 7033–41.

47. Lazarevic V, Nolt D, Flynn JL. Long-Term Control of Mycobacterium tuberculosis Infection Is Mediated by Dynamic Immune Responses. *J Immunol* 2005; **175**: 1107–17.

48. Diedrich CR, Flynn JAL. HIV-1/Mycobacterium tuberculosis coinfection immunology: How does HIV-1 exacerbate tuberculosis? *Infect Immun* 2011; **79**: 1407–17.

49. Shankar EM, Vignesh R, Ellegård R, *et al.* HIV-Mycobacterium tuberculosis co-infection: A 'danger-couple model' of disease pathogenesis. *Pathog Dis* 2014; **70**: 110–8.

50. Vanham G, Edmonds K, Qing L, *et al.* Generalized immune activation in pulmonary

tuberculosis: Co-activation with HIV infection. *Clin Exp Immunol* 1996; **103**: 30–4.

51. Rosas-Taraco AG, Arce-Mendoza AY, Caballero-Olín G, Salinas-Carmona MC. Mycobacterium tuberculosis upregulates coreceptors CCR5 and CXCR4 while HIV modulates CD14 favoring concurrent infection. *AIDS Res Hum Retroviruses* 2006; **22**: 45–51.

52. Pau AK, George JM. Antiretroviral therapy: Current drugs. *Infect Dis Clin North Am* 2014; **28**: 371–402.

53. Desai M, Iyer G, Dikshit RK. Antiretroviral drugs: Critical issues and recent advances. *Indian J Pharmacol* 2012; **44**: 288–98.

54. Atta MG, De Seigneux S, Lucas GM. Clinical pharmacology in HIV therapy. *Clin J Am Soc Nephrol* 2019; **14**: 435–44.

55. WHO (World Health Organization). Update of Recommendations on First-and Second-Line Antiretroviral Regimens. *World Heal Organ* 2019: 16.

56. Western Cape Health Department. The Western Cape Consolidated Guidelines for HIV Treatment: Prevention of Mother- to- Child Transmission of HIV (PMTCT), Children, Adolescents and Adults. 2018 (Amended Version). 2020; **2020**: 78.

57. South African National Department of Health, DoH. 2019 ART Clinical Guidelines for the Management of HIV in Adults, Pregnancy, Adolescents, Children, Infants and Neonates. 2019: 26. Available at: https://sahivsoc.org/Files/2019 ART Guideline 28042020 pdf.pdf.

58. Letang E, Ellis J, Naidoo K, *et al.* Tuberculosis-HIV Co-Infection: Progress and Challenges After Two Decades of Global Antiretroviral Treatment Roll-Out. *Arch Bronconeumol* 2020; **56**: 446–54.

59. Yuen GJ, Weller S, Pakes GE. A review of the pharmacokinetics of abacavir. *Clin*

Pharmacokinet 2008; **47**: 351–71.

60. Bergshoeff A, Burger D, Verweij C, *et al.* Plasma pharmacokinetics of once- versus twice-daily lamivudine and abacavir: simplification of combination treatment in HIV-1-infected children (PENTA-13). *Antivir Ther* 2005; **10**: 239–46.

61. Kumar PN, Sweet DE, McDowell JA, *et al.* Safety and pharmacokinetics of abacavir (1592U89) following oral administration of escalating single doses in human immunodeficiency virus type 1-infected adults. *Antimicrob Agents Chemother* 1999; **43**: 603–8.

62. Zhao W, Cella M, Della Pasqua O, *et al.* Population pharmacokinetics and maximum a posteriori probability Bayesian estimator of abacavir: Application of individualized therapy in HIV-infected infants and toddlers. *Br J Clin Pharmacol* 2012; **73**: 641–50.

63. Sleasman J, Robbins B, Cross S, *et al.* Abacavir Pharmacokinetics During Chronic Therapy in HIV1 Infected Adolescents and Young Adults. *Am Soc Clin Pharmacol Ther* 2009; **85**: 394–401.

64. Zhao W, Piana C, Danhof M, Burger D, Della Pasqua O, Jacqz-Aigrain E. Population pharmacokinetics of abacavir in infants, toddlers and children. *Br J Clin Pharmacol* 2013; **75**: 1525–35.

65. Jullien V, Urien S, Chappuy H, *et al.* Abacavir pharmacokinetics in human immunodeficiency virus-infected children ranging in age from 1 month to 16 years: a population analysis. *J Clin Pharmacol* 2005; **45**: 257–64.

66. Waters LJ, Moyle G, Bonora S, *et al.* Abacavir plasma pharmacokinetics in the absence and presence of atazanavir/ritonavir or lopinavir/ritonavir and vice versa in HIV-infected patients. *Antivir Ther* 2007; **12**: 825–30.

67. Nahirya-Ntege P, Musiime V, Naidoo B, *et al.* Low incidence of abacavir hypersensitivity

reaction among african children initiating antiretroviral therapy. *Pediatr Infect Dis J* 2011; **30**: 535–7.

68. Blumberg HM, Burman WJ, Chaisson RE, *et al.* American Thoracic Society/Centers for Disease Control and Prevention/Infectious Diseases Society of America: treatment of tuberculosis. *Am J Respir Crit Care Med* 2003; **167**: 603–62.

69. Peloquin CA, Bulpitt AE, Jaresko GS, Jelliffe RW, Childs JM, Nix DE. Pharmacokinetics of ethambutol under fasting conditions, with food, and with antacids. *Antimicrob Agents Chemother* 1999; **43**: 568–72.

70. Bekker A, Schaaf HS, Draper HR, *et al.* Pharmacokinetics of rifampin, isoniazid, pyrazinamide, and ethambutol in infants dosed according to revised whorecommended treatment guidelines. *Antimicrob Agents Chemother* 2016; **60**: 2171–9.

71. Breda M, Benedetti MS, Bani M, *et al.* Effect of rifabutin on ethambutol pharmacokinetics in healthy volunteers. *Pharmacol Res* 1999; **40**: 351–6.

72. Lee CS, Gambertoglio JG, Craig Brater D, Benet LZ. Kinetics of oral ethambutol in the normal subject. *Clin Pharmacol Ther* 1977; **22**: 615–21.

73. Zhu M, Burman WJ, Starke JR, *et al.* Pharmacokinetics of ethambutol in children and adults with tuberculosis. *Int J Tuberc Lung Dis* 2004; **8**: 1360–7.

74. Hall RG, Swancutt MA, Meek C, Leff RD, Gumbo T. Ethambutol pharmacokinetic variability is linked to body mass in overweight, obese, and extremely obese people. *Antimicrob Agents Chemother* 2012; **56**: 1502–7.

75. Denti P, Jeremiah K, Chigutsa E, *et al.* Pharmacokinetics of isoniazid, pyrazinamide, and ethambutol in newly diagnosed pulmonary TB patients in Tanzania Subbian S, ed. *PLoS One*

2015; **10**: e0141002.

76. Jönsson S, Davidse A, Wilkins J, *et al.* Population pharmacokinetics of ethambutol in South African tuberculosis patients. *Antimicrob Agents Chemother* 2011; **55**: 4230–7.

77. Smythe WA. Characterizing population pharmacokinetic/pharmacodynamic relationships in pulmonary tuberculosis infected adults using nonlinear mixed effects modelling. 2016.

78. McIlleron H, Wash P, Burger A, Norman J, Folb PI, Smith P. Determinants of rifampin, isoniazid, pyrazinamide, and ethambutol pharmacokinetics in a cohort of tuberculosis patients. *Antimicrob Agents Chemother* 2006; **50**: 1170–7.

79. Donald PR, Maher D, Maritz JS, Qazi S. Ethambutol dosage for the treatment of children: Literature review and recommendations. *Int J Tuberc Lung Dis* 2006; **10**: 1318–30.

80. Alsultan A, Peloquin CA. Therapeutic drug monitoring in the treatment of tuberculosis: An update. *Drugs* 2014; **74**: 839–54.

81. Girling DJ. The hepatic toxicity of antituberculosis regimens containing isoniazid, rifampicin and pyrazinamide. *Tubercle* 1977; **59**: 13–32.

82. Croxtall JD, Perry CM. LopinavirRitonavir: A review of its use in the management of HIV-1 infection. *Drugs* 2010; **70**: 1885–915.

83. Teply R, Goodman M, Destache CJ. Lopinavir/ritonavir: A review for 2011. *Clin Med Insights Ther* 2011; **3**: 93–102.

84. Oldfield V, Plosker GL. Lopinavir/ritonavir: A review of its use in the management of HIV infection. *Drugs* 2006; **66**: 1275–99.

85. Acocella G. Clinical Pharmacokinetics of Rifampicin. *Clin Pharmacokinet* 1978; **3**: 108–27.

86. Saktiawati AMI, Sturkenboom MGG, Stienstra Y, *et al.* Impact of food on the

pharmacokinetics of first-line anti-TB drugs in treatment-naive TB patients: a randomized cross-over trial. *J Antimicrob Chemother* 2016; **71**: 703–10.

87. Acocella G. Pharmacokinetics and metabolism of rifampin in humans. *Rev Infect Dis* 1983; **5**: S428–32.

88. Boman G, Ringberger VA. Binding of rifampicin by human plasma proteins. *Eur J Clin Pharmacol* 1974; **7**: 369–73.

89. Chen J, Raymond K. Roles of rifampicin in drug-drug interactions: Underlying molecular mechanisms involving the nuclear pregnane X receptor. *Ann Clin Microbiol Antimicrob* 2006; **5**: 3.

90. Niemi M, Backman JT, Fromm MF, Neuvonen PJ, Kivistö KT. Pharmacokinetic interactions with rifampicin: Clinical relevance. *Clin Pharmacokinet* 2003; **42**: 819–50.

91. Caniglia EC, Phillips A, Porter K, *et al.* Commonly Prescribed Antiretroviral Therapy Regimens and Incidence of AIDS-Defining Neurological Conditions. *J Acquir Immune Defic Syndr* 2018; **77**: 102–9.

92. McDonagh EM, Lau JL, Alvarellos ML, Altman RB, Klein TE. PharmGKB summary: Efavirenz pathway, pharmacokinetics. *Pharmacogenet Genomics* 2015; **25**: 363–76.

93. Avery LB, Sacktor N, McArthur JC, Hendrix CW. Protein-free efavirenz concentrations in cerebrospinal fluid and blood plasma are equivalent: Applying the law of mass action to predict protein-free drug concentration. *Antimicrob Agents Chemother* 2013; **57**: 1409–14.

94. Faucette SR, Zhang TC, Moore R, *et al.* Relative activation of human pregnane X receptor versus constitutive androstane receptor defines distinct classes of CYP2B6 and CYP3A4 inducers. *J Pharmacol Exp Ther* 2007; **320**: 72–80.

95. Svärd J, Spiers JP, Mulcahy F, Hennessy M. Nuclear receptor-mediated induction of CYP450 by antiretrovirals: Functional consequences of NR1I2 (PXR) polymorphisms and differential prevalence in whites and sub-Saharan Africans. *J Acquir Immune Defic Syndr* 2010; **55**: 536–49.

96. Adkins JC, Noble S. Efavirenz. *Drugs* 1998; **56**: 1055–64.

97. Hariparsad N, Nallani SC, Sane RS, Buckley DJ, Buckley AR, Desai PB. Induction of CYP3A4 by efavirenz in primary human hepatocytes: Comparison with rifampin and phenobarbital. *J Clin Pharmacol* 2004; **44**: 1273–81.

98. Whiting B, Kelman AW, Grevel J. Population Pharmacokinetics Theory and Clinical Application. *Clin Pharmacokinet* 1986; **11**: 387–401.

99. Gobburu JVS. Pharmacometrics 2020. *J Clin Pharmacol* 2010; **50**.

100. Barrett JS, Fossler MJ, Cadieu KD, Gastonguay MR. Pharmacometrics: A multidisciplinary field to facilitate critical thinking in drug development and translational research settings. *J Clin Pharmacol* 2008; **48**: 632–49.

101. Gisleskog PO, Karlsson MO, Beal SL. Use of prior information to stabilize a population data analysis. *J Pharmacokinet Pharmacodyn* 2002; **29**: 473–505.

102. Manolis E, Osman TE, Herold R, *et al.* Role of modeling and simulation in pediatric investigation plans. *Paediatr Anaesth* 2011; **21**: 214–21.

103. Wickham H. Mastering Shiny. 2019: 298.

104. Beeley C, Sukhdeve SR. *Web Application Development with R using Shiny*. 2018.

105. Mulenga V, Musiime V, Kekitiinwa A, *et al.* Abacavir, zidovudine, or stavudine as paediatric tablets for African HIV-infected children (CHAPAS-3): an open-label, parallel-group, randomised controlled trial. *Lancet Infect Dis* 2016; **16**: 169–79.

106. Gibb DM. Routine versus clinically driven laboratory monitoring and fi rst-line antiretroviral therapy strategies in African children with HIV (ARROW): A 5-year open-label randomised factorial trial. *Lancet* 2013; **381**: 1391–403.

107. Musiime V, Kendall L, Bakeera-Kitaka S, *et al.* Pharmacokinetics and acceptability of once- versus twice-daily lamivudine and abacavir in HIV type-1-infected Ugandan children in the ARROW Trial. *Antivir Ther* 2010; **15**: 1115–24.

108. Rabie H, Tikiso T, Lee J, *et al.* Abacavir exposure in children cotreated for tuberculosis with rifampin and superboosted lopinavir-ritonavir. *Antimicrob Agents Chemother* 2020; **64**.

109. Rabie H, Denti P, Lee J, *et al.* Lopinavir–ritonavir super-boosting in young HIV-infected children on rifampicin-based tuberculosis therapy compared with lopinavir–ritonavir without rifampicin: a pharmacokinetic modelling and clinical study. *Lancet HIV* 2019; **6**: e32–42.

110. Archary M, McLlleron H, Bobat R, *et al.* Population Pharmacokinetics of Lopinavir in Severely Malnourished HIV-infected Children and the Effect on Treatment Outcomes. *Pediatr Infect Dis J* 2018; **37**: 349–55.

111. Archary M, Mcllleron H, Bobat R, *et al.* Population pharmacokinetics of abacavir and lamivudine in severely malnourished human immunodeficiency virus-infected children in relation to treatment outcomes. *Br J Clin Pharmacol* 2019; **85**: 2066–75.

112. Chabala C, Turkova A, Thomason MJ, *et al.* Shorter treatment for minimal tuberculosis (TB) in children (SHINE): A study protocol for a randomised controlled trial. *Trials* 2018; **19**: 237.

113. McIlleron H, Hundt H, Smythe W, *et al.* Bioavailability of two licensed paediatric rifampicin suspensions: Implications for quality control programmes. *Int J Tuberc Lung Dis* 2016; **20**: 915–9.

114. Sheiner LB, Ludden TM. Population pharmacokinetics/dynamics. *Annu Rev Pharmacol Toxicol* 1992; **32**: 185–209.

115. Mould DR, Upton RN. Basic concepts in population modeling, simulation, and model-based drug development-part 2: introduction to pharmacokinetic modeling methods. *CPT pharmacometrics Syst Pharmacol* 2013; **2**: e38.

116. Bonate PL. *Pharmacokinetic-Pharmacodynamic Modeling and Simulation*. Springer US; 2011.

117. Ette E, Roy A. *Pharmacometrics : The Science of Quantitative Pharmacology*. John Wiley & Sons; 2007.

118. Laveille M. *Mixed Effects Models for the Population Approach Models , Tasks , Methods and Tools*. Chapman and Hall/CRC; 2014.

119. Gibiansky L, Gibiansky E, Bauer R. Comparison of Nonmem 7.2 estimation methods and parallel processing efficiency on a target-mediated drug disposition model. *J Pharmacokinet Pharmacodyn* 2012; **39**: 17–35.

120. Keizer RJ, Karlsson MO, Hooker A. Modeling and Simulation Workbench for NONMEM: Tutorial on Pirana, PsN, and Xpose. *CPT pharmacometrics Syst Pharmacol* 2013; **2**: e50.

121. Savic RM, Jonker DM, Kerbusch T, Karlsson MO. Implementation of a transit compartment model for describing drug absorption in pharmacokinetic studies. *J Pharmacokinet Pharmacodyn* 2007; **34**: 711–26.

122. Beal SL. Ways to fit a PK model with some data below the quantification limit. *J Pharmacokinet Pharmacodyn* 2001; **28**: 481–504.

123. Foster DM. Noncompartmental Versus Compartmental Appoaches To Pharmacokinetic

Analysis. *Princ Clin Pharmacol* 2007: 102–30.

124. Van Hasselt JGC, van Eijkelenburg NKA, Beijnen JH, Schellens JHM, Huitema ADR. Optimizing drug development of anti-cancer drugs in children using modelling and simulation. *Br J Clin Pharmacol* 2013; **76**: 30–47.

125. Manolis E, Pons G. Proposals for model-based paediatric medicinal development within the current European Union regulatory framework. *Br J Clin Pharmacol* 2009; **68**: 493–501.

126. Collart L, Blaschke TF, Boucher F, Prober CG. Potential of population pharmacokinetics to reduce the frequency of blood sampling required for estimating kinetic parameters in neonates. *Dev Pharmacol Ther* 1992; **18**: 71–80.

127. Cella M, Zhao W, Jacqz-Aigrain E, Burger D, Danhof M, Della Pasqua O. Paediatric drug development: are population models predictive of pharmacokinetics across paediatric populations? *Br J Clin Pharmacol* 2011; **72**: 454–64.

128. Cella M, Gorter de Vries F, Burger D, Danhof M, Della Pasqua O. A model-based approach to dose selection in early pediatric development. *Clin Pharmacol Ther* 2010; **87**: 294–302.

129. De Cock RFW, Piana C, Krekels EHJ, Danhof M, Allegaert K, Knibbe C a J. The role of population PK-PD modelling in paediatric clinical research. *Eur J Clin Pharmacol* 2011; **67 Suppl 1**: 5–16.

130. Cella M, Knibbe C, Danhof M, Della Pasqua O. What is the right dose for children? *Br J Clin Pharmacol* 2010; **70**: 597–603.

131. Johnson TN. Modelling approaches to dose estimation in children. *Br J Clin Pharmacol* 2005; **59**: 663–9.

132. Tod M, Jullien V, Pons G. Facilitation of drug evaluation in children by population methods

and modelling. *Clin Pharmacokinet* 2008; **47**: 231–43.

133. Gobburu JVS, Marroum PJ. Utilisation of pharmacokinetic-pharmacodynamic modelling and simulation in regulatory decision-making. *Clin Pharmacokinet* 2001; **40**: 883–92.

134. Bellanti F, Della Pasqua O. Modelling and simulation as research tools in paediatric drug development. *Eur J Clin Pharmacol* 2011; **67 Suppl 1**: 75–86.

135. World Health Organization. *Updated recommendations on first-line and second-line antiretroviral regimens and post-exposure prophylaxis and recommendations on early infant diagnosis of HIV.* World Health Organization; 2019.

136. Jacqz-Aigrain E, Harrison L, Zhao W, *et al.* Pharmacokinetic study of once-daily versus twice-daily abacavir and lamivudine in HIV type-1-infected children aged 3-<36 months. *Antivir Ther* 2010; **15**: 297–305.

137. Western Cape Health Department. *The Western Cape Consolidated Guidelines for HIV Treatment: Prevention of Mother- to- Child Transmission of HIV (PMTCT), Children, Adolescents and Adults. 2018 (Amended Version)*. 2018.

138. McDowell JA, Chittick GE, Stevens CP, Edwards KD, Stein DS. Pharmacokinetic interaction of abacavir (1592U89) and ethanol in human immunodeficiency virus-infected adults. *Antimicrob Agents Chemother* 2000; **44**: 1686–90.

139. Yuen GJ, Weller S, Pakes GE. A review of the pharmacokinetics of abacavir. *Clin Pharmacokinet* 2008; **47**: 351–71.

140. Lindsey JC, Hughes MD, Violari A, *et al.* Predictors of Virologic and Clinical Response to Nevirapine versus Lopinavir/Ritonavir-based Antiretroviral Therapy in Young Children With and Without Prior Nevirapine Exposure for the Prevention of Mother-to-child HIV Transmission.

Pediatr Infect Dis J 2014; **33**: 846–54.

141. Violari A, Lindsey JC, Hughes MD, *et al.* Nevirapine versus Ritonavir-Boosted Lopinavir for HIV-Infected Children. *N Engl J Med* 2012; **366**: 2380–9.

142. Kumar GN, Jayanti VK, Johnson MK, *et al.* Metabolism and disposition of the HIV-1 protease inhibitor lopinavir (ABT-378) given in combination with ritonavir in rats, dogs, and humans. *Pharm Res* 2004; **21**: 1622–30.

143. Perloff MD, Von Moltke LL, Marchand JE, Greenblatt DJ. Ritonavir induces P-glycoprotein expression, multidrug resistance-associated protein (MRP1) expression, and drug transporter-mediated activity in a human intestinal cell line. *J Pharm Sci* 2001; **90**: 1829–37.

144. Gordon LA, Malati CY, Hadigan C, *et al.* Lack of an Effect of Ritonavir Alone and Lopinavir-Ritonavir on the Pharmacokinetics of Fenofibric Acid in Healthy Volunteers. *Pharmacotherapy* 2016; **36**: 49–56.

145. Mugundu G, Hariparsad N, Desai P. Impact of Ritonavir, Atazanavir and Their Combination on the CYP3A4 Induction by Efavirenz in Primary Human Hepatocytes. *Drug Metab Lett* 2010; **4**: 45–50.

146. Fahmi OA, Ripp SL. Evaluation of models for predicting drug–drug interactions due to induction. *Expert Opin Drug Metab Toxicol* 2010; **6**: 1399–416.

147. Fahmi OA, Kish M, Boldt S, Scott Obach R. Cytochrome P450 3A4 mRNA is a more reliable marker than CYP3A4 activity for detecting pregnane X receptor-activated induction of drug-metabolizing enzymes. *Drug Metab Dispos* 2010; **38**: 1605–11.

148. B-Lajoie MR, Drouin O, Bartlett G, *et al.* Incidence and Prevalence of Opportunistic and Other Infections and the Impact of Antiretroviral Therapy among HIV-infected Children in Low-

and Middle-income Countries: A Systematic Review and Meta-analysis. *Clin Infect Dis* 2016; **62**: 1586–94.

149. Dresser GK, Spence JD, Bailey DG. Pharmacokinetic-pharmacodynamic consequences and clinical relevance of cytochrome P450 3A4 inhibition. *Clin Pharmacokinet* 2000; **38**: 41–57.

150. Mahatthanatrakul W, Nontaput T, Ridtitid W, Wongnawa M, Sunbhanich M. Rifampin, a cytochrome P450 3A inducer, decreases plasma concentrations of antipsychotic risperidone in healthy volunteers. *J Clin Pharm Ther* 2007; **32**: 161–7.

151. Johnson LF, Davies M-A, Moultrie H, *et al.* The Effect of Early Initiation of Antiretroviral Treatment in Infants on Pediatric AIDS Mortality in South Africa A Model-based Analysis. *HIV REPORTS Pediatr Infect Dis J* 2012; **31**.

152. Rabie H, Denti P, Lee J, *et al.* Lopinavir-ritonavir super-boosting in young HIV-infected children on rifampicin-based tuberculosis therapy compared with lopinavir-ritonavir without rifampicin: a pharmacokinetic modelling and clinical study. *lancet HIV* 2018; **6**: e32–42.

153. Boeckmann AJ, Beal SL, Sheiner LB. NONMEM User's Guide, Part V. Introductory Guide. *NONMEM Proj Gr* 1998: 48.

154. Anderson BJ, Holford NHG. Mechanism-based concepts of size and maturity in pharmacokinetics. *Annu Rev Pharmacol Toxicol* 2008; **48**: 303–32.

155. World Health Organization. *WHO child growth standards : head circumference-for-age, arm circumference-for-age, triceps skinfold-for-age and subscapular skinfold-for-age : methods and development*. 2007.

156. Dosne AG, Bergstrand M, Harling K, Karlsson MO. Improving the estimation of parameter uncertainty distributions in nonlinear mixed effects models using sampling importance

resampling. *J Pharmacokinet Pharmacodyn* 2016; **43**: 583–96.

157. Svensson EM, Yngman G, Denti P, McIlleron H, Kjellsson MC, Karlsson MO. Evidence-Based Design of Fixed-Dose Combinations: Principles and Application to Pediatric Anti-Tuberculosis Therapy. *Clin Pharmacokinet* 2018; **57**: 591–9.

158. Yuen GJ, Weller S, Pakes GE. A review of the pharmacokinetics of abacavir. *Clin Pharmacokinet* 2008; **47**: 351–71.

159. Weller S, Radomski KM, Lou Y, Daniel S, Stein DS. Population Pharmacokinetics and Pharmacodynamic Modeling of Abacavir Trial with Human Immunodeficiency Virus-Infected Subjects Population Pharmacokinetics and Pharmacodynamic Modeling of Abacavir (1592U89) from a Dose-Ranging , Double-Blind , Randomized. *Antimicrob Agents Chemother* 2000; **44**: 2052–60.

160. Jackson A, Moyle G, Dickinson L, *et al.* Pharmacokinetics of abacavir and its anabolite carbovir triphosphate without and with darunavir/ritonavir or raltegravir in HIV-infected subjects. *Antivir Ther* 2012; **17**: 19–24.

161. Hughes W, McDowell JA, Shenep J, *et al.* Safety and single-dose pharmacokinetics of abacavir (1592U89) in human immunodeficiency virus type 1-infected children. *Antimicrob Agents Chemother* 1999; **43**: 609–15.

162. Van Heeswijk RPG, Bourbeau M, Seguin I, Giguere P, Garber GE, Cameron DW. Absence of circadian variation in the pharmacokinetics of lopinavir/ritonavir given as a once daily dosing regimen in HIV-1-infected patients. *Br J Clin Pharmacol* 2005; **59**: 398–404.

163. Kline MW, Blanchard S, Fletcher C V., *et al.* A phase I study of abacavir (1592U89) alone and in combination with other antiretroviral agents in infants and children with human

immunodeficiency virus infection. AIDS Clinical Trials Group 330 Team. *Pediatrics* 1999; **103**: e47–e47.

164. Chittick GE, Gillotin C, McDowell JA, *et al.* Abacavir: Absolute Bioavailability, Bioequivalence of Three Oral Formulations, and Effect of Food. *Pharmacotherapy* 1999; **19**: 932–42.

165. Quellet D, Hsu A, Granneman GR, *et al.* Pharmacokinetic interaction between ritonavir and clarithromycin. *Clin Pharmacol Ther* 1998; **64**: 355–62.

166. Hsu A, Granneman GR, Witt G, *et al.* Multiple-dose pharmacokinetics of ritonavir in human immunodeficiency virus-infected subjects. *Antimicrob Agents Chemother* 1997; **41**: 898–905.

167. Bienczak A, Cook A, Wiesner L, *et al.* The impact of genetic polymorphisms on the pharmacokinetics of efavirenz in African children. *Br J Clin Pharmacol* 2016; **82**: 185–98.

168. Panhard X, Goujard C, Legrand M, Taburet AM, Diquet B, Mentré F. Population pharmacokinetic analysis for nelfinavir and its metabolite M8 in virologically controlled HIV-infected patients on HAART. *Br J Clin Pharmacol* 2005; **60**: 390–403.

169. Lemmer B, Nold G. Circadian changes in estimated hepatic blood flow in healthy subjects. *Br J Clin Pharmacol* 1991; **32**: 627–9.

170. Moyle G, Boffito M, Fletcher C, *et al.* Steady-state pharmacokinetics of abacavir in plasma and intracellular carbovir triphosphate following administration of abacavir at 600 milligrams once daily and 300 milligrams twice daily in human immunodeficiency virus-infected subjects. *Antimicrob Agents Chemother* 2009; **53**: 1532–8.

171. UNAIDS. Factsheet - July 2018: 2017 Global Hiv Statistics. *Unaids* 2018: 6. Available at: https://www.unaids.org/en/resources/fact-sheet.

172. Bergshoeff A, Burger D, Verweij C, *et al.* Plasma pharmacokinetics of once- versus twice-daily lamivudine and abacavir: Simplification of combination treatment in HIV-1-infected children (PENTA-13). *Antivir Ther* 2005; **10**: 239–46.

173. Zhao W, Piana C, Danhof M, Burger D, Della Pasqua O, Jacqz-Aigrain E. Population pharmacokinetics of abacavir in infants, toddlers and children. *Br J Clin Pharmacol* 2013; **75**: 1525–35.

174. Archary M, Mcllleron H, Bobat R, *et al.* Population pharmacokinetics of abacavir and lamivudine in severely malnourished human immunodeficiency virus-infected children in relation to treatment outcomes. *Br J Clin Pharmacol* 2019; **85**: 2066–75.

175. Rabie H, Tikiso T, Lee J, *et al.* Abacavir exposure in children co-treated for tuberculosis with rifampicin and super-boosted lopinavir-ritonavir. *Antimicrob Agents Chemother* 2020.

176. Rhodin MM, Anderson BJ, Peters AM, *et al.* Human renal function maturation: A quantitative description using weight and postmenstrual age. *Pediatr Nephrol* 2009; **24**: 67–76.

177. Anderson BJ, Holford NHG. Mechanistic Basis of Using Body Size and Maturation to Predict Clearance in Humans. *Drug Metab Pharmacokinet* 2009; **24**: 25–36.

178. Svensson E, van der Walt JS, Barnes KI, *et al.* Integration of data from multiple sources for simultaneous modelling analysis: Experience from nevirapine population pharmac okinetics. *Br J Clin Pharmacol* 2012; **74**: 465–76.

179. Karlsson MO, Sheiner LB. The importance of modeling interoccasion variability in population pharmacokinetic analyses. *J Pharmacokinet Biopharm* 1993; **21**: 735–50.

180. Germovsek E, Barker CIS, Sharland M, Standing JF. Scaling clearance in paediatric pharmacokinetics: All models are wrong, which are useful? *Br J Clin Pharmacol* 2017; **83**: 777–

90.

181. Germovsek E, Barker CIS, Sharland M, Standing JF. Pharmacokinetic–Pharmacodynamic Modeling in Pediatric Drug Development, and the Importance of Standardized Scaling of Clearance. *Clin Pharmacokinet* 2019; **58**: 39–52.

182. Group WMGRS. WHO Child Growth Standards: Head circumference-for-age, arm circumference-for-age, triceps skinfold-for-age and subscapular skinfold-for-age: Methods and. *Geneva World Heal …* 2007.

183. CHMP. *Ziagen - ANNEX I SUMMARY OF PRODUCT CHARACTERISTICS*. 2014. Available at: https://www.ema.europa.eu/documents/product-information/trulicity-epar-product-information_en.pdf.

184. Venkatesan K. Pharmacokinetic Drug Interactions with Rifampicin. *Clin Pharmacokinet* 1992; **22**: 47–65.

185. Barry M, Feely J. Enzyme induction and inhibition. *Pharmacol Ther* 1990; **48**: 71–94.

186. Lee LS, Pham P, Flexner C. Unexpected drug-drug interactions in human immunodeficiency virus (HIV) therapy: Induction of ugt1a1 and bile efflux transporters by efavirenz. *Ann Acad Med Singapore* 2012; **41**: 559–62.

187. Lang CH, Frost RA, Nairn AC, MacLean DA, Vary TC. TNF-α impairs heart and skeletal muscle protein synthesis by altering translation initiation. *Am J Physiol - Endocrinol Metab* 2002; **282**.

188. Kaysen GA. Association between inflammation and malnutrition as risk factors of cardiovascular disease. *Blood Purif* 2006; **24**: 51–5.

189. Kaysen GA, Chertow GM, Adhikarla R, Young B, Ronco C, Levin NW. Inflammation and

dietary protein intake exert competing effects on serum albumin and creatinine in hemodialysis patients. *Kidney Int* 2001; **60**: 333–40.

190. Richardson TA, Sherman M, Kalman D, Morgan ET. Expression of UDP-glucuronosyltransferase isoform mRNAs during inflammation and infection in mouse liver and kidney. *Drug Metab Dispos* 2006; **34**: 351–3.

191. Wu KC, Lin CJ. The regulation of drug-metabolizing enzymes and membrane transporters by inflammation: Evidences in inflammatory diseases and age-related disorders. *J Food Drug Anal* 2019; **27**: 48–59.

192. Kruk A, Bannister W, Podlekareva DN, *et al.* Tuberculosis among HIV-positive patients across Europe. *AIDS* 2011; **25**: 1505–13.

193. Alghamdi WA, Al-Shaer MH, Peloquin CA. Protein binding of first-line antituberculosis drugs. *Antimicrob Agents Chemother* 2018; **62**.

194. Aaron L, Saadoun D, Calatroni I, *et al.* Tuberculosis in HIV-infected patients: A comprehensive review. *Clin Microbiol Infect* 2004; **10**: 388–98.

195. Peloquin CA, Macphee AA, Berning SE. Malabsorption of Antimycobacterial Medications. *N Engl J Med* 1993; **329**: 1122–3.

196. Antwi S, Yang H, Enimil A, *et al.* Pharmacokinetics of the first-line antituberculosis drugs in Ghanaian children with tuberculosis with or without HIV coinfection. *Antimicrob Agents Chemother* 2017; **61**.

197. National Center for Biotechnology Information. PubChem Compound Summary for CID 14051, Ethambutol Hydrochloride. Available at: https://pubchem.ncbi.nlm.nih.gov/compound/Ethambutol-Hydrochloride.

198. National Center for Biotechnology Information. PubChem Compound Summary for CID 14052, Ethambutol. Available at: https://pubchem.ncbi.nlm.nih.gov/compound/Ethambutol.

199. Svensson E, van der Walt JS, Barnes KI, *et al.* Integration of data from multiple sources for simultaneous modelling analysis: Experience from nevirapine population pharmac okinetics. *Br J Clin Pharmacol* 2012; **74**: 465–76.

200. Anderson BJ, Holford NHG. Mechanism-Based Concepts of Size and Maturity in Pharmacokinetics. *Annu Rev Pharmacol Toxicol* 2008; **48**: 303–32.

201. Graham SM, Bell DJ, Nyirongo S, Hartkoorn R, Ward SA, Molyneux EM. Low levels of pyrazinamide and ethambutol in children with tuberculosis and impact of age, nutritional status, and human immunodeficiency virus infection. *Antimicrob Agents Chemother* 2006; **50**: 407–13.

202. Verhagen LM, López D, Hermans PWM, *et al.* Pharmacokinetics of anti-tuberculosis drugs in Venezuelan children younger than 16years of age: Supportive evidence for the implementation of revised WHO dosing recommendations. *Trop Med Int Heal* 2012; **17**: 1449–56.

203. Hiruy H, Rogers Z, Mbowane C, *et al.* Subtherapeutic concentrations of first-line anti-TB drugs in South African children treated according to current guidelines: The PHATISA study. *J Antimicrob Chemother* 2014; **70**: 1115–23.

204. Mukherjee A, Velpandian T, Singla M, Kanhiya K, Kabra SK, Lodha R. Pharmacokinetics of isoniazid, rifampicin, pyrazinamide and ethambutol in Indian children. *BMC Infect Dis* 2015; **15**: 126.

205. Hartkoorn RC, Chandler B, Owen A, *et al.* Differential drug susceptibility of intracellular and

extracellular tuberculosis, and the impact of P-glycoprotein. *Tuberculosis* 2007; **87**: 248–55.

206. Kirby BJ, Collier AC, Kharasch ED, Whittington D, Thummel KE, Unadkat JD. Complex drug interactions of HIV protease inhibitors 1: Inactivation, induction, and inhibition of cytochrome P450 3A by ritonavir or nelfinavir. *Drug Metab Dispos* 2011; **39**: 1070–8.

207. Marzolini C, Gibbons S, Khoo S, Back D. Cobicistat versus ritonavir boosting and differences in the drug-drug interaction profiles with co-medications. *J Antimicrob Chemother* 2016; **71**: 1755–8.

208. Patel KB, Belmonte R, Crowe HM. Drug Malabsorption and Resistant Tuberculosis in HIV-Infected Patients. *N Engl J Med* 1995; **332**: 336–7.

209. Gurumurthy P, Ramachandran G, Hemanth Kumar AK, *et al.* Malabsorption of Rifampin and Isoniazid in HIV-Infected Patients With and Without Tuberculosis. *Clin Infect Dis* 2004; **38**: 280–3.

210. Pinheiro VGF, Ramos LMA, Monteiro HSA, *et al.* Intestinal permeability and malabsorption of rifampin and isoniazid in active pulmonary tuberculosis. *Brazilian J Infect Dis* 2006; **10**: 374–9.

211. Daskapan A, Idrus LR, Postma MJ, *et al.* A Systematic Review on the Effect of HIV Infection on the Pharmacokinetics of First-Line Tuberculosis Drugs. *Clin Pharmacokinet* 2019; **58**: 747–66.

212. Richey RH, Shah UU, Peak M, *et al.* Manipulation of drugs to achieve the required dose is intrinsic to paediatric practice but is not supported by guidelines or evidence. *BMC Pediatr* 2013; **13**.

213. Matsuo Y, Ishibashi T, Shimamura K, Wajima T. Prediction of Pharmacokinetics and Pharmacodynamics of Doripenem in Pediatric Patients. *J Pharm Sci* 2015; **104**: 3194–8.

214. Dunne J, Rodriguez WJ, Murphy MD, *et al.* Extrapolation of adult data and other data in pediatric drug-development programs. *Pediatrics* 2011; **128**: e1242–9.

215. Holford N, Heo YA, Anderson B. A pharmacokinetic standard for babies and adults. *J Pharm Sci* 2013; **102**: 2941–52.

216. WHO (World Health Organization). Toolkit for research and development of paediatric antiretroviral drugs and formulations. 2018. Available at: https://www.who.int/hiv/pub/research-dev-toolkit-paediatric-arv-drug-formulation/en/.

217. Paolo Denti, Nandita Sugandhi, Tim R. Cressey, Mark Mirochnick, Edmund V. Capparelli MP. AN EASY-TO-USE PAEDIATRIC DOSING TOOL: ONE MG/KG DOSE DOES NOT FIT ALL. In: Seattle, Washington, 2017. Available at: https://www.croiconference.org/abstract/easy-use-paediatric-dosing-tool-one-mgkg-dose-does-not-fit-all/.

218. RStudio Team. RStudio Inc. shiny: Web Application Framework for R.R package version 1.5.0. 2020.

219. R Core Team. R: a language and environment for statistical computing. 2020. Available at: http://www.r-project.org/.

220. Wojciechowski J, Hopkins AM, Upton RN. Interactive pharmacometric applications using R and the Shiny package. *CPT Pharmacometrics Syst Pharmacol* 2015; **4**: 146–59.

221. Marc Lavielle. mlxR: Simulation of Longitudinal Data. R package version 4.1.0. 2019. Available at: https://cran.r-project.org/package=mlxR.

Appendix 1: NONMEM scripts

Final NONMEM scripts for results presented in chapter 3

```
$SIZES     PD=-1000 LVR=-150 LTH=-200 MAXFCN=10000000 LNP4=-150000
$PROBLEM   ABACAVIR_DNDI
$INPUT     ID DATE_ORG=DROP TIME_ORG=DROP VISIT OCC
           TIME WHAT=DROP EVID NIGHT AMT SS=DROP II=DROP DV
           DVID MDV FLAG BLQ SEX AGE WT HT HAZ WAZ BAZ COMMENTS=DROP
$DATA      DNDI_20190502_SH.csv IGNORE=@ IGNORE=(FLAG.GT.0)
           IGNORE=(DVID.GT.1)
$SUBROUTINE ADVAN13 TRANS1 TOL=9 SSTOL=3,SSATOL=3 ; 2 compartments
$MODEL     NCOMPARTMENTS=3 COMP=(ABS DEFDOSE) COMP=(CENTRAL DEFOBSERVATION)COMP=(PERI1)
;-------------------------------------------------------------------------
$PK
; ---------- BOV----------
   BOVBIO = ETA(10)
   BOVKA  = ETA(16)
   BOVMTT = ETA(22)

IF (OCC==1) THEN
   BOVBIO = ETA(11)
   BOVKA  = ETA(17)
   BOVMTT = ETA(23)
ENDIF
IF (OCC==2) THEN
   BOVBIO = ETA(12)
   BOVKA  = ETA(18)
   BOVMTT = ETA(24)
ENDIF
IF (OCC==3) THEN
   BOVBIO = ETA(13)
   BOVKA  = ETA(19)
   BOVMTT = ETA(25)
ENDIF
IF (OCC==4) THEN
   BOVBIO = ETA(14)
   BOVKA  = ETA(20)
   BOVMTT = ETA(26)
ENDIF
IF (OCC==5) THEN
   BOVBIO = ETA(15)
   BOVKA  = ETA(21)
   BOVMTT = ETA(27)
ENDIF

BOVCL = ETA(7)
```

```
IF(VISIT==1) THEN
  BOVCL = ETA(8)
ENDIF
 IF(VISIT==2) THEN
  BOVCL = ETA(9)
ENDIF
; ------- BSV-------------
BSVCL  = ETA(1)
BSVV   = ETA(2)
BSVKA  = ETA(3)
BSVBIO = ETA(4)
BSVV3  = ETA(5)
BSVQ   = ETA(6)

VISIT_BIO=1
IF(VISIT==1.OR.VISIT==2) VISIT_BIO = THETA(14)

;----------Accounting for variability in BIO in un-observed occasions--------
OCC_BOVBIO=1

IF(OCC==1.OR.OCC==3.OR.OCC==5) OCC_BOVBIO = THETA(11)

BOVBIO =  BOVBIO * OCC_BOVBIO
;-------ACCOUNTING FOR DIFFRENT BIOAVALIBITY IN in un-observed occasions--
OCC_BIO=1
IF(OCC==1.OR.OCC==3.OR.OCC==5) OCC_BIO = THETA(12)

NIGHT_CL=1
IF(NIGHT==1) NIGHT_CL = THETA(15)

; ---------- Calculation of Fat-free Mass
; These formulas require WT in KG and HT in m !!!

; Conversion from cm to m
HTM = HT/100

IF (SEX.EQ.0) THEN  ; female
   WHSMAX=37.99
   WHS50=35.98
ELSE       ;males
   WHSMAX=42.92
   WHS50=30.93
ENDIF
;HTM2 = HTM**2
;FFM = (WHSMAX*HTM2*WT)/(WHS50*HTM2+WT)
;FAT = WT-FFM

; ------- Typical values of covariates
TVWT = 9.4
;TVFAT = 16
;TVFFM = 47
;--------- Allometric scaling and covariates
ALLMCL_WT = (WT/TVWT)**0.75
```

```
ALLMV_WT  = (WT/TVWT)
;--------------Maturation----------------------------------------------
AGE_YRS = AGE

PGA = AGE_YRS + 9/12    ; assumed AGE in years. Adding 0.75 years (9 months) for standard gestation

LOGPGA50 = THETA(13) ; this is the log of age50, so the estimate is in the log scale
GAMMA    = THETA(10)
MATCL    = 0
IF (PGA>0) MATCL=1/(1+EXP(-GAMMA*(LOG(PGA)-LOGPGA50)))
;---------Typical values---------------------------------------------------
TVCL  =  THETA(1)*ALLMCL_WT* MATCL*NIGHT_CL
TVV   =  THETA(2)*ALLMV_WT
TVKA  =  THETA(3)
TVBIO =  THETA(4)*VISIT_BIO*OCC_BIO
TVMTT =  THETA(7)
TVV3  =  THETA(8)*ALLMV_WT
TVQ   =  THETA(9)*ALLMCL_WT
TVNN = THETA(16)
;-----------Define parameters-------------------------------------------------------
CL  =  TVCL*EXP(BSVCL+BOVCL)     ; CLEARANCE
V   =  TVV*EXP(BSVV)             ; CENTRAL VOL.
KA  =  TVKA*EXP(BSVKA+BOVKA)     ; ABS. RATE CONSTANT
BIO =  TVBIO*EXP(BSVBIO+BOVBIO)  ; BIOAVAILABILITY
MTT=  TVMTT*EXP(BOVMTT)          ; MTT TIME
V3  =  TVV3*EXP(BSVV3)           ; PERIPH VOL
Q   =  TVQ*EXP(BSVQ)             ; INTER COMPT CL
NN  = TVNN ; Number of transit compartments
;-----------------------------------------------------------------------------
; re-parameterization

K    =  CL/V ;(rate constant of elimination)
K23  =  Q/V   ; (rate constant from central to peripheral 1)
K32  =  Q/V3 ;(rate constant from peripheral 1 to central)
F1   =  BIO
S2   =  V    ; necessary for these ADVANs (1-4,12,12)
;-----------------------------------------------------------------------------
TVLAG = THETA(17)

BVVLAG = ETA(28)
IF (VISIT==2) BVVLAG = ETA(29)
IF (VISIT==3) BVVLAG = ETA(30)

LAG = TVLAG*EXP(BVVLAG)

ALAG1 = 0
IF (NIGHT==1) ALAG1 = LAG; LAG TIME

; Transit compartment absorption
F1=0 ; I need to set bioavailability in compartment 1 to 0 for this implementation of the transit compartment
absorption

KTR = (NN+1)/MTT
```

```
IF (NEWIND/=2.OR.EVID>=3) THEN ; new individual, or reset event
   ; The values read here will be stored in TDOS and PD in this very PK call.
   TNXD=TIME ; Time of the dose
   PNXD=AMT ; Amount. If it's zero, the DE is deactivated.
ENDIF

DOSTIME = DOSTIM
TDOS=TNXD ; This will either save here the temporary values if it's a new individual...
PD=PNXD ; ...or the values which were read one record ahead during the execution of the previous record.

;IF(AMT>0) THEN ; This reads one record ahead and stores the data to be used when running the following record
 IF(AMT.GT.0.AND.ALAG1.EQ.0) THEN ; Use this INSTEAD if there is ALAG, as it will also checks if the ALAG is not 0.
Note that you normally do not want to include both ALAG and transit, this is a very exceptional case
   TNXD=TIME
   PNXD=AMT
ENDIF

; Uncomment this if you have ALAG or if you use ADDL
 IF (DOSTIM .NE. 0) THEN ; This will account for the ADDL or lagged doses. It will overwrite the time, if it a non-
event record
   TNXD=DOSTIM
   PNXD=AMT
 ENDIF
;LNGAM = NN*LOG(NN)-NN+LOG(NN*(1+4*NN*(1+2*NN)))/6+0.572364942
; To speed up the computation, I calculate here all the non-time-varying quantities used in $DES
PIZZA = LOG(BIO*PD*KTR + 0.00001) - GAMLN(NN+1)   ; without +0.00001, it won't work with ETAs in
bioavailability

; Initialisation
A_0(1) = 0.001
A_0(2) = 0.001
A_0(3) = 0.001
$DES
TEMPO = T-TDOS ; this is time after dose for the transit, it should always be >= 0
KTT = 0
TRANSIT = 0

IF(PD.GT.0.AND.TEMPO.GT.0) THEN ; This happens only id PD>0, so only if a dose has been detected
   KTT = KTR*(TEMPO)
   TRANSIT = EXP(PIZZA+NN*LOG(KTT)-KTT)
ENDIF

DADT(1) = TRANSIT -KA*A(1)
DADT(2) = KA*A(1)-K23*A(2)+K32*A(3)-K*A(2)
DADT(3) = K23*A(2)-K32*A(3)

;-----------------------------------------------------------------------
$ERROR

IPRED = A(2)/V                  ;  individual Plasma concentration of drug
LLOQ = 0.0243 ;DNDI
```

```
; ERROR COMPONENTS
PROP = IPRED*THETA(5)
ADD = 0.2*LLOQ + THETA(6)


; For BLQ==1 (i.e. first BLQ value in a series), we add extra additive error on the concentrations, since the value in DV has been imputed
IF(ICALL.NE.4.AND.BLQ==1) ADD = ADD + (LLOQ/2)

IF(ICALL.NE.4.AND.BLQ==2) THEN
   PROP = 0
   ADD = 100000000
ENDIF

W = SQRT(ADD**2+PROP**2)

Y = IPRED + W*ERR(1)
; Protective code if the W is 0, but it should never happen in this case, as ADD cannot be 0
IF (W.LE.0.000001) W=0.000001

IRES = DV-IPRED
IWRES = IRES/W

; To prevent simulation (ICALL==4) of negative values. It set a positive lower bound for Y, so that VPCs in the log-scale can be plotted
IF (ICALL==4.AND.Y<=LLOQ) Y = LLOQ/2

; To calculate time after dose.
IF(AMT.GT.0) THEN
   TIMEDOSE = TIME
   AMOUNTDOSE = AMT
ENDIF

TAD = TIME-TIMEDOSE
;----------------RETRIEVE AMOUNT IN EACH COMPARTMENT-----------------
AA1 = A(1)
AA2 = A(2)
AA3 = A(3)

VARCL = BSVCL + BOVCL
VARBIO = BSVBIO + BOVBIO
VARAUC = BSVBIO + BOVBIO - BSVCL - BOVCL
;------------------------------------------------------------------------
$THETA
(0, 9.02,30) ; 1 CL [L/h]
(0, 7.85,30) ; 2 V [L]
(0, 2.09,6) ; 3 KA [1/h]
(1) FIX ; 4 BIO
(0, 0.231,1) ; 5 PROP []
(0, 0.00034,3) ; 6 ADD [mg/L]
(0, 0.0988,5) ; 7 MTT
(0, 3.38,10) ; 8 V3 [L]
(0, 1.44,5) ; 9 Q [L/h]
```

```
(0.5, 4.5,6) ; 10 GAMMA []
(0, 1,3) FIX ; 11 OCC_BOVBIO
(0, 1,3) FIX ; 12 OCC_BIO
(-10, -0.156,10) ; 13 logPGA50 [yrs] [log]
(0, 0.606,3) ; 14 VISIT_BIO
(0, 1,5) FIX ; 15 NIGHT_CL
(0, 0.861,50) ; 16 NN
(0, 2.54,5) ; 17 LAG

$OMEGA 0.0207 ;   1 BSV CL
$OMEGA 0 FIX  ;   2 BSV V
$OMEGA 0 FIX  ;   3 BSV KA
$OMEGA 0 FIX  ;  4 BSV BIO
$OMEGA 0.0559 ;   5 BSVV3
$OMEGA 0.0166 ;    6 BSVQ
;-------------------------------------------------
$OMEGA  BLOCK(1)
 0.038 ; 7 BOV CLEARANCE
$OMEGA  BLOCK(1) SAME
$OMEGA  BLOCK(1) SAME
;-------------------------------------------------------
$OMEGA  BLOCK(1)
 0.195 ;  10 BOVBIO
$OMEGA  BLOCK(1) SAME
$OMEGA  BLOCK(1) SAME
$OMEGA  BLOCK(1) SAME
$OMEGA  BLOCK(1) SAME
$OMEGA  BLOCK(1) SAME
;-------------------------------------------------
$OMEGA  BLOCK(1)
 0.284 ;   16 BOVKA
$OMEGA  BLOCK(1) SAME
$OMEGA  BLOCK(1) SAME
$OMEGA  BLOCK(1) SAME
$OMEGA  BLOCK(1) SAME
$OMEGA  BLOCK(1) SAME
;-------------------------------------------------
$OMEGA  BLOCK(1)
 2.09 ;  22 BOVMTT
$OMEGA  BLOCK(1) SAME
$OMEGA  BLOCK(1) SAME
$OMEGA  BLOCK(1) SAME
$OMEGA  BLOCK(1) SAME
$OMEGA  BLOCK(1) SAME
;-----------------------------------------
$OMEGA  BLOCK(1)
 0.00986 ; 28 BVVDELAY
$OMEGA  BLOCK(1) SAME
$OMEGA  BLOCK(1) SAME
;-----------------------------------------------------------------
$SIGMA 1 FIX  ; Scaled RUV variance - IT'S A VARIANCE SO FIXED TO "0" AND ALL ERROR IS GOING TO THE THETAS
AND IT MAKES A SD
;-----------------------------------------------------------------
```

```
$ESTIMATION MSFO=run3042c.msf MAXEVAL=9999 PRINT=1 METHOD=1 INTER
NOABORT NSIG=3 NONINFETA=1 ETASTYPE=1 ATOL=9 SIGL=9
;As the model becomes more complex, you can use MATRIX=S and then remove the $COVARIANCE step
completely when the model is too complex to obtain precisions
;$COVARIANCE PRINT=E ; MATRIX=S
$TABLE WRESCHOL FILE=sdtab3042c.csv ID OCC VISIT TIME TAD AA1 AA2
AA3 TDOS TNXD PD PNXD TEMPO LAG ALAG1 DOSTIME ; AA4
Y DV PRED RES WRES IPRED IRES IWRES CWRESI OBJI NOPRINT
NOAPPEND ONEHEADER FORMAT=,
$TABLE FILE=patab3042c.csv ID OCC CL V KA BIO MTT V3 Q BSVCL BSVV
BSVKA BSVBIO BSVV3 BSVQ BOVCL BOVKA BOVBIO BOVMTT NOPRINT
NOAPPEND ONEHEADER FORMAT=,
$TABLE FILE=cotab3042c.csv ID OCC WT HT AGE VARAUC VARCL NOPRINT
NOAPPEND ONEHEADER FORMAT=,
$TABLE FILE=catab3042c.csv ID OCC SEX VISIT NOPRINT NOAPPEND
ONEHEADER FORMAT=,
$TABLE FILE=mytab3042c.csv ID OCC VISIT TIME TAD Y DV AA1 AA2 ; AA3 AA4
PRED RES WRES IPRED IRES IWRES CWRESI OBJI CL V KA BIO MTT
V3 Q BSVCL BSVV BSVKA BSVBIO BSVV3 BSVQ SEX WT HT AGE
VARAUC VARCL ;T_SYNCH;BOVCL BOVKA BOVBIO BOVLAG BMI FFM FAT
NOPRINT NOAPPEND ONEHEADER FORMAT=,
```

Final NONMEM scripts for results presented in chapter 4

```
$SIZES     PD=-1000 LVR=-150 LTH=-200 MAXFCN=10000000 LNP4=-150000
$PROBLEM    ABACAVIR_POOLED
$INPUT     ID DATE_ORG=DROP TIME_ORG=DROP VISIT OCC TIME WHAT=DROP
          EVID NIGHT CMT AMT SS=DROP II=DROP DV DVID MDV FLAG STUDY BLQ
          SEX AGE WT HT TB LPVRTV RTV=DROP FORMULATION RAND HAZ WAZ
          BAZ INITM ARV_INITIATION TIME_TO_SUP COMMENT=DROP
$DATA     MACHANDI_20190910_SUP_AUC_fix_swap4.csv IGNORE=@ IGNORE=(DVID.GT.1)IGNORE=(FLAG.GT.0)
;-------------------------------------------------------------------------
$ABBREVIATED COMRES=4
$SUBROUTINE ADVAN13 TRANS1 TOL=9 SSTOL=3,SSATOL=3
$MODEL     NCOMPARTMENTS=4 COMP=(ABS DEFDOSE) COMP=(CENTRAL DEFOBSERVATION)COMP=(PERI1)
COMP=(AUC)
;-------------------------------------------------------------------------
$PK
; ---------- BOV----------;
   BOVBIO = ETA(10)
   BOVKA  = ETA(16)
   BOVMTT = ETA(22)
IF (OCC==1) THEN
   BOVBIO = ETA(11)
   BOVKA  = ETA(17)
   BOVMTT= ETA(23)
ENDIF
IF (OCC==2) THEN
   BOVBIO = ETA(12)
   BOVKA  = ETA(18)
   BOVMTT = ETA(24)
ENDIF
IF (OCC==3) THEN
   BOVBIO = ETA(13)
   BOVKA  = ETA(19)
   BOVMTT = ETA(25)
ENDIF
IF (OCC==4) THEN
   BOVBIO = ETA(14)
   BOVKA  = ETA(20)
   BOVMTT = ETA(26)
ENDIF
IF (OCC==5) THEN
   BOVBIO = ETA(15)
   BOVKA  = ETA(21)
   BOVMTT = ETA(27)
ENDIF

BOVCL = ETA(7)
IF(VISIT==1) THEN
  BOVCL = ETA(8)
ENDIF
 IF(VISIT==2) THEN
```

```
 BOVCL = ETA(9)
ENDIF
; ------- BSV----------;
BSVCL  = ETA(1)
BSVV   = ETA(2)
BSVKA  = ETA(3)
BSVBIO = ETA(4)
BSVV3  = ETA(5)
BSVQ   = ETA(6)


;----COV effects-----------------------------------------------------------
TB_BIO=1
IF(TB==1) TB_BIO = THETA(12)  ; BIO of visits where TB medication was given

EARLY_CL = 1
IF(STUDY==4 .AND. VISIT==1 .AND. RAND==1) EARLY_CL = THETA(13)  ;account for slow MATCH(STUDY 4) early
ARV initiation visit 1 clearance

VISIT_CL = 1
IF(STUDY==4 .AND. VISIT==1) VISIT_CL  = THETA(16) ; account for MATCH visit that has not been induced

SLOPE = THETA(18)

SPACE_HOLDER = THETA(20)

BIO_SUP_EXP=1
IF(STUDY==4) BIO_SUP_EXP = 1 + THETA(17)*EXP(-SLOPE*TIME_TO_SUP)

CL_SUP_EXP=1
IF(STUDY==4) CL_SUP_EXP = 1 + THETA(19)*EXP(-SLOPE*TIME_TO_SUP)

FORM_ABS=1
IF(FORMULATION==2) FORM_ABS = THETA(21);Tablets

MATCH_BOVBIO = 1
IF(STUDY==4) MATCH_BOVBIO  = THETA(22)  ;
BOVBIO=  BOVBIO * MATCH_BOVBIO

MATCH_BOVCL=1
IF(STUDY==4) MATCH_BOVCL  = THETA(23)   ;
BOVCL=  BOVCL * MATCH_BOVCL

EFV_BIO=1

EFV_CL=1
IF(LPVRTV==0) THEN  ; EFV
   EFV_BIO = THETA(24)
   EFV_CL = THETA(25)
ENDIF
; Remove EFV effect if Match visti 1, since they were un-induced
IF(STUDY==4 .AND. VISIT==1) THEN
   EFV_BIO = 1
```

```
   EFV_CL = 1
ENDIF
; ---------- Calculation of Fat-free Mass
; These formulas require WT in KG and HT in m !!!

; Conversion from cm to m
HTM = HT/100

IF (SEX.EQ.0) THEN  ; female
   WHSMAX=37.99
   WHS50=35.98
ELSE       ;males
   WHSMAX=42.92
   WHS50=30.93
ENDIF

; ------- Typical values of covariates
TVWT = 9.8

;--------- Allometric scaling and covariates
ALLMCL_WT = (WT/TVWT)**0.75
ALLMV_WT  = (WT/TVWT)

;--------------Maturation----------------------------------------------;
AGE_YRS = AGE

PGA = AGE_YRS + 9/12    ; assumed AGE in years. Adding 0.75 years (9 months) for standard gestation

LOGPGA50 = THETA(11) ; this is the log of age50, so the estimate is in the log scale
GAMMA    = THETA(10)
MATCL    = 1
IF (PGA>0) MATCL=1/(1+EXP(-GAMMA*(LOG(PGA)-LOGPGA50)))
;---------Typical values----------------------------------------------------;
TVCL  =  THETA(1)*ALLMCL_WT*MATCL*VISIT_CL*EARLY_CL*CL_SUP_EXP*EFV_CL
TVV   =  THETA(2)*ALLMV_WT
TVKA  =  THETA(3)*FORM_ABS
TVBIO =  THETA(4)*TB_BIO*BIO_SUP_EXP*EFV_BIO
TVMTT =  THETA(7)/FORM_ABS
TVV3  =  THETA(8)*ALLMV_WT
TVQ   =  THETA(9)*ALLMCL_WT
TVNN  =  THETA(14)

;----------Define parameters-------------------------------------------------
CL  =  TVCL*EXP(BSVCL+BOVCL)    ; CLEARANCE
V   =  TVV*EXP(BSVV)            ; CENTRAL VOL.
KA  =  TVKA*EXP(BSVKA+BOVKA)    ; ABS. RATE CONSTANT
BIO =  TVBIO*EXP(BSVBIO+BOVBIO) ; BIOAVAILABILITY
MTT=  TVMTT*EXP(BOVMTT)         ; MTT TIME
V3  =  TVV3*EXP(BSVV3)          ; PERIPH VOL
Q   =  TVQ*EXP(BSVQ)            ; INTER COMPT CL
NN  = TVNN                      ; Number of transit compartments
;----------------------------------------------------;
; re-parameterization
```

```
K    = CL/V ;(rate constant of elimination)
K23  = Q/V  ; (rate constant from central to peripheral 1)
K32  = Q/V3 ;(rate constant from peripheral 1 to central)
F1   = BIO
S2   = V    ; necessary for these ADVANs (1-4,12,12)
;-------------------------------------------------------------------------;
;Account for high pre-dose concentrations
TVLAG = THETA(15)

BVVLAG = ETA(28)
IF (VISIT==1) BVVLAG = ETA(29)
IF (VISIT==2) BVVLAG = ETA(30)

LAG = TVLAG*EXP(BVVLAG)

ALAG1 = 0
IF (NIGHT==1) ALAG1 = LAG; LAG TIME

; Transit compartment absorption
F1=0 ; I need to set bioavailability in compartment 1 to 0 for this implementation of the transit compartment
absorption

KTR = (NN+1)/MTT

IF (NEWIND/=2.OR.EVID>=3) THEN ; new individual, or reset event
  ; The values read here will be stored in TDOS and PD in this very PK call.
   TNXD=TIME ; Time of the dose
   PNXD=AMT ; Amount. If it's zero, the DE is deactivated.
ENDIF

DOSTIME = DOSTIM
TDOS=TNXD ; This will either save here the temporary values if it's a new individual...
PD=PNXD ; ...or the values which were read one record ahead during the execution of the previous record.

;IF(AMT>0) THEN ; This reads one record ahead and stores the data to be used when running the following record
 IF(AMT.GT.0.AND.ALAG1.EQ.0) THEN ; Use this INSTEAD if there is ALAG, as it will also checks if the ALAG is not 0.
   TNXD=TIME
   PNXD=AMT
ENDIF

; Uncomment this if you have ALAG or if you use ADDL
IF (DOSTIM .NE. 0) THEN ; This will account for the ADDL or lagged doses. It will overwrite the time, if it a non-
event record
   TNXD=DOSTIM
   PNXD=AMT
 ENDIF

; To speed up the computation, I calculate here all the non-time-varying quantities used in $DES
PIZZA = LOG(BIO*PD*KTR + 0.00001) - GAMLN(NN+1)   ; without +0.00001, it won't work with ETAs in
bioavailability

; Initialisation
```

```
A_0(1) = 0.000001
A_0(2) = 0.000001
A_0(3) = 0.000001

; RESET code for Cmax Tmax
IF (NEWIND/=2.OR.EVID>=3) THEN
   COM(1)=0
   COM(2)=0
   COM(3)=1000
   COM(4)=0
   TIMEDOSE = TIME
   AMOUNTDOSE = AMT
ENDIF
;---------------------------------------------------------------
$DES

CP = A(2)/V ; PLASMA CONCENTRATION
TEMPO = T-TDOS ; this is time after dose for the transit, it should always be >= 0
KTT = 0
TRANSIT = 0

IF(PD.GT.0.AND.TEMPO.GT.0) THEN ; This happens only id PD>0, so only if a dose has been detected
   KTT = KTR*(TEMPO)
   TRANSIT = EXP(PIZZA+NN*LOG(KTT)-KTT)
ENDIF

DADT(1) = TRANSIT -KA*A(1)
DADT(2) = KA*A(1)-K23*A(2)+K32*A(3)-K*A(2)
DADT(3) = K23*A(2)-K32*A(3)
DADT(4) = CP

;================================
TIMEATERDOSE=TIME-TIMEDOSE; TIME AFTER DOSE

IF (CP.GE.COM(1)) THEN
   COM(1) = CP         ; CMAX
   COM(2) = TIMEATERDOSE         ; TIME OF CMAX
ENDIF
IF (CP.LE.COM(3)) THEN
   COM(3) = CP         ; CMin
   COM(4) = TIMEATERDOSE       ; TIME of CMIN
ENDIF

;-------------------------------------------------------------------------;

$ERROR
; In the dataset, the DV of each BLQ value must imputed to LLOQ/2
; Additionally, all BLQ values must be flagged as BLQ=1 if the first in a series, or BLQ=2 if trailing values in a series

IPRED = A(2)/V

; DEFINE LLOQ VALUE
; LLOQ could be study-specific, e.g if you have data from different labs in your analysis
```

```
; In that case, you can use IFs, or you can define the values as covariates in the dataset
LLOQ = 0.0243 ;DNDI
IF (STUDY==1) LLOQ = 0.0243 ;ARROW
IF (STUDY==2) LLOQ = 0.0238 ; CHAPAS
IF (STUDY==4) LLOQ = 0.0238 ; MATCH

; Censoring threshold, generally the same as LLOQ, but not if the LLOQ data was released.
; If censoring threshold is not explocitly indicated, we can estimate it based on LLOQ.
; The signal-to-noise ratio assumed to be 10 at the LLOQ, and 3 for the LOD (generally the censoring threshold
when BLQ values are reported)
; https://en.wikipedia.org/wiki/Detection_limit;

CENS_THR = LLOQ
IF (STUDY==2) CENS_THR = 0.3*LLOQ ; imputing the Censoring thresold based on the declared LLOQ

; ERROR COMPONENTS
ADD = 0.2*LLOQ + THETA(6) ; each sample has at least 20% of LLOQ
PROP = IPRED*THETA(5)

; For BLQ==1 (i.e. first CENSORED value in a series, which was imputed to CENS_THR/2), we add extra additive
error on the concentrations, since the value in DV has been imputed
IF(ICALL/=4.AND.BLQ==1) ADD = ADD + 0.5*CENS_THR ; Each imputed sample has 50% of the censoring threshol
Each imputed sample has at least 20% or LLOQ or 50% of the censoring threshold

IF(ICALL/=4.AND.BLQ==2) THEN
   PROP = 0
   ADD = 1000000000
ENDIF

W = SQRT(ADD**2+PROP**2)

; Protective code if the W is 0, but it should never happen in this case, as ADD cannot be 0
IF (W.LE.0.000001) W=0.000001

IRES = DV-IPRED
IWRES = IRES/W

Y = IPRED + W*ERR(1)
                ; Model prediction of observed PK value with additive + proportional error

; To prevent simulation (ICALL==4) of negative values. It set a positive lower bound for Y, so that VPCs in the log-
scale can be plotted
IF (ICALL==4.AND.Y<=CENS_THR) Y = CENS_THR/2

; This puts a huge error on the BLQ data, so that it is virtually removed

; To calculate time after dose.
IF(AMT.GT.0) THEN
   TIMEDOSE = TIME
   AMOUNTDOSE = AMT
ENDIF

TAD = TIME-TIMEDOSE
```

```
;-----------------RETRIEVE AMOUNT IN EACH COMPARTMENT----------------------
AA1 = A(1)
AA2 = A(2)
AA3 = A(3)
; AA4 = A(4)

; For Cmax Tmax
C_MAX = COM(1) ; CMAX
T_MAX = COM(2) ; TIME OF CMAX
C_MIN = COM(3) ; CMIN
T_MIN = COM(4) ; TIME OF CMIN

IF(AMT.GT.0) THEN
   TIMEDOSE = TIME
   AMOUNTDOSE = AMT
; Reset CMAX code when a new dose is given
   COM(1)=0
   COM(2)=0
   COM(3)=1000
   COM(4)=0
ENDIF

TIMEAFTDOSE = TIME-TIMEDOSE

AUC = A(4) ; AUC as obtained integrating the concentration in $DES
AUC_INF = AMT * BIO / CL ; this works for any linear model, it is the theoretical A

VARCL = BSVCL + BOVCL
VARBIO = BSVBIO + BOVBIO
VARAUC = BSVBIO + BOVBIO - BSVCL - BOVCL

;======================VPC STRATIFICATION===============;
STUDY_VISIT=0
;EFV
IF(STUDY==1 .AND. VISIT==1) STUDY_VISIT=1
IF(STUDY==2 .AND. VISIT==1) STUDY_VISIT=1
IF(STUDY==4 .AND. RAND==1 .AND. VISIT==1 .AND. LPVRTV==0) STUDY_VISIT=1
IF(STUDY==4 .AND. RAND==1 .AND. VISIT==2 .AND. LPVRTV==0) STUDY_VISIT=1
IF(STUDY==4 .AND. RAND==0 .AND. VISIT==2 .AND. LPVRTV==0) STUDY_VISIT=1
IF(STUDY==4 .AND. RAND==0 .AND. VISIT==1 .AND. LPVRTV==0) STUDY_VISIT=1

;CHAPAS
IF(STUDY==1 .AND. VISIT==2) STUDY_VISIT=2
IF(STUDY==2 .AND. VISIT==2) STUDY_VISIT=2

;LPV/RIF
IF(STUDY==3 .AND. VISIT==1) STUDY_VISIT=3
IF(STUDY==3 .AND. VISIT==2) STUDY_VISIT=3
IF(STUDY==4 .AND. RAND==0 .AND. VISIT==2 .AND. LPVRTV==1) STUDY_VISIT=3
IF(STUDY==4 .AND. RAND==1 .AND. VISIT==2 .AND. LPVRTV==1) STUDY_VISIT=3

;LPV
IF(STUDY==3 .AND. VISIT==3) STUDY_VISIT=4
```

```
IF(STUDY==4 .AND. RAND==1 .AND. VISIT==1 .AND. LPVRTV==1) STUDY_VISIT=4
IF(STUDY==4 .AND. RAND==0 .AND. VISIT==1 .AND. LPVRTV==1) STUDY_VISIT=4
;------------------------------------------------------------------- ;
$THETA
(0, 11.8,30)  ; 1 CL [L/h]
(0, 11.6,30)  ; 2 V [L]
(0, 2.01,6)  ; 3 KA [1/h]
(1) FIX ; 4 BIO
(0, 0.235,1)  ; 5 PROP []
(0, 0.00215,3)  ; 6 ADD [mg/L]
(0, 0.054,3)  ; 7 MTT
(0, 3.8,10)  ; 8 V3 [L]
(0, 1.26,5)  ; 9 Q [L/h]
(0.5, 2.29,6)  ; 10 GAMMA []
(-10, -0.343,10)  ; 11 logPGA50 [yrs] [log]
(0, 0.684,3)  ; 12 TB_BIO
(0, 1,5) FIX ; 13  CL_V1_EARLY
(0, 10.6,50)  ; 14 NN
(0, 2.48,8)  ; 15 NIGHT_LAG
(0, 0.856,5)  ; 16 CL_NO-INDUC
(-5, 1.01,15)  ; 17 init_BIO
(-8, 0.0332,5) ; 18  SLOPE
(-10, -0.7,15)  ; 19 init_CL
(-8, 0,5) FIX ; 20  SPACE_HOLDER
(0, 0.743,5)  ; 21 FORMULATION
(0, 1.41,5)  ; 22  BOVBIO_MATCH
(0, 3.19,5)  ; 23 BOVCL_MATCH
(0, 1,5) FIX ; 24 EFV_BIO
(0, 1,5)  ; 25 EFV_CL

$OMEGA 0.022 ;    1 BSVCL
$OMEGA 0 FIX  ;    2 BSVV
$OMEGA 0 FIX  ;    3 BSVKA
$OMEGA 0 FIX  ;   4 BSVBIO
$OMEGA 0.183 ;    5 BSVV3
$OMEGA 0 FIX  ;    6 BSVQ
;-----------------------------------------------
$OMEGA  BLOCK(1)
 0.0291 ;    7 BOVCL
$OMEGA  BLOCK(1) SAME
$OMEGA  BLOCK(1) SAME
;-----------------------------------------------
$OMEGA  BLOCK(1)
 0.144 ;  10 BOVBIO
$OMEGA  BLOCK(1) SAME
$OMEGA  BLOCK(1) SAME
$OMEGA  BLOCK(1) SAME
$OMEGA  BLOCK(1) SAME
$OMEGA  BLOCK(1) SAME
;-----------------------------------------------
$OMEGA  BLOCK(1)
 0.48 ;   16 BOVKA
$OMEGA  BLOCK(1) SAME
```

```
$OMEGA  BLOCK(1) SAME
$OMEGA  BLOCK(1) SAME
$OMEGA  BLOCK(1) SAME
$OMEGA  BLOCK(1) SAME
;----------------------------------------------
$OMEGA  BLOCK(1)
 3.79 ;  22 BOVMTT
$OMEGA  BLOCK(1) SAME
$OMEGA  BLOCK(1) SAME
$OMEGA  BLOCK(1) SAME
$OMEGA  BLOCK(1) SAME
$OMEGA  BLOCK(1) SAME
;-----------------------------------
$OMEGA  BLOCK(1)
 0 FIX  ; 28 BVVDELAY
$OMEGA  BLOCK(1) SAME
$OMEGA  BLOCK(1) SAME
;-----------------------------------------------------------------;
$SIGMA 1 FIX  ; Scaled RUV variance - IT'S A VARIANCE SO FIXED TO "0" AND ALL ERROR IS GOING TO THE THETAS
AND IT MAKES A SD
;-----------------------------------------------------------------;
$ESTIMATION MSFO=run6f.msf MAXEVAL=9999 PRINT=1 METHOD=1 INTER
NOABORT NSIG=3 NONINFETA=1 ETASTYPE=1 ATOL=9 SIGL=9;MCETA=50 ;RANMETHOD=P ;SADDLE_RESET=1

$TABLE WRESCHOL FILE=sdtab6f.csv ID OCC VISIT TIME TAD ALAG1
DOSTIME AA1 AA2 AA3
Y DV PRED RES WRES IPRED IRES IWRES CWRESI OBJI NOPRINT
NOAPPEND ONEHEADER FORMAT=,
$TABLE FILE=patab6f.csv ID OCC CL V KA BIO MTT LAG V3 Q C_MAX T_MAX C_MIN T_MIN AUC_INF AUC BSVCL
BSVV BSVKA BSVBIO BSVV3 BSVQ BOVCL BOVKA BOVBIO BOVMTT
NOPRINT NOAPPEND ONEHEADER FORMAT=,
$TABLE FILE=cotab6f.csv ID OCC WT HT AGE HAZ WAZ BAZ VARAUC
VARCL NOPRINT NOAPPEND ONEHEADER FORMAT=,
$TABLE FILE=catab6f.csv ID OCC SEX VISIT TB RAND LPVRTV STUDY
STUDY_VISIT NOPRINT NOAPPEND ONEHEADER FORMAT=,
$TABLE FILE=mytab6f.csv ID OCC VISIT TIME TAD Y DV AA1 AA2
PRED RES WRES IPRED IRES IWRES CWRESI OBJI CL V KA BIO MTT
LAG V3 Q BSVCL BSVV BSVKA BSVBIO BSVV3 BSVQ SEX WT HT AGE
STUDY_VISIT HAZ WAZ EARLY_CL BAZ VISIT_CL TB RAND LPVRTV
ALAG1 DOSTIME VARAUC VARCL TIME_TO_SUP STUDY C_MAX T_MAX C_MIN T_MIN AUC_INF AUC
NOPRINT NOAPPEND ONEHEADER FORMAT=,
```

Final NONMEM scripts for results presented in chapter 5

```
$SIZES      PD=-1000 LVR=-150 LTH=-200 MAXFCN=10000000 LNP4=-150000
$PROBLEM    DATIC_ETH

$INPUT ID ORG_ID=DROP DAT1=DROP OCC TIME VPC_TIME WHAT=DROP EVID AMT SS II DV MDV BLQ STUDY
WT HT AGE SEX FFM HAZ WAZ BAZ BMI ALB HEMO HIV ALT BIOCREAT BIOBILI LPVRTV ADMIN SITE_ID EFV NVP
ABC X3TC ZDV MULTIVIT IRON GESTATION ADJ_ADMIN STUDY_AGE LAB_ID=DROP VOMIT
COMMENT_VOMIT=DROP ON_ETH SITE=DROP DATE_START_TB=DROP DRUG_CHANGED_LAST_WEEK=DROP
PROBLEM COMMENT=DROP
$DATA   ETH_FULL3_GEST.csv
IGNORE=@ IGNORE=(PROBLEM.GT.1) IGNORE=(ON_ETH.EQ.0) IGNORE=(ID.EQ.136) IGNORE=(ID.EQ.481)
$SUBROUTINE ADVAN13 TRANS1 TOL=9
$MODEL
NCOMPARTMENTS = 3 COMP=(ABS DEFDOSE) COMP=(CENTRAL DEFOBSERVATION)
COMP=(PERI1)
;-----------PRIOR-------------------------------------------------
;Sim_start
$PRIOR      NWPRI NPEXP=1 PLEV=0.9999
;Sim_end

$PK
; ---------- BOV
BOVCL = ETA(9)
BOVBIO = ETA(11)
BOVKA = ETA(13)
BOVMTT = ETA(15)
IF (OCC==2) THEN
   BOVCL = ETA(10)
   BOVBIO = ETA(12)
   BOVKA = ETA(14)
   BOVMTT = ETA(16)
ENDIF
; ------- BSV
BSVCL   = ETA(1)
BSVV   = ETA(2)
BSVKA   = ETA(3)
BSVBIO = ETA(4)
BSVCLMET = ETA(5)
BSVVMET = ETA(6)
BSVQ   = ETA(7)
BSVVP   = ETA(8)

SCALE_BOVBIO = 1
IF (OCC==1) SCALE_BOVBIO=THETA(18)

BOVBIO = SCALE_BOVBIO*BOVBIO
; ---------- Calculation of Fat-free Mass
; Conversion from cm to m
HTM = HT/100
; These formulas require WT in KG and HT in m, and AGE in years !!!
```

```
; Formulas for Children
IF (SEX.EQ.0) THEN  ; female ; IN DATIC females were "1" and males "0" I changed that and made females "0" just as in DNDI
      ALALPHA=1.11 ; lower bound of sigmoid hyperbolic function
      A50=7.1      ; ffm maturation half-time (years)
      ALGAMMA=1.1  ; Sigmoidicity coefficient
      WHSMAX=37.99
      WHS50=35.98
ELSE       ;males
      ALALPHA=0.88
      A50=13.4
      ALGAMMA=12.7
      WHSMAX=42.92
      WHS50=30.93
ENDIF

HTM2 = HTM**2    ; IMPORTANT: HEIGHT is used in meters!!!
AGEGAM=AGE**ALGAMMA  ; Compute this once and use many times
A50GAM=A50**ALGAMMA  ; Compute this once and use many times

FFM_CH = ((AGEGAM+ALALPHA*A50GAM)/(AGEGAM+A50GAM))*((WHSMAX*HTM2*WT)/(WHS50*HTM2+WT))
FAT_CH = WT-FFM_CH
PERFAT_CH = FAT_CH/WT
; ------- Typical values of covariates
TVWT = 10
TVFAT = 3 ; from datic only
TVFFM = 7.7
TVPERFAT = 0.2; from datic only
;--------- Allometric scaling and covariates
ALLMCL_WT = (WT/TVWT)**0.75
ALLMV_WT = (WT/TVWT)

ALLMCL_FAT_CH = (FAT_CH/TVFAT)**0.75
ALLMV_FAT_CH = (FAT_CH/TVFAT)

ALLMCL_FFM_CH = (FFM_CH/TVFFM)**0.75
ALLMV_FFM_CH = (FFM_CH/TVFFM)

STUDY_ABS = 1
IF(STUDY>1) STUDY_ABS= THETA (13); absorption of other studies relative to DATIC

;LPV/r impact on BIO
LPVR = 0
IF (LPVRTV>0) LPVR = 1

LPVR_BIO=1
IF(LPVR==1) LPVR_BIO= THETA (14)

; EFFECT OF AGE ON BIO
BRK_AGE = THETA(15)

AGE_BIO=1
```

```
IF(AGE<BRK_AGE) AGE_BIO = (1 + THETA(16)*(AGE - BRK_AGE))
IF(AGE>BRK_AGE) AGE_BIO = (1 + THETA(17)*(AGE - BRK_AGE))

; Maturation of CL
PMAGE = AGE + GESTATION/52

LOGPMAGE50 = THETA(1)
GAMMA = EXP(THETA(2))

MATCL=0
IF (PMAGE>0) MATCL=1/(1+EXP(-GAMMA*(LOG(PMAGE)-LOGPMAGE50)))

;---------Typical values----------------------------------------------------
TVCL = THETA(3)*ALLMCL_FFM_CH*MATCL
TVV = THETA(4)*ALLMV_FFM_CH
TVKA = THETA(5)*STUDY_ABS
TVBIO = THETA(6)*AGE_BIO*LPVR_BIO
TVMTT = THETA(9)/STUDY_ABS
TVNN = THETA(12)
TVQ = THETA(10)*ALLMCL_FFM_CH
TVVP = THETA(11)*ALLMV_FFM_CH
;----------Define parameters-------------------------------------------------
CL  = TVCL*EXP(BSVCL+BOVCL) ; CLEARANCE
V   = TVV*EXP(BSVV) ; CENTRAL VOL.
KA  = TVKA*EXP(BSVKA+BOVKA) ; ABS. RATE CONSTANT
BIO = TVBIO*EXP(BSVBIO+BOVBIO) ; BIOAVAILABILITY
MTT = TVMTT*EXP(BOVMTT) ; MTT TIME
NN  = TVNN ; Number of transit compartments
Q   = TVQ*EXP(BSVQ)
VP  = TVVP*EXP(BSVVP)

K = CL/V
K23 = Q/V
K32 = Q/VP

;-------------------------------------------------------------------------
F1=0 ; I need to set bioavailability in compartment 1 to 0 for this implementation of the transit compartment
absorption

KTR = (NN+1)/MTT

IF (NEWIND/=2.OR.EVID>=3) THEN ; new individual, or reset event
   ; The values read here will be stored in TDOS and PD in this very PK call.
   TNXD=TIME ; Time of the dose
   PNXD=AMT ; Amount. If it's zero, the DE is deactivated.
ENDIF

TDOS=TNXD ; This will either save here the temporary values if it's a new individual...
PD=PNXD ; ...or the values which were read one record ahead during the execution of the previous record.

IF(AMT>0) THEN ; This reads one record ahead and stores the data to be used when running the following record
; IF(AMT.GT.0.AND.ALAG1.EQ.0) THEN ; Use this INSTEAD if there is ALAG, as it will also checks if the ALAG is not 0.
Note that you normally do not want to include both ALAG and transit, this is a very exceptional case
```

```
   TNXD=TIME
   PNXD=AMT
ENDIF

PIZZA = LOG(BIO*PD*KTR + 0.00001) - GAMLN(NN+1)  ; without +0.00001, it won't work with ETAs in bioavailability

; Initialisation
A_0(1) = 0.000001
A_0(2) = 0.000001
A_0(3) = 0.000001
$DES
TEMPO = T-TDOS ; this is time after dose for the transit, it should always be >= 0

KTT = 0
DADT(1) = -KA*A(1)

IF(PD.GT.0.AND.TEMPO.GT.0) THEN ; This happens only if PD>0, so only if a dose has been detected
   KTT = KTR*(TEMPO)
   DADT(1) = EXP(PIZZA+NN*LOG(KTT)-KTT) -KA*A(1)
ENDIF

DADT(2) = KA*A(1)-K23*A(2)+K32*A(3)-K*A(2)
DADT(3) = K23*A(2)-K32*A(3)

;-----------------------------------------------------------------------------
$ERROR
LLOQ = 0.084 ; nominal EMB LLOQ = 0.084

CENS_THR=LLOQ

IF (STUDY==1) CENS_THR = 0.0252 ; inferred EMB LOD = 30% of LLOQ = 0.0252

IPRED = A(2)/V

IRES = DV-IPRED

PROP = IPRED*THETA(7)
; ADD is defined as 20% of LLOQ + THETA(.)
ADD = LLOQ/5 + THETA(8)

; For BLQ==1 (i.e. first CENSORED value in a series, which was imputed to CENS_THR/2), we add extra additive
error on the concentrations,
; since the value in DV has been imputed and therefore more uncertain.
IF (ICALL==2.AND.BLQ==1) THEN
   ADD = ADD + CENS_THR/2
ENDIF

NO_FIT = 0

IF (ICALL==2.AND.BLQ==2) THEN
   ADD = 1000000000
   PROP = 0
   NO_FIT = 1
```

```
ENDIF

W = SQRT(ADD**2+PROP**2)

; Protective code if the W is 0, but it should never happen in this case, as ADD cannot be 0
IF (W.LE.0.000001) W=0.000001

IWRES = IRES/W

Y = IPRED + W*ERR(1)

; To prevent simulation (ICALL==4) of negative values. It set a positive lower bound for Y, so that VPCs in the log-scale can be plotted
IF (ICALL==4.AND.Y<=CENS_THR) Y = CENS_THR/2

; To calculate time after dose.
IF(AMT>0) THEN
   TIMEDOSE = TIME
   AMOUNTDOSE = AMT
ENDIF

TAD = TIME-TIMEDOSE

VARCL = BSVCL + BOVCL
VARBIO = BSVBIO + BOVBIO
VARKA   = BSVKA + BOVKA
VARAUC = BSVBIO + BOVBIO - BSVCL - BOVCL

AA1=A(1)
AA2=A(2)
AA3=A(3)

NGT = 0
IF (STUDY==1 .AND. ADMIN==3) NGT=1

AGE_LT1 = 0
IF (AGE<1) AGE_LT1 = 1

HIV_POS = 0
IF (HIV==2) HIV_POS = 1; was 2 the only ones with HIV in datic? ; In the dataset all DNDI should have HIV==2 since they were all possitive

;-----VPC STRATIFICATION----------
STUDY_ADMIN=0

; DATIC
IF(STUDY==1 .AND. ADMIN==0) STUDY_ADMIN= 1; WHOLE
IF(STUDY==1 .AND. ADMIN==1) STUDY_ADMIN= 2 ;CRUSHED SWALLOWED
IF(STUDY==1 .AND. ADMIN==2) STUDY_ADMIN= 3; CRUSHED SYRINGE
IF(STUDY==1 .AND. ADMIN==3) STUDY_ADMIN= 4;; NGT
IF(STUDY==1 .AND. ADMIN==4) STUDY_ADMIN= 5;TYGERB

DND_ADMIN=0
```

```
IF(STUDY==2 .AND. AGE<3) DND_ADMIN= 1;CRUSHED
IF(STUDY==2 .AND. AGE>3) DND_ADMIN= 2;FULL

;DNDI
IF(STUDY==2 .AND. DND_ADMIN==1) STUDY_ADMIN= 6;ADMIN==0 = FULL TABLETS
IF(STUDY==2 .AND. DND_ADMIN==2) STUDY_ADMIN= 7
;SHINE
IF(STUDY==3 .AND. ADMIN==0) STUDY_ADMIN= 8;;
IF(STUDY==3 .AND. ADMIN==1) STUDY_ADMIN= 9;WHOLE

SITE_ADMIN=0
; D
IF(SITE_ID==1 .AND. ADMIN==2) SITE_ADMIN= 1
IF(SITE_ID==1 .AND. ADMIN==3) SITE_ADMIN= 2
;M
IF(SITE_ID==2 .AND. ADMIN==0) SITE_ADMIN= 3
IF(SITE_ID==2 .AND. ADMIN==1) SITE_ADMIN= 4
IF(SITE_ID==2 .AND. ADMIN==2) SITE_ADMIN= 5
;X
IF(SITE_ID==3 .AND. ADMIN==0) SITE_ADMIN= 6
IF(SITE_ID==3 .AND. ADMIN==1) SITE_ADMIN= 7
IF(SITE_ID==3 .AND. ADMIN==2) SITE_ADMIN= 8
;T
IF(SITE_ID==4 .AND. ADMIN==4) SITE_ADMIN= 9
;DNDI
IF(SITE_ID==5 .AND. ADMIN==6) SITE_ADMIN= 10

SITE_ADMIN_OC2=0
; D
IF(OCC==2 .AND. SITE_ID==1 .AND. ADMIN==2) SITE_ADMIN_OC2= 1
IF(OCC==2 .AND. SITE_ID==1 .AND. ADMIN==3) SITE_ADMIN_OC2= 2
;M
IF(OCC==2 .AND. SITE_ID==2 .AND. ADMIN==0) SITE_ADMIN_OC2= 3
IF(OCC==2 .AND. SITE_ID==2 .AND. ADMIN==1) SITE_ADMIN_OC2= 4
IF(OCC==2 .AND. SITE_ID==2 .AND. ADMIN==2) SITE_ADMIN_OC2= 5
;X
IF(OCC==2 .AND. SITE_ID==3 .AND. ADMIN==0) SITE_ADMIN_OC2= 6
IF(OCC==2 .AND. SITE_ID==3 .AND. ADMIN==1) SITE_ADMIN_OC2= 7
IF(OCC==2 .AND. SITE_ID==3 .AND. ADMIN==2) SITE_ADMIN_OC2= 8
;T
IF(OCC==2 .AND. SITE_ID==4 .AND. ADMIN==4) SITE_ADMIN_OC2= 9
;DNDI
IF(OCC==2 .AND. SITE_ID==5 .AND. ADMIN==6) SITE_ADMIN_OC2= 10
;----------------------------------------------------------------------
$THETA
(-3, -0.102,5) ; 1 PMAGE50 yrs [log]
(-2, 1.15,3) ; 2 GAMMA_AGE [log]
(1, 21.8,60) ; 3 CL [L/h]
(1, 61.3,300) ; 4 V [L]
(0.5, 1.45,5) ; 5 KA [1/h]
(1) FIX ; 6 BIO
(0, 0.177,0.5) ; 7 PROP []
(0, 0,1) FIX ; 8 ADD [mg/L]
```

```
(0, 0.681,3) ; 9 MTT [h]
(0.1, 15.8,100) ; 10 Q [L/h]
(0.1, 117,600) ; 11 VP [L]
(-2, 4.86,15) ; 12 NN []
(0.01, 0.782,5) ; 13 DNDI_SHINE_ABS
(0.01, 0.684,5) ; 14  LPVR_BIO
(-4, 3.17,5) ; 15 BRK_AGE
(-1, 0.0963,5) ; 16 SLOPE
(-1, 0,5) FIX ; 17 FLAT_FIXED_LINE
(0.1, 1.37,10) ; 18 PREDOSE BOVBIO []

;**********DONE
; PRIORS
;Sim_start
$THETAP
-0.08906 FIX; 1 PMAGE50 yrs
 1.23 FIX ; 2 GAMMA_AGE [
;Sim_end
;---------------------------------------
; UNCERTAINTY IN PRIORS
;Sim_start
$THETAPV  BLOCK(2) FIX
0.01  ;
0 0.01
;Sim_end
$OMEGA  BLOCK(1)
 0.0246 ;   1 BSV CL
$OMEGA  BLOCK(1)
 0 FIX  ;    2 BSV V
$OMEGA  BLOCK(1)
 0 FIX  ;   3 BSV KA
$OMEGA  BLOCK(1)
 0 FIX  ;  4 BSV BIO
$OMEGA  BLOCK(1)
 0 FIX  ; 5 BSV CLMET
$OMEGA  BLOCK(1)
 0 FIX  ; 6 BSV VMET
$OMEGA  BLOCK(1)
 0 FIX  ;     7 BSVQ
$OMEGA  BLOCK(1)
 0 FIX  ;    8 BSVVP
;-----------------------------------------------------------------------
$OMEGA  BLOCK(1)
 0 FIX  ;    9 BOVCL
$OMEGA  BLOCK(1) SAME
;-----------------------------------------------------------------------
$OMEGA  BLOCK(1)
 0.199 ;  11 BOVBIO
$OMEGA  BLOCK(1) SAME
;-----------------------------------------------------------------------
$OMEGA  BLOCK(1)
 0.403 ;   13 BOVKA
$OMEGA  BLOCK(1) SAME
```

```
;-----------------------------------------------------------------------
$OMEGA  BLOCK(1)
 0.233 ;  15 BOVMTT
$OMEGA  BLOCK(1) SAME

$SIGMA 1 FIX
;-----------------------------------------------------------------------
;Sim_start

$ESTIMATION MSFO=run500d.msf MAXEVAL=9999 PRINT=1 METHOD=1 INTER
NOABORT NONINFETA=1 ETASTYPE=1 NSIG=3 ATOL=9 SIGL=9 SADDLE_RESET=1 MCETA=500 RANMETHOD=4P
REPEAT
;$SIMULATION (12345) ONLYSIMULATION
$TABLE WRESCHOL FILE=sdtab500d.csv ID OCC TIME
TAD BLQ AA1 AA2 AA3 Y DV PRED RES
WRES IPRED IRES IWRES CWRES OBJI NOPRINT NOAPPEND
ONEHEADER FORMAT=,
$TABLE FILE=patab500d.csv ID OCC CL V KA BIO MTT NN Q VP BSVCL
BSVV BSVKA BSVBIO BSVCLMET BSVVMET BOVCL BOVKA BOVBIO
BOVMTT VARCL VARBIO VARAUC NOPRINT NOAPPEND ONEHEADER
FORMAT=,
$TABLE FILE=cotab500d.csv ID OCC WT HT AGE FFM_CH FAT_CH PERFAT_CH BMI
HEMO HAZ WAZ BAZ BIOCREAT BIOBILI ALT NOPRINT NOAPPEND ONEHEADER FORMAT=,
$TABLE FILE=catab500d.csv ID OCC SEX ADMIN SITE_ID
HIV NGT AGE_LT1 HIV_POS LPVR LPVRTV NVP EFV ABC X3TC ZDV STUDY STUDY_AGE SITE_ADMIN
SITE_ADMIN_OC2 STUDY_ADMIN
NOPRINT NOAPPEND ONEHEADER FORMAT=,
$TABLE FILE=mytab500d.csv ID OCC TIME TAD Y DV AA1
AA2 AA3 AGE_BIO PRED RES WRES IPRED IRES IWRES CWRES OBJI
CL V KA BIO MTT NN Q VP BSVCL BSVV BSVKA BSVBIO BSVCLMET VARKA VPC_TIME
BSVVMET BOVCL BOVKA BOVBIO BOVMTT VARCL VARBIO VARAUC WT
HT AGE FFM_CH FAT_CH PERFAT_CH HEMO SEX ADMIN STUDY_ADMIN
SITE_ID HIV NGT AGE_LT1 HIV_POS STUDY
LPVR STUDY_AGE SITE_ADMIN SITE_ADMIN_OC2 BIOCREAT BIOBILI ALT WAZ HAZ NOPRINT NOAPPEND
ONEHEADER FORMAT=,
```

Shinyapp script for the application presented in chapter 6. This is a prototype, the current version is still under revision

UI.R

```
library(shiny) # basic shiny related functions and features
library(shinydashboardPlus)
library(plotly)
library(shinydashboard) # for dashboard related functions and features
library(shinyBS)
library(shinyjs) # easy javascript functionalities with shiny
library(DT) # for interactive data tables
library(ggplot2) # for ggplot plot
library(shinycssloaders) # for spinner while data / plot loads
#HEADER
header <- dashboardHeader(title = "Dosing Tool")
#SIDEBAR
sidebar <- dashboardSidebar(disable = TRUE)
#BODY
body <- dashboardBody(
  useShinyjs(),
  tabPanel("Plot",
           tabsetPanel( id="tabs", type="pills",
                        #=============generic tool==============
                        tabPanel("GENERIC TOOL",id="tabs3",
                        # A box that will include dosage and parameter inputs
                                 fluidRow(
                                   br(), br(),  # line spacing
                                   tabBox( id = "tabset3", height =
"780px",width = 3,# The id lets us use input$tabset1 on the server to find
the current tab
                       tabPanel("WHO",
                            box( width = 12,height = 100, status = "warning",
                          fluidRow(
                               box(width = 5, height = 80, status = "danger",

div(style="display: inline-block; width: 95%;",numericInput('WGT', 'Adult
weight (kg)', value = 40, min = 1, max = 200))),
                              box(width = 5, height = 80, status = "success",

div(style="display: inline-block; width: 95%;",numericInput('adult_dose',
'Adult dose (mg)', value = 2000, min = 1, max = 10000)))
                                                    )#end of fluidrow adults
                                                  ),#end of box
                             box( width = 12,height = 100,status = "warning",
                              box(width = 8, height = 80, status = "success",

numericInput('amount5', 'Target dose (mg)',  value = 500, min = 20, max =
4000))),
                              box(width = 12,height = 450,status = "warning",
                                                fluidRow(
```

```
                                                                box(width =
7,height = 440,status = "danger",  icon = "fas fa-pills",

div(style="display: inline-block; width:
95%;height:65px;",selectInput('genband1', 'Select weightband (Kg)',
                                    c( "3-5.9",
                                      "6-9.9",
                                     "10-13.9",
                                     "14-19.9",
                                     "20-24.9",
                                      "25-35"),
                                  selected = "3-5.9")),


div(style="display: inline-block; width:
95%;height:65px;",selectInput('genband2', '',
                                    c( "3-5.9",
                                      "6-9.9",
                                     "10-13.9",
                                     "14-19.9",
                                     "20-24.9",
                                      "25-35"),
                                  selected = "6-9.9")),


div(style="display: inline-block; width:
95%;height:65px;",selectInput('genband3', '',
                                    c( "3-5.9",
                                      "6-9.9",
                                     "10-13.9",
                                     "14-19.9",
                                     "20-24.9",
                                      "25-35"),
                                 selected = "10-13.9")),

div(style="display: inline-block; width:
95%;height:65px;",selectInput('genband4', '',
                                    c( "3-5.9",
                                      "6-9.9",
                                     "10-13.9",
                                     "14-19.9",
                                     "20-24.9",
                                      "25-35"),
                                 selected = "14-19.9")),

div(style="display: inline-block; width:
95%;height:65px;",selectInput('genband5', '',
                                    c( "3-5.9",
                                      "6-9.9",
                                     "10-13.9",
                                     "14-19.9",
                                     "20-24.9",
                                      "25-35"),
                                 selected = "20-24.9")),

div(style="display: inline-block; width:
95%;height:65px;",selectInput('genband6', '',
```

```
                                    c( "3-5.9",
                                      "6-9.9",
                                     "10-13.9",
                                     "14-19.9",
                                     "20-24.9",
                                      "25-35"),
                                  selected = "25-35"))
                                                    ),#box for weigth band#,

                                   box(width = 5,height = 440,status = "success",


div(style="display: inline-block; width:
95%;height:65px;",numericInput('gentab1', 'Number of tablets',

value = 0.25, min = 0, max = 5,step =0.25)),
div(style="display: inline-block; width:
95%;height:65px;",numericInput('gentab2', '',
value = 0.5, min = 0, max = 5,step =0.25)),
div(style="display: inline-block; width:
95%;height:65px;",numericInput('gentab3', '',
value = 1, min = 0, max = 5,step =0.25)),
div(style="display: inline-block; width:
95%;height:65px;",numericInput('gentab4', '',
value = 1.5, min = 0, max = 5,step =0.25)),
div(style="display: inline-block; width:
95%;height:65px;",numericInput('gentab5', '',
value = 1.5, min = 0, max = 5,step =0.25)),
div(style="display: inline-block; width:
95%;height:65px;",numericInput('gentab6', '',
value = 2, min = 0, max = 5,step =0.25))
                                                       ) #end box tablets

                                                     )#,#fluidrow weightband 1

                                                     )#,

                                                ),#end of WHO tabpanel dosage
#================================================================================

                          ) #END tabpane data input
            )#end tabsetpanel
  )#end tabPanel
)))
dashboardPage(header, sidebar, body,skin = "black")
```

Server. R

```
library(shiny)
library(ggplot2)
library(dplyr)
library(gridExtra)
library(grid)
library(mlxR)
library(tidyverse)
library(plyr)
library(purrr)
library(plotly)


server <-  function(input, output, session) {

  observeEvent(input$showh,
               show("txt")) # show() is shiny js function, pass the
element/widget ID as the argument

  observeEvent(input$hideh,
               hide("txt")) # hide() is shiny js function, pass the
element/widget ID as the argument

 #============================
  boys= read.csv("boys.csv",stringsAsFactors = FALSE) # DNDI STRUCTURE

  girls= read.csv("girls.csv",stringsAsFactors = FALSE) # DNDI STRUCTURE

  #============================

  # Define model file-----
  model.file <- inlineModel("

                            [LONGITUDINAL]
                            input = {F,Tlag, ka, V, Cl}

                            PK:
                            Cc = pkmodel(p=F, Tlag, ka, V, Cl)

                            [INDIVIDUAL]
                            input = {F_pop, gamma_F, Tlag_pop, gamma_Tlag,
ka_pop, gamma_ka, V_pop, beta_V_tWeight, tWeight, omega_V, Cl_pop,
beta_Cl_tWeight, omega_Cl}

                            DEFINITION:
                            F = {distribution=lognormal, typical=F_pop,
varlevel=id*occ, sd=gamma_F}
                            Tlag = {distribution=lognormal, typical=Tlag_pop,
varlevel=id*occ, sd=gamma_Tlag}
                            ka = {distribution=lognormal, typical=ka_pop,
varlevel=id*occ, sd=gamma_ka}
                            V = {distribution=lognormal, typical=V_pop,
covariate=tWeight, coefficient=beta_V_tWeight, sd=omega_V}
                            Cl = {distribution=lognormal, typical=Cl_pop,
covariate=tWeight, coefficient=beta_Cl_tWeight, sd=omega_Cl}
```

```
                            [COVARIATE]
                            input = {Weight}

                            EQUATION:
                            ; The centering median has been computed from the
data column 'Weight'.
                            tWeight = log(Weight) - log(52)
                            ")
  #=============================================Reference model=======
  plot <- eventReactive(input$up,{
    # Define population parameters ----

    p.pop <- c( F_pop = 1,
                gamma_F = 0,
                Tlag_pop = input$Tlag, #  0.419,
                gamma_Tlag = 0,
                ka_pop = 3.04,#input$Ka
                gamma_ka = 0,
                V_pop = input$V,  #33,
                beta_V_tWeight = 1,
                omega_V = 0.151,
                Cl_pop = input$CL, #2.97,
                beta_Cl_tWeight = 0.75,
                omega_Cl = 0.301)

    Weight <- c(seq(3,35,by = 0.1))
    Ncov<- 321#input$subjects

    # Define global parameters----
    SSDOSES <- 10 # Number of doses to steady state
    DOSEINT <- input$time_int # Dosing interval
    TABLETSIZE = input$amount
    NSIM = 1000

    cov.data <- data.frame(id=1:Ncov, Weight)

    # Define treatment design ----
    tstart = (SSDOSES - 1)*DOSEINT
    tstop  = SSDOSES*DOSEINT
    treat.des <- list(time = seq(0, tstart, DOSEINT), amount = TABLETSIZE)

    # Define simulation output ----
    out.var <- list(name = c("Cc","Weight"), time = c(tstart:tstop))

    #-------------------------------------------------
    # Simulate exposure----
    #-------------------------------------------------
    res <- exposure(model = model.file,
                    parameter = list(p.pop,cov.data),
                    output = out.var,
                    treatment = treat.des,
                    settings = list(seed = 12345))

    #list to data.frame
    res_expo <- res$Cc
    res_conc <- res$output$Cc
```

```
res_cov <- res$output$parameter
resx <-left_join(res_expo,res_conc,by="id" )
res_xp <- left_join(resx,res_cov,by="id"  )
res_xp$WTBAND <- 0

res_xp$WTBAND[res_xp$Weight>=3 & res_xp$Weight<3.99]     <- 3
res_xp$WTBAND[res_xp$Weight>=4 & res_xp$Weight<4.99]     <- 4
res_xp$WTBAND[res_xp$Weight>=5 & res_xp$Weight<5.99]     <- 5
res_xp$WTBAND[res_xp$Weight>=6 & res_xp$Weight<6.99]     <- 6
res_xp$WTBAND[res_xp$Weight>=7 & res_xp$Weight<7.99]     <- 7
res_xp$WTBAND[res_xp$Weight>=8 & res_xp$Weight<8.99]     <- 8
res_xp$WTBAND[res_xp$Weight>=9 & res_xp$Weight<9.99]     <- 9
res_xp$WTBAND[res_xp$Weight>=10 & res_xp$Weight<10.99]   <- 10

res_xp$WTBAND[res_xp$Weight>=11 & res_xp$Weight<11.99]   <- 11
res_xp$WTBAND[res_xp$Weight>=12 & res_xp$Weight<12.99]   <- 12
res_xp$WTBAND[res_xp$Weight>=13 & res_xp$Weight<13.99]   <- 13
res_xp$WTBAND[res_xp$Weight>=14 & res_xp$Weight<14.99]   <- 14
res_xp$WTBAND[res_xp$Weight>=15 & res_xp$Weight<15.99]   <- 15
res_xp$WTBAND[res_xp$Weight>=16 & res_xp$Weight<16.99]   <- 16
res_xp$WTBAND[res_xp$Weight>=17 & res_xp$Weight<17.99]   <-17
res_xp$WTBAND[res_xp$Weight>=18 & res_xp$Weight<18.99]   <-18
res_xp$WTBAND[res_xp$Weight>=19 & res_xp$Weight<19.99]   <-19
res_xp$WTBAND[res_xp$Weight>=20 & res_xp$Weight<20.99]   <-20

res_xp$WTBAND[res_xp$Weight>=21 & res_xp$Weight<21.99] <- 21
res_xp$WTBAND[res_xp$Weight>=22 & res_xp$Weight<22.99] <-22
res_xp$WTBAND[res_xp$Weight>=23 & res_xp$Weight<23.99] <-23
res_xp$WTBAND[res_xp$Weight>=24 & res_xp$Weight<24.99] <-24
res_xp$WTBAND[res_xp$Weight>=25 & res_xp$Weight<25.99] <-25
res_xp$WTBAND[res_xp$Weight>=26 & res_xp$Weight<26.99] <-26
res_xp$WTBAND[res_xp$Weight>=27 & res_xp$Weight<27.99] <-27
res_xp$WTBAND[res_xp$Weight>=28 & res_xp$Weight<28.99] <-28
res_xp$WTBAND[res_xp$Weight>=29 & res_xp$Weight<29.99] <-29
res_xp$WTBAND[res_xp$Weight>=30 & res_xp$Weight<30.99] <-30

res_xp$WTBAND[res_xp$Weight>=31 & res_xp$Weight<31.99] <-31
res_xp$WTBAND[res_xp$Weight>=32 & res_xp$Weight<32.99] <-32
res_xp$WTBAND[res_xp$Weight>=33 & res_xp$Weight<36] <-33

res_xp$WeightBD[res_xp$Weight>=3 & res_xp$Weight<5.99]   <- "3-5.9"
res_xp$WeightBD[res_xp$Weight>=6 & res_xp$Weight<9.99]   <- "6-9.9"
res_xp$WeightBD[res_xp$Weight>=10 & res_xp$Weight<13.99]   <- "10-13.9"

res_xp$WeightBD[res_xp$Weight>=14 & res_xp$Weight<19.99]   <- "14-19.9"
res_xp$WeightBD[res_xp$Weight>=20 & res_xp$Weight<24.99]   <- "20-24.9"
res_xp$WeightBD[res_xp$Weight>=25 & res_xp$Weight<36]     <- "25-35"


resPLOT1 <- res_xp %>%
  filter(WeightBD=="3-5.9") %>%
  select(id,time,auc,cmin,cmax,WeightBD,WTBAND,Weight) %>%
  mutate(aucTAB=auc*0.25) %>%
  mutate(cminTAB=cmin*0.25) %>%
  mutate(cmaxTAB=cmax*0.25)

resPLOT2 <- res_xp %>%
```

```
    filter(WeightBD=="6-9.9") %>%
    select(id,time,auc,WeightBD,cmin,cmax,WTBAND,Weight) %>%
    mutate(aucTAB=auc*0.5) %>%
    mutate(cminTAB=cmin*0.5) %>%
    mutate(cmaxTAB=cmax*0.5)

  resPLOT3 <- res_xp %>%
    filter(WeightBD=="10-13.9") %>%
    select(id,time,auc,WeightBD,cmin,cmax,WTBAND,Weight) %>%
    mutate(aucTAB=auc*1) %>%
    mutate(cminTAB=cmin*1) %>%
    mutate(cmaxTAB=cmax*1)

  resPLOT4 <- res_xp %>%
    filter(WeightBD=="14-19.9") %>%
    select(id,time,auc,WeightBD,cmin,cmax,WTBAND,Weight) %>%
    mutate(aucTAB=auc*1.5) %>%
    mutate(cminTAB=cmin*1.5) %>%
    mutate(cmaxTAB=cmax*1.5)

  resPLOT5 <- res_xp %>%
    filter(WeightBD=="20-24.9") %>%
    select(id,time,auc,WeightBD,cmin,cmax,WTBAND,Weight) %>%
    mutate(aucTAB=auc*1.5) %>%
    mutate(cminTAB=cmin*1.5) %>%
    mutate(cmaxTAB=cmax*1.5)

  resPLOT6 <- res_xp %>%
    filter(WeightBD=="25-35") %>%
    select(id,time,auc,WeightBD,cmin,cmax,WTBAND,Weight) %>%
    mutate(aucTAB=auc*2) %>%
    mutate(cminTAB=cmin*2) %>%
    mutate(cmaxTAB=cmax*2)

  resAUC1  <- full_join(
resPLOT1,resPLOT2,by=c("id","time","aucTAB","WeightBD","WTBAND","cmaxTAB","cm
inTAB","Weight"))
  resAUC2  <- full_join(
resAUC1,resPLOT3,by=c("id","time","aucTAB","WeightBD","WTBAND","cmaxTAB","cmi
nTAB","Weight"))
  resAUC3  <- full_join(
resAUC2,resPLOT4,by=c("id","time","aucTAB","WeightBD","WTBAND","cmaxTAB","cmi
nTAB","Weight"))
  resAUC4  <- full_join(
resAUC3,resPLOT5,by=c("id","time","aucTAB","WeightBD","WTBAND","cmaxTAB","cmi
nTAB","Weight"))
  resAUC5  <- full_join(
resAUC4,resPLOT6,by=c("id","time","aucTAB","WeightBD","WTBAND","cmaxTAB","cmi
nTAB","Weight"))
  resaucPLOT <- select(resAUC5,WeightBD,aucTAB )
  resaucPLOT$WeightBD = factor(resaucPLOT$WeightBD , levels=c('3-5.9','6-
9.9','10-13.9','14-19.9','20-24.9','25-35'))# arrange order

  #define the summary function
  fsummary <- function(x) {
    r <- quantile(x, probs = c(0.025, 0.25, 0.5, 0.75, 0.975))
    names(r) <- c("ymin", "lower", "middle", "upper", "ymax")
```

```
    }

    c<- ggplot(data = na.omit(resaucPLOT), aes(as.factor(WeightBD),
group=WeightBD))+
      stat_summary(fun.data = fsummary, geom="boxplot",(aes(y=aucTAB,fill =
"green")),position=position_dodge(1))+
      xlab("Weight (kg)") +
      ylab(expression(paste('AUC'[0-12]," (mg.h/L)"))) +
      theme_minimal() +
      theme(legend.position = "none")+
      theme(plot.title = element_text(hjust = 0.5)) +
      geom_hline(yintercept = 363, linetype ="dashed",color = "red", size =
0.75) #+

    resaucPLOT2 <- select(resAUC5,WTBAND,aucTAB )
    c2<- ggplot(data = na.omit(resaucPLOT2), aes(as.factor(WTBAND),
group=WTBAND))+
      stat_summary(fun.data = fsummary, geom="boxplot",(aes(y=aucTAB,fill =
"green")),position=position_dodge(1))+
      xlab("Weight (kg)") +
      ylab(expression(paste('AUC'[0-12]," (mg.h/L)"))) +
      theme_minimal() +
      theme(legend.position = "none")+
      theme(plot.title = element_text(hjust = 0.5)) +
      geom_hline(yintercept = 363, linetype ="dashed",color = "red", size =
0.75) #+

    #=======exposures
    #exposure tables in WHO weightbands
    cmax_R<- ddply(resAUC5, .(WeightBD), summarise,
                   cmax = median(cmaxTAB))
    cmin_R<- ddply(resAUC5, .(WeightBD), summarise,
                   cmin = median(cminTAB))
    auc_R<- ddply(resAUC5, .(WeightBD), summarise,
                  auc = median(aucTAB))

    list(c=c,c2=c2,cmax_R=cmax_R,cmin_R=cmin_R,auc_R=auc_R)

  })

##############################OUTPUT#############################################
#######

  #simulations plot of reference model
  output$Plot1 <- renderPlot({
    plot()$c
  })

  output$Plot111 <- renderPlot({
    plot()$c2
  })

  #Cmax for individual WHO weightbands
  output$table5 <- renderTable({
    wplot()$cmax_R
  })
```

```
  #Cmin for individual WHO weightbands
  output$table6 <- renderTable({
    wplot()$cmin_R
  })

  #auc for individual WHO weightbands
  output$table7  <- renderTable({
    wplot()$auc_R

    output$whosum <- renderTable({
      wplot()$tabwho
    })

  })

   #============================Repoert============

  output$report <- downloadHandler(
    # For PDF output, change this to "report.pdf"
    filename = "report.html",
    content = function(file) {
      # Copy the report file to a temporary directory before processing it,
in
      # case we don't have write permissions to the current working dir
(which
      # can happen when deployed).
      tempReport <- file.path(tempdir(), "report.Rmd")
      file.copy("report.Rmd", tempReport, overwrite = TRUE)

      # Set up parameters to pass to Rmd document
      params <- list(n = input$WGT,
                     m = input$adult_dose,
                     L = input$amount5,
                     p = pl(),
                     t = tb())

g in the `params` list, and eval it in a
      # child of the global environment (this isolates the code in the
document
      # from the code in this app).
      rmarkdown::render(tempReport, output_file = file,
                        params = params,
                        envir = new.env(parent = globalenv()))


    }

  )
}
```